

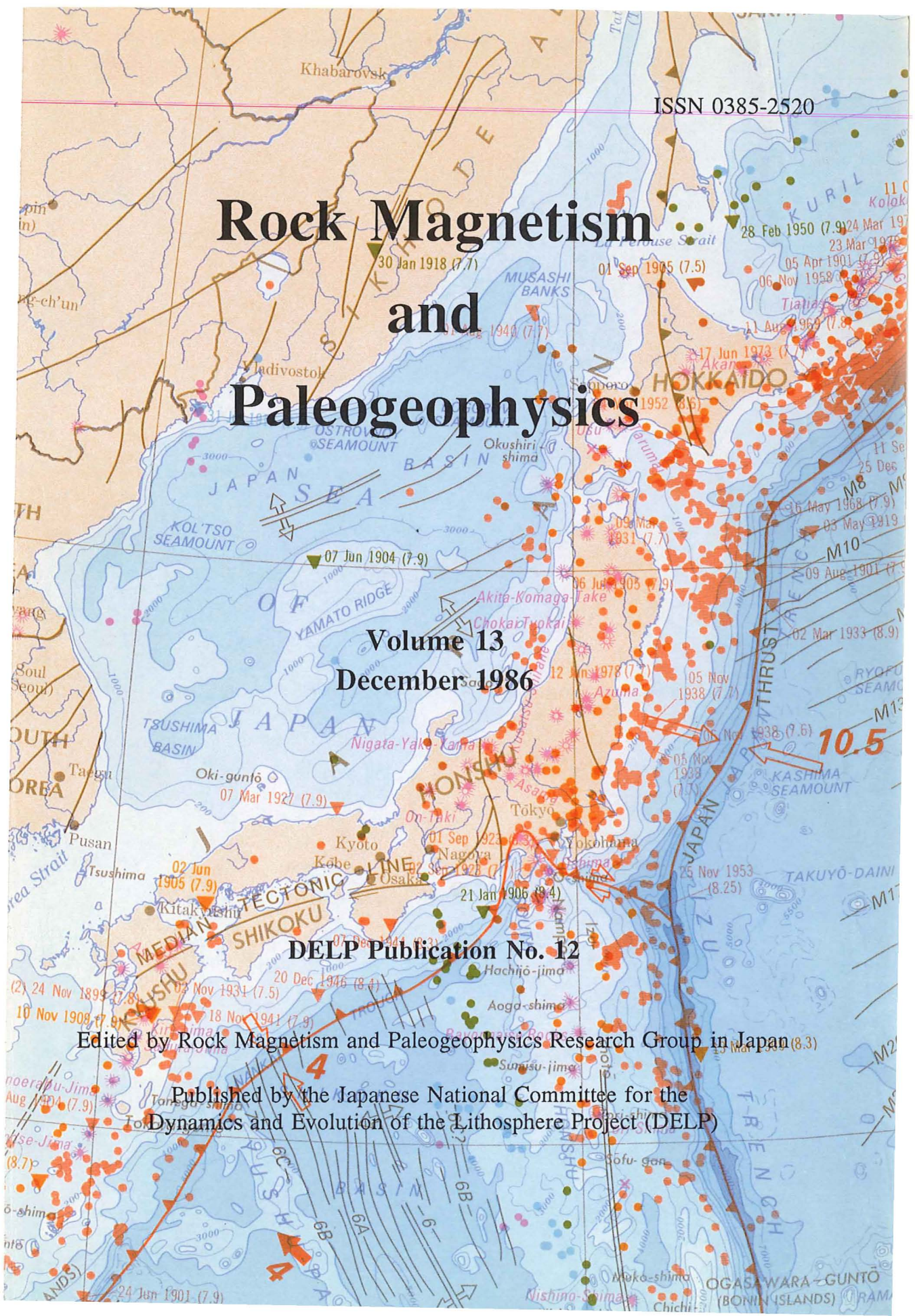
Rock Magnetism and Paleogeophysics

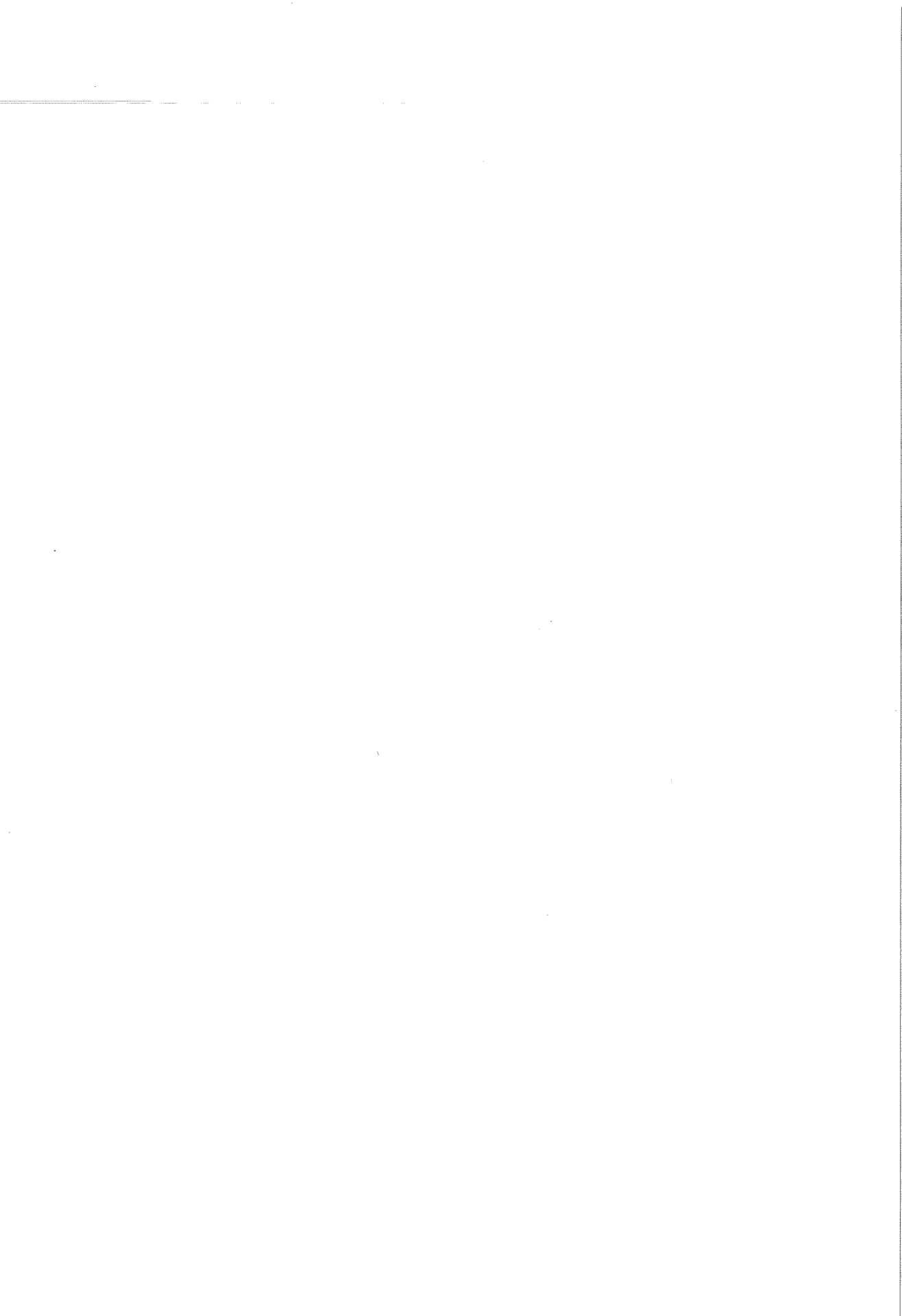
Volume 13
December 1986

DELP Publication No. 12

Edited by Rock Magnetism and Paleogeophysics Research Group in Japan

Published by the Japanese National Committee for the
Dynamics and Evolution of the Lithosphere Project (DELP)





Rock Magnetism and Paleogeophysics

**Volume 13
December 1986**

DELP Publication No. 12

Edited by Rock Magnetism and Paleogeophysics Research Group in Japan

Published by the Japanese National Committee for the
Dynamics and Evolution of the Lithosphere Project (DELP)

まえがき

本書は岩石磁気学・古地磁気学研究グループの1986年度の年次研究報告書であり、「国際リソフェア探査開発計画 (Dynamics and Evolution of the Lithosphere Project, DELP)」の成果報告 (DELP Publications) 第12号として刊行されるものである。

岩石磁気学・古地磁気学研究グループでは、以前から Annual Report として英文の報文集を刊行してきた。(Annual Progress Report of the Rock Magnetism (Paleogeophysics) Research Group in Japan, 1963, 1964, 1965, 1969; Rock Magnetism and Paleogeophysics, 1973-present)。これらの報文集は図書館などからの寄贈要請も多く、諸外国の関連分野の研究者によってかなり広く利用されている。このような経過からこの報告書も全て英文によって編集された。日本国内の方々には幾分不自由をおかけすることになると思うが、以上の事情によることを御理解いただきたい。

DELP計画は昭和60年度から開始されすでに2年が経過した。我々の研究グループは課題5「日本列島の構造発達」に参加し、日本列島及びその周辺のテクニクな発展の歴史を解明しようと努力を続けている。今年は7月24日、25日の両日、島根大学において研究会(シンポジウム)を開き、研究成果の発表を行った。このシンポジウムのプログラムは目次のあとに示されており、また、ここで発表された論文の多くは本研究報告に収められている。なお、本書はあくまでも extended abstract 集であり、ここに収録された研究はいずれ正式の論文として発表されることになる。投稿中のものや投稿予定のはっきりしているものについては各報文の最後にそのことが示されているので、引用される場合にはできるだけ正式の論文を参照していただくようお願いしたい。

本書の刊行及び研究会の開催については、文部省国際共同研究等経費「リソフェア探査開発計画 (DELP)」(代表: 秋本俊一)より援助を受けた。ここに記して感謝の意を表する。

1986年12月

岩石磁気・古地磁気研究グループ

PREFACE

This volume is the annual progress report of the Rock Magnetism and Paleogeophysics Research Group in Japan for the year 1986. We have published annual reports with a title "Annual Progress Report of the Rock Magnetism (Paleogeophysics) Research Groups in Japan" four times since 1963. Since 1973, the title changed to the present one and the reports were published annually (except 1976).

As the previous reports were so, this volume contains a collection of summaries, extended abstracts or brief notes of the research works carried out in our group this year. Many of the reports contain materials which may undergo a significant change or may be revised as the research activity continues. In this respect, the readers are warned to regard them as tentative, and are also requested to refer from a complete paper if such is published as a final result. (Names of journals appear at the end of individual articles if they are in press, submitted, or in preparation for submission to some scientific journals).

This volume is published with a financial aid from Ministry of Education, Science and Culture for the Dynamics and Evolution of the Lithosphere Project (DELP). It is Publication No. 12 of the Japanese DELP Program. We thank other members of the Lithosphere Project for help and encouragements.

Tokyo
December 1986

Masaru Kono
Editor

Rock Magnetism and Paleogeophysics
Research Group in Japan

Table of Contents

まえがき	i
Preface	ii
Table of Contents	iii
Rock Magnetism and Paleogeophysics Symposium 18	v

PALEOMAGNETISM AND TECTONIC PROBLEMS

M. Torii and N. Ishikawa	1
Paleomagnetic Directions from Middle Miocene Igneous Rocks In Central Eastern Kyushu Islands	
Y. Otofujii and T. Matsuda	6
Amount of Clockwise Rotation of Southwest Japan -- Fan Shape Opening of the Southwestern Part of the Japan Sea --	
N. Ishikawa and M. Torii	8
Westerly Deflected Remanent Direction of the Middle Miocene Granite from the Osumi Peninsula	
Y. Itoh	12
Differential Rotation of the Eastern Part of Southwest Japan: Paleomagnetic Study of Cretaceous and Neogene Rocks in the Chubu Area	
Y. Fujiwara and R. Sugiyama	15
Post-Oligocene Tectonic Rotation of Southeast Hokkaido - From Paleomagnetic Evidence -	
T. Yamazaki	19
Paleomagnetic Stratigraphy of Deep-Sea Sediments in the Central Equatorial Pacific	
K. Fukuma and M. Torii	26
Late Cretaceous Paleomagnetic Pole from the Koto Rhyolite, Southwest	

Japan

H. Ito and S. Nishimura	30
Short Duration of Magnetic Activity of the late Cretaceous Koto Rhyolite: New Evidence from Fission Track Age Dating	
M. Funaki and M. Yoshida	35
Paleomagnetic Studies of Paleozoic Rocks from the Ellsworth Mountains, West Antarctica	
P. Gautam	39
A Paleomagnetic Reconnaissance of Some Late Precambrian to Early Paleo- zoic Rocks of Tansen Area, Lesser Himalaya, Nepal	

AGE DATING, ROCK MAGNETISM, AND GEOMAGNETISM

I. Kaneoka, K. Notsu, Y. Takigami, K. Fujioka, and H. Sakai	48
K-Ar,40 Ar-39 Ar Age and Sr Isotope Studies on Volcanic Rocks of Seamounts from the Japan Sea	
H. Morinaga, H. Inokuchi, K. Yaskawa, T. Miki, and M. Ikeya	51
Paleomagnetism of a Phosphorite Module Collected from off New Zealand	
M. Funaki and H. Sakai	55
NRM Acquisition Mechanisms for Snow Involving Rock Dusts	
H. Ueno	60
Chemical Composition of Magnetite from the Hydrothermal Alteration Zone of Quartz Diorite Bodies, Chichibu Mining Area, Japan	
H. Domen	66
Thermomagnetic Study on Rocks from Ryoke Belt in Yanai-Oshima Dis- tricts, South-East End of Yamaguchi Prefecture, West Japan	
M. Kono	71
Rikitake Two-Disk Dynamo and Paleomagnetism	
Author Index	77

ROCK MAGNETISM AND PALEOGEOPHYSICS SYMPOSIUM 18

24 July Morning

1. H. Domen (Yamaguchi Univ.) and H. Muneoka (NDB., Ozaki Base)
Thermomagnetic analysis of the slime from a bore-hole at Uda Spa, Yamaguchi City, West Japan
2. H. Sibuya (Univ. of Osaka Pref.), N. Natsuhara, Y. Miyazaki (Natsuhara Co.) and T. Nakajima (Univ. of Fukui)
Yet another ring-core spinner magnetometer
3. T. Yamazaki and A. Nishimura (Geol. Surv. of Japan)
Paleomagnetic study of deep-sea pelagic clay
4. E. Kikawa (ERI, Univ. of Tokyo)
Magnetization of oceanic crust: a brief review
5. K. Fukuma (Kyoto Univ.)
Analysis of multicomponent magnetization

24 July Afternoon

6. N. Ishikawa and M. Torii (Kyoto Univ.)
Paleomagnetism of Kyushu Islands
7. K. Hirookam H. Nakamura and A. Takeuchi (Toyama Univ.)
Paleomagnetic study in Koshiki Islands
8. K. Tokieda, S. Omagari, T. Watanabe and H. Ito (Shimane Univ.)
Paleomagnetism of volcanic rocks exposed in Shimane peninsula
9. Y. Ito (Kyoto Univ.)
Paleomagnetic study in the Chubu district
10. M. Koyama (Tokyo Inst. Tech.) and K. Amano (Ibaragi Univ.)
Deformation model of the Jizodo section of the Ashigara Group based on paleomagnetism
11. N. Niitsuma (Shizuoka Univ.)
Collision in the South Fossa Magna area, central Japan
12. A. Hayashida (Doshisya Univ.), H. Tsurudome and M. Torii (Kyoto Univ.)
Paleomagnetism of some volcanic rocks in Northeast Japan
13. Y. Fujiwara (Hokkaido Univ.)
Paleomagnetism of the southeastern Hokkaido, North Japan
14. K. Kodama (Kochi Univ.)
A magnetic shielded room for paleomagnetic study at Kochi University

25 July Morning

15. M. Yoshida (Tribhuvan Univ.)
"Post-Collisional stage" in the Nepal Himalaya: its geological and paleomagnetic interpretation
16. P. Gautam (Hokkaido Univ.)
A Paleomagnetic reconnaissance of some Late Precambrian to Early Paleozoic sedimentary rocks in Lesser Himalayas, Tansen area, Nepal
17. K. Maenaka and S. Sasajima (Hanazono Univ.)
Tectonics of East Asia estimated from paleomagnetism
18. M. Kono (Tokyo Inst. Tech.)
Mountain building in the Central Andes
19. M. Torii (Kyoto Univ.)
News of Ocean Drilling Program

**PALEOMAGNETIC DIRECTIONS FROM MIDDLE MIOCENE IGNEOUS ROCKS
IN CENTRAL EASTERN KYUSHU ISLANDS**

Masayuki TORII and Naoto ISHIKAWA

Dept. Geology and Mineralogy, Kyoto University, Kyoto 606, Japan

Paleomagnetic directions from middle Miocene rocks in the main part of Southwest Japan can be categorized into two characteristic declinations: one group of the site-mean directions shows considerable clockwise deflection from the paleomeridian and the other points north-south direction. This fact interpreted as evidence that Southwest Japan land block has undergone regional clockwise rotation at middle Miocene time within very short time interval (Otofuji et al., 1986). Contemporaneous rock units on the eastern toe of Southwest Japan show fairly smaller magnitude of clockwise deflection of the remanent magnetism. This small deflection may imply differential rotation within the land block, particularly in the vicinity of its margin (Itoh, 1986). From this context, paleomagnetic directions of the other toe, the western part of Southwest Japan, is quite interesting and more data should be extensively collected to test the regional rotation hypothesis.

Middle Miocene igneous complex field is paleomagnetically studied in the central eastern Kyushu Islands. Pre-Neogene geologic system of eastern Kyushu Islands indicates a coherent structural trend with the main part of Southwest Japan, that is, the coeval tectonic rotation is expected as a part of the rotated land block. Paleomagnetic sample collection were carried out in the following three middle Miocene igneous field; Ono andesite and rhyolite volcanic field, Sobosan-Okueyama volcano-plutonic complex field, and Osuzuyama rhyolite volcanic field, from north to south (Fig. 1).

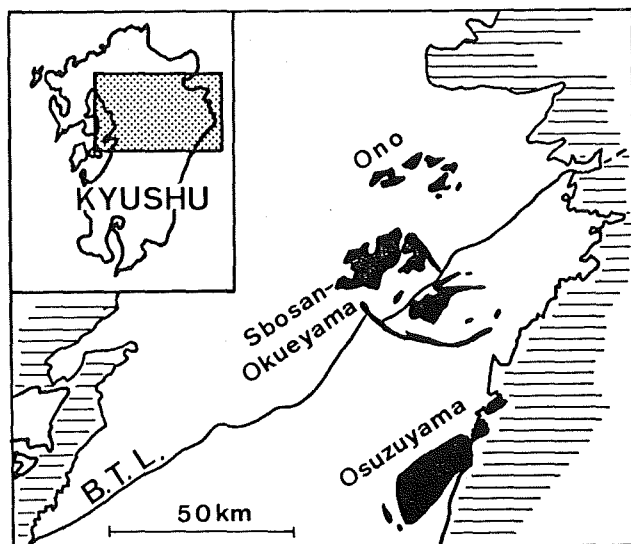


Fig. 1 Index map of studied area in central eastern Kyushu. Three igneous field are indicated by solid pattern. B.T.L. is Butuzo Tectonic Line.

Samples were collected at three sites in Ono area. One site is from lower Miyakeyama rhyolitic welded tuff which comprise many horizontally elongated pumice lenses. The other two site are from Daisangoyama andesite lava flow which shows prominent vertical columnar joint system. Shibata and Ono (1974) reported mean K-Ar age as 14.3 ± 0.4 Ma for Miyakeyama welded tuff. Daisangoyama andesite yielded K-Ar ages of 14.2 ± 0.8 Ma (Shibata and Ono, 1974) and 13.2 ± 0.7 Ma (Tatsumi et al., 1982). Alternating field and thermal demagnetization experiments proved that those volcanic rocks carry stable remanence as shown in the vector-demagnetiza-

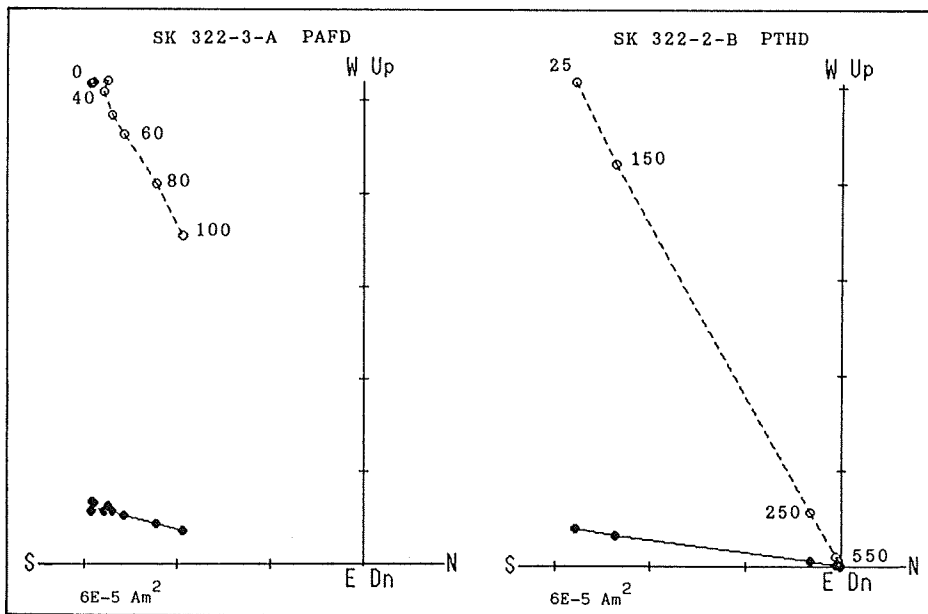


Fig. 2 Examples of vector-demagnetization diagrams of progressive alternating field (left) and thermal (right) demagnetizations of Ono volcanics (Daisangoyama andesite lava). Solid and open circles are projections of vector end-points on the horizontal and N-S vertical planes, respectively. Demagnetization levels are indicated in mT and $^{\circ}\text{C}$. Unit of the axis is Am^2 .

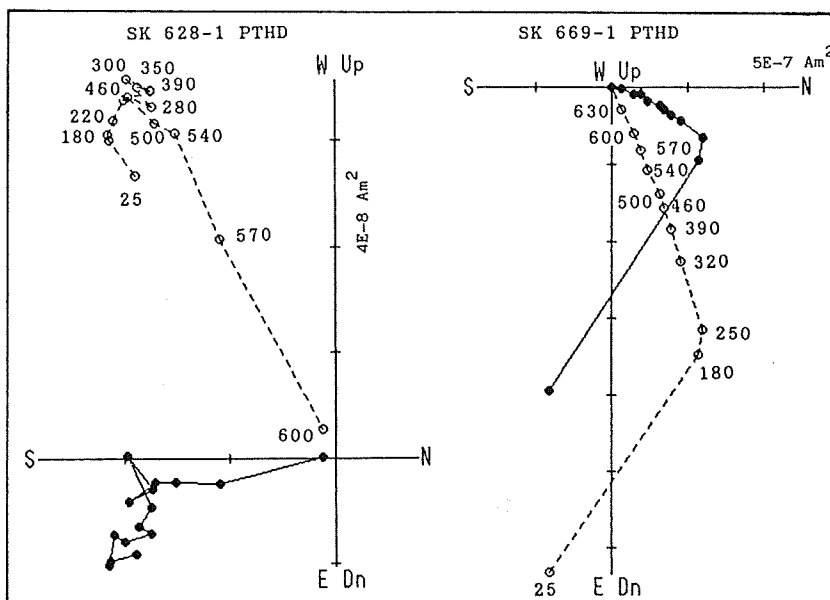


Fig. 3 Vector-demagnetization diagrams of progressive thermal demagnetization of the granite (Okueyama batholith: left) and Kunimidake rhyolite welded tuff (right) are shown as examples. See Fig. 2 for explanation.

tion diagrams in Fig. 2. Paleomagnetic directions from three sites are all pointing north-south direction (Table 1).

Our sampling localities were distributed at 13 sites in Sobosan-Okueyama area. Two sites are located in the underlying Sobosan volcanics. The granite porphyry ring dikes which are fringing the igneous field were sampled at two sites. The latest intrusive body of granite (Okueyama batholith) were sampled at eight sites, which yielded K-Ar age of 13.8 ± 0.9 Ma (Shibata, 1978). The well-documented vertical zoned pluton enable us to confirm that whole rock units have not been tilted since the final magmatism in this area (Takahashi, 1986). Most of the samples, however, could not reveal stable direction when examined by mean of thermal demagnetization. Finally four sites were accepted as to give paleomagnetic data (Fig. 3 & Table 1).

Welded tuff samples were collected at five sites, and satellitic intrusion of granite porphyry were sampled at three sites in Osuzuyama area. The welded tuff is extending about 250 Km^2 and showing distinct flow unit boundaries and elongated glass lenses as evidence for gentle tectonic attitude (Nakada, 1978). Two K-Ar ages have been reported by Shibata and Nozawa (1968); 15 ± 2 Ma for the welded tuff and 13 ± 2 Ma for the granite porphyry. We have very much disappointed by really meager behaviors of the rocks from this area. All samples failed to reveal stable direction by both alternating field and thermal demagnetizations. During the progressive demagnetizations, irregular increase of intensity and capricious directional flips were often observed which made us impossible to estimate a primary remanent direction (Fig. 4). Large pyrrhotite crystals are commonly observed under the reflecting light microscope. The presence of pyrrhotite would be a reason of an instability of remanence. Thus the all sites were finally discarded from the further consideration.

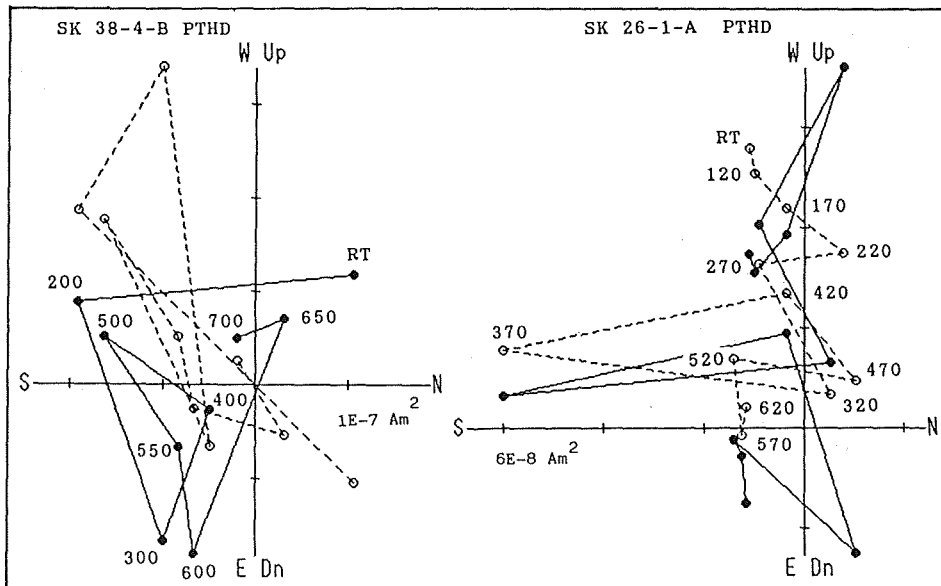


Fig. 4 Unsuccessful results of stepwise thermal demagnetizations of Osuzuyama area. Left diagram is an example of welded tuff (W.T. 2; Nakada, 1978), and right is granite porphyry. See Fig. 2 for explanation.

Table 1. Summary of Paleomagnetic Data from Middle Miocene Igneous Rocks in Central Eastern Kyushu Islands

Site	Rock type	Demag	N	Dec	Inc	α_{95}	k
[Ono volcanic field]							
SK-4	Daisangoyama andesite lava	50mT	6	-161.0	-36.5	4.6	211
SK-17	Daisangoyama andesite lava	40mT	6	178.1	-59.2	2.4	759
SK-14	Miyakeyama rhyolitic welded tuff	30mT	6	-16.1	52.3	3.9	289
MEAN			3	3.4	50.3	25.7	24
[Sobosan-Okueyama volcano-plutonic field]							
SO-6	Okueyama batholith (granite)	540°C	4	171.2	-45.9	26.4	13
SO-4	Ring dike (granite porphyry)	500°C	6	14.8	52.0	12.7	29
SO-12	Ring dike (granite porphyry)	500°C	7	-13.1	50.1	10.0	38
SO-13	Kunimidake rhyolitic welded tuff	600°C	8	1.9*	65.6*	3.7	226
MEAN			4	-2.0	53.9	13.0	51

*: tilt corrected

Our paleomagnetic results are listed in Table 1. Quite simply, all site-mean directions are pointing parallel direction with the present north. The mean direction of Ono area is $D=3.4^\circ$ and $I=50.3^\circ$, and that of Sobosan-Okueyama area is $D=-2.0^\circ$ and $I=53.9^\circ$. It can be said that the studied area has not been subjected to any regional rotation since the igneous activities of middle Miocene age. Volcanic field of Ono area has been considered as the western extension of the Setouchi Volcanic Belt mainly from view point of radiometric age (Tatsumi et al., 1982). The characteristic paleomagnetic direction of the Setouchi Volcanic Rocks is parallel to the present north-south direction that implies the post-rotational direction (Torii, 1983). The north-south direction of Ono volcanic rocks supports to locate the western extension of the Setouchi Volcanic Belt in the eastern Kyushu Islands. On the other hand, Sobosan-Okueyama volcano-plutonic complex has been considered as a part of felsic rocks in the so-called Outer Zone of Southwest Japan (Nakada and Takahashi, 1979). Paleomagnetic direction from the 'Outer Zone' volcanic field so far reported have been all showing considerable clockwise deflection (Tagami, 1982; Torii and Ishikawa, 1986). Therefore, the magmatic activities has been thought to precede the timing of rotation of Southwest Japan in the trench-side area ('Outer Zone'). Our result from Sobosan-Okueyama area is not consistent to the results of the previous studies. Undelected paleomagnetic directions from central eastern Kyushu Islands may imply that the magmatic activity in the trench-side area has partly survived after the rotation of Southwest Japan at 15 Ma.

References:

- Itoh, Y. (1986) *J. Geomag. Geoelectr.*, **38**, 325.
 Nakada, S. (1978) *J. Geol. Soc. Japan*, **84**, 243.
 Nakada, S. and M. Takahashi (1979) *J. Geol. Soc. Japan*, **85**, 571.
 Otofujii, Y., A. Hayashida and M. Torii (1986) in 'Formation of Active Ocean Margins', eds., N. Nasu et al., TERRAPUB, 551.
 Shibata, K. (1978) *Bull. Geol. Surv. Japan*, **29**, 551.
 Shibata, K. and T. Nozawa (1968) *Bull. Geol. Surv. Japan*, **19**, 7.

- Shibata, K. and K. Ono (1974) Bull. Geol. Surv. Japan, **25**, 55.
- Tagami, T. (1982) NOM (News of Osaka Micropaleontologist), **9**, 23.
- Takahashi, M. (1986) J. Vol. Geotherm. Res., **29**, 33.
- Tatsumi, Y, M. Torii and K. Ishizaka (1982), Bull. Vol. Soc. Japan, **25**,
171.
- Torii, M. (1983), Rock Mag. Paleogeophys., **10**, 77.
- Torii, M. and N. Ishikawa (1986) J. Geomag. Geoelectr., **38**, 523.

AMOUNT OF CLOCKWISE ROTATION OF SOUTHWEST JAPAN
 -- FAN SHAPE OPENING OF THE SOUTHWESTERN PART OF
 THE JAPAN SEA --

YO-ichiro OTOFUJI* and Takaaki MATSUDA**

* Department of Earth Sciences, Faculty of Science,
 Kobe University, Kobe 657, Japan

** Department of Geology, Himeji Institute of Technology,
 Himeji 671-22, Japan

Paleomagnetic measurements have been carried out on welded tuffs ranging in age between 58 Ma and 112 Ma from Yamaguchi and Go river areas in central part of Southwest Japan. The new data, together with those of younger igneous rocks published previously, define the change of paleomagnetic field direction during late Mesozoic-Cenozoic period for Southwest Japan. The paleomagnetic direction from Southwest Japan has pointed $56^\circ \pm 3^\circ$ clockwise from the expected field direction estimated from APWP (apparent polar wandering path) of the whole of Eurasia during the period between 100 Ma and 20 Ma. In comparison with the expected one from the eastern margin of Eurasia (Korea, China, Siberia), the Cretaceous field direction of Southwest Japan shows the clockwise deflection by 44° to 49° . These results establish that while the eastern margin of Eurasia including Southwest Japan was rotated more or less with respect to the main part of Eurasia during last 100 Ma, Southwest Japan was rotated clockwise through more than 40 degrees with respect

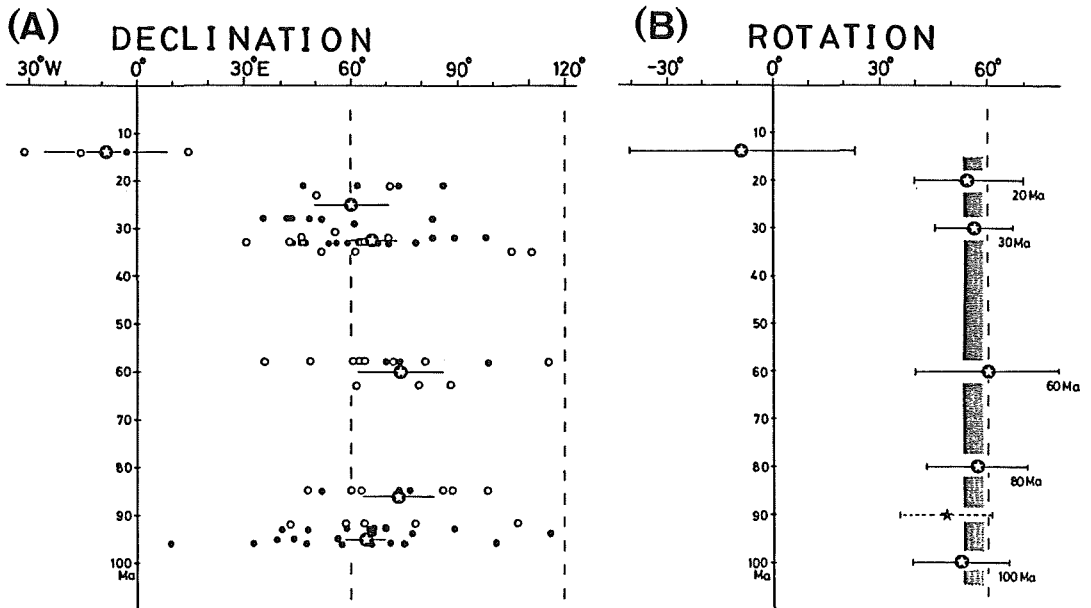


Fig. 1. (A) Mean declination data versus age for each site and each stage of 13.9 Ma, 20-30 Ma, 30-35 Ma, 58-63 Ma, 80-92 Ma and 85-112 Ma. Closed (open) circles show the data with normal (reversed) polarity. (B) Rotation with respect to Eurasia versus age for each stage of 13.9 Ma, 20 Ma, 30 Ma, 60 Ma, 80 Ma and 100 Ma. Rotation with respect to the eastern part of Eurasia is shown as closed star. The error bar in declination and rotation for each stage is ΔD and ΔR values. Shaded declination zone is the standard error of rotation.

to the eastern margin of Eurasia since 20 Ma. The large amount of rotation for Southwest Japan implies that Southwest Japan is rotated by an opening of the southwestern part of the Japan Sea, which widens northeastward (fan shape opening). The tectonic feature of Southwest Japan and the Japan Sea is analogous to that of Corso-Sardinia and the Ligurian Sea in the Mediterranean, indicating that the fan shape opening is a specific feature of the rifting of the continental sliver at continental rim.

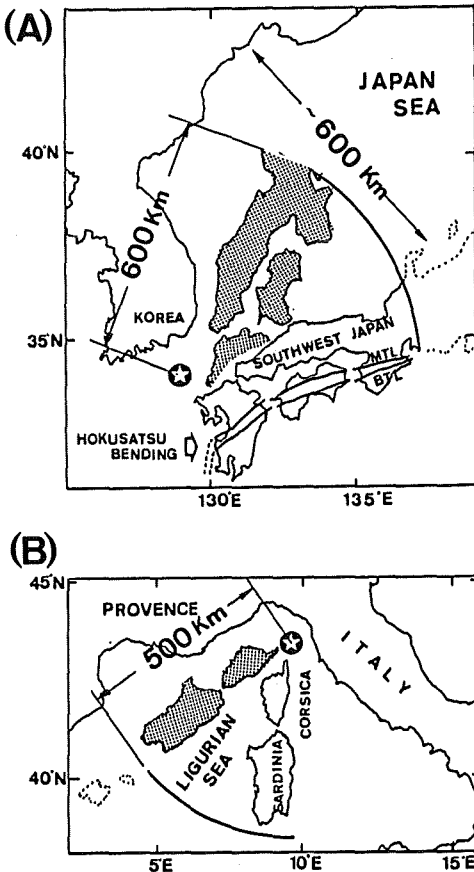


Fig. 2. A comparison of rotation of the continental sliver. (A) Southwest Japan is rotated about the rotation pivot 129°E , 34°N through 47° associated with the fan shape opening of the southwestern part of the Japan Sea. MTL: Median tectonic line. BTL: Butsuzo tectonic line which is a boundary between the Sambosan and Shimanto Groups. (B) Corso-Sardinia block is estimated to be rotated about the pivot $9^{\circ}38'\text{E}$, $43^{\circ}22'\text{N}$ through 49° associated with the fan shape opening of the Ligurian Sea.

(Submitted to Earth Planet. Sci. Lett.)

WESTERLY DEFLECTED REMANENT DIRECTION OF THE MIDDLE MIOCENE GRANITE
FROM THE OSUMI PENINSULA

Naoto ISHIKAWA and Masayuki TORII

Dept. Geology and Mineralogy, Kyoto University, Kyoto 606, Japan

Middle Miocene felsic igneous rocks are widely distributed in the southern coastal area, so-called the Outer Zone of Southwest Japan. The zonal arrangement of these rocks runs parallel to the Nankai Trough extending almost 800 km long from the Kii Peninsula to Yakushima Island (Fig. 1(A)). These trench-side magmatism have been thought as one of the middle Miocene episodic igneous activities observed in the whole area of Southwest Japan (Nakada and Takahashi, 1979). Radiometric age data obtained for these rocks concentrated around 14 Ma (Shibata, 1978). Paleomagnetic directions for these rocks have been previously reported from the Kumano Acidic Rocks, in the eastern part of the zonal distribution (Tagami, 1982). The remanent vector from the Kumano area

point clockwise deflected direction which has been interpreted as a result of the clockwise rotation of Southwest Japan at 15Ma (Otofuji et al., 1986). It is indispensable to collect much more paleomagnetic directions from the wide area of the trench-side igneous field to characterize tectonic movements occurred after middle Miocene.

The Osumi granite is regarded as the largest exposure of those trench-side felsic rocks, which is distributed in almost whole area of the Osumi Peninsula, the southernmost Kyushu Islands (Fig. 1(B)). The Osumi granite is discordantly intruded into the Mesozoic and early Tertiary Shimanto Group, and is exposed more than 400 km². Radiometric ages ranging 13 to 14 Ma were obtained by K-Ar method on biotite crystals (Shibata, 1978), and by fission track method on zircon crystals (Miyachi, 1985).

Paleomagnetic analysis

Samples for the paleomagnetic study were collected at 28 sites (Fig. 1(B)). About ten hand samples were collected in each site, and oriented by using a magnetic compass. More than two cylindrical specimens about 25 mm in diameter and height were prepared from each hand sample.

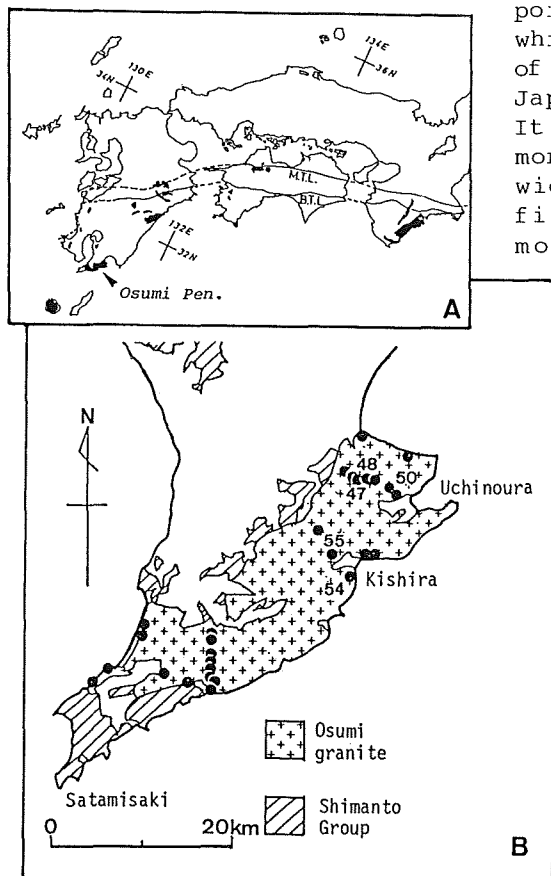


Fig. 1.(A): Map showing the distribution of Middle Miocene felsic igneous rocks in the trench-side area of Southwest Japan. (B): Distribution of the Osumi granite and site location. Solid circles show sampling sites. Numerals indicate site number.

Remanent magnetization was measured with a cryogenic magnetometer (SCT C-112). In order to assess the stability of natural remanent magnetization, progressive thermal and alternating field demagnetizations were carried out for two or more pilot specimens per site.

As results of the demagnetization experiments, all but a few sites were discarded from the further analysis. Because the pilot specimens of discarded sites showed an erratic behavior with irregular change of intensity and direction at each step of the demagnetization (Fig. 2 (a), (b)). Such unstable behaviors could be attributed to the abundant occurrence of pyrrhotite crystals (e.g., Tsusue, 1973). The abundant occurrence of pyrrhotite was confirmed by the reflecting light microscopy, particularly in the samples of the discarded site. These pyrrhotite is considered to be a dominant magnetic minerals in the Osumi granite, which could not be a stable remanence carrier but a source of magnetic noise

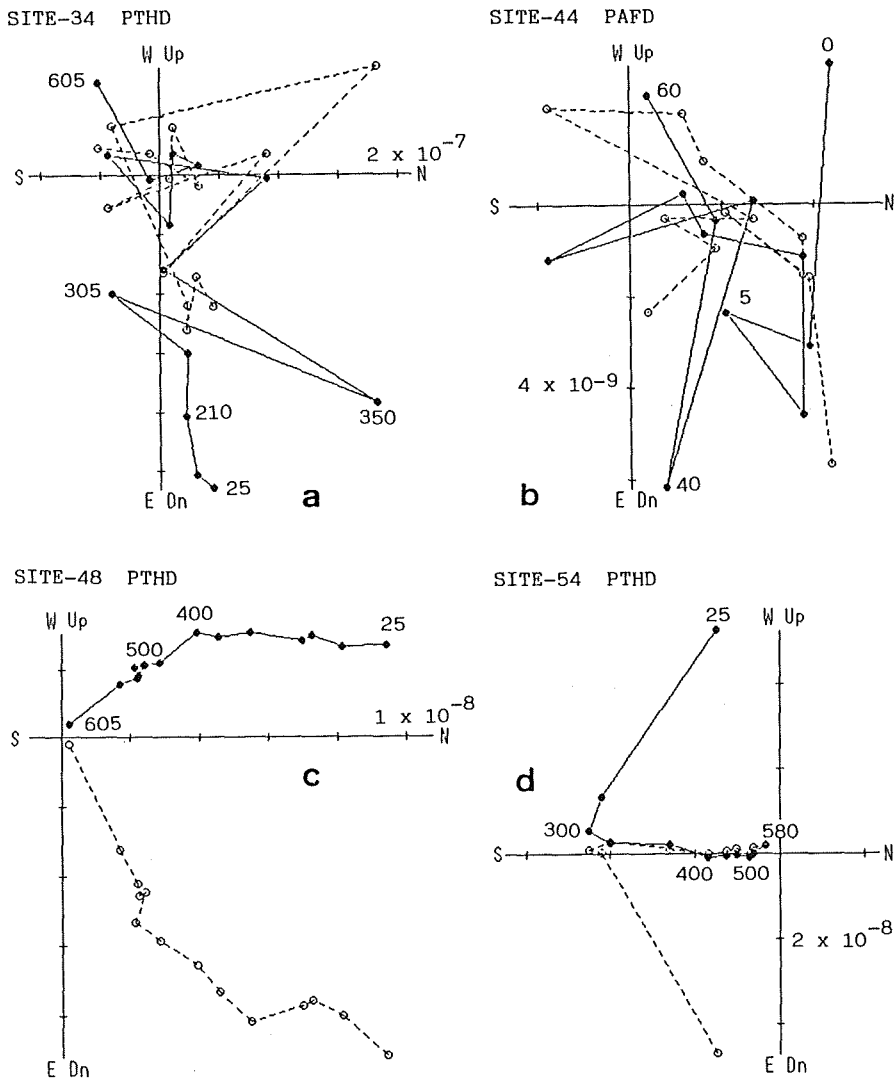


Fig. 2. Typical examples of vector-demagnetization diagrams of progressive thermal demagnetization (PTHD) and progressive alternating field demagnetization (PAFD). Solid (open) circles are projection on horizontal (N-S vertical) plane. Numerals denote demagnetization level in $^{\circ}\text{C}$ or mT. Unit of coordinate is bulk intensity in Am^2 .

during the thermal experiment.

Fortunately, we could obtain stable remanent magnetization in several sites, after the progressive thermal treatment. The stable magnetization can be discriminated as a linear trend of vector end-points on the vector-demagnetization diagram at the temperature range higher than 400°C (Fig. 2(c), (b)). Under the reflecting light, samples of stable remanence show smaller numbers of pyrrhotite crystals relative to the discarded samples. All the rest specimens of the site which share stable pilot specimens were submitted to the progressive thermal demagnetization. Then the specimens of stable magnetization were selected by using vector-demagnetization diagrams. Site-mean directions were calculated combining the each direction which constitutes the linear trend of vector end-points of the stepwise demagnetization. A site-mean direction with the smallest radius of 95% confidence circle ($<30^\circ$) is regarded as a stable remanent direction of each site.

Five site-mean directions were finally obtained from site-47, 48, 50, 54, and 55 (Fig. 3, Table 1). These mean directions of site-47, 48, 50 are making a cluster of normal polarity, and the mean direction of site-55 is showing approximately antipodal relation to the others. The mean direction of site-54 is of very shallow inclination. We consider this anomalous direction as a record of transient feature of the geomagnetic field or a result of local tectonic movement. Therefore, formation-mean direction is calculated by combining four site-mean directions except site-54; $D_m = -45.3^\circ$, $I_m = 45.7^\circ$, $\alpha_{95} = 21.4^\circ$, and $k = 19.5$. This westerly deflected direction is regarded as a characteristic remanent direction of the Osumi granite.

Discussion

To explain westerly deflected mean direction, two simple tectonic models are discussed as follows; (a) a tilting movement about a horizontal axis, and (b) a combination of rotation about a vertical axis and north-south translation after Beck (1980). For the sake of the further calculation, the expected field direction at about 15 Ma is calculated from the geocentric axial dipole: $D_{exp} = 0.0^\circ$, and $I_{exp} = 50.6^\circ$.

(a) To fit the formation-mean direction to the expected field direction, a rotation through the dip of $30.1^\circ E$ about the line of strike in the direction of $N13.2^\circ W$ is required.

(b) To obtain same fitting, $45.3^\circ \pm 31.5^\circ$ rotation about a vertical axis in counter-clockwise sense, and northward translation of $4.9^\circ \pm 21.4^\circ$ are necessary. Which tectonic model is more realistic for the case of the present study?

Nozawa and Ota (1967) reported the excellent development of nearly

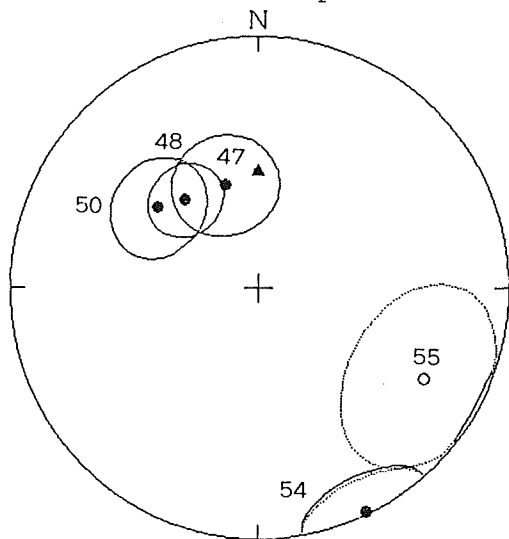


Fig. 3. Equal-area projection of site-mean directions. Ovals around the mean directions indicate 95% confidence limit. Numerals denote site number. Solid (open) symbol is on the lower (upper) hemisphere. Triangle symbol shows field direction of axial geocentric dipole field at the representative sampling location ($31.3^\circ N$, $131.0^\circ E$).

Table 1. Paleomagnetic data from the Osumi granite

SITE	LAT	Lon	DMG	D	I	α_{95}	k	N
47	31.30	131.01	500	-18.2	54.1	17.3	16.0	6
48	31.30	131.02	500	-40.1	52.0	12.2	21.6	8
50	31.30	131.05	500	-51.6	46.8	16.2	12.7	8
54	31.21	131.01	550	153.9	0.8	15.6	13.6	8
55	31.22	130.96	450	118.8	-25.2	27.1	7.1	6
MEAN*				-45.3	45.7	21.4	19.5	4

LAT, LON: latitude ($^{\circ}$ N) and longitude ($^{\circ}$ E) of sampling site. DMG: demagnetization level in $^{\circ}$ C. D, I: mean declination and inclination in degree. α_{95} : radius of 95% confidence circle. k: precision parameter. N: number of specimens. **MEAN***: formation-mean direction calculated from site-mean directions of site-47, 48, 50, 55.

vertical joint system in the Osumi granitic body of Uchinoura area. Shigeno (1980) stressed the ubiquitous existence of the conjugated joint sets with vertical dip in the granitic bodies of Osumi Peninsula, Okinoshima Island and Yakushima Island. In their paper, the formation of those joint sets were attributed to the regional tensile stress field which should be a stress condition during the uplift and subsequent erosion after the solidification of granitic magma at the shallow level of the crust. The vertical joint system may suggest that the granite body have not been significantly tilted after its emplacement. Therefore, we prefer the model (b), that is, the westerly deflected remanent direction may imply a counter-clockwise rotation of the Osumi Peninsula through 45° about a vertical axis sometime after the intrusion of the granite.

The counter-clockwise deflection of the remanent direction from the Osumi granite is quite different from the previously obtained clockwise deflected directions from the eastern part of the trench-side igneous zone (Tagami, 1982; Torii and Ishikawa, 1986). As discussed in the former paragraph, it may be possible to attribute anomalous paleomagnetic direction to the counter-clockwise rotation of the studies area. If so, the supposed rotation is opposite sense to the rotation of the main part of Southwest Japan, that is, a different tectonic movement might have taken place around the Osumi Peninsula since the intrusion of the granite.

References:

Beck, M. E. Jr. (1980) *J. Geophys. Res.*, **85**, 7115.
 Miyachi, M. (1985) *J. Japan. Assoc. Min. Petr. Econ. Geol.*, **80**, 406.
 Nakada, S. and M. Takahashi (1979) *J. Geol. Soc. Japan*, **85**, 571.
 Nozawa, T. and R. Ota (1967) in 'Geological Map of Uchinoura', Geol. Surv. Japan, Quad. Ser., 1:50,000, no. 102, 37.
 Otofujii, Y., A. Hayashida and M. Torii (1986) in 'Formation of Active Ocean Margins', eds., N. Nasu et al., TERRAPUB, 551.
 Shibata, K. (1978) *Bull. Geol. Surv. Japan*, **29**, 551.
 Shigeno, H. (1980) *Sci. Rept. Dept. Geol., Kyushu Univ.*, **13**, 145.
 Tagami, T. (1982) *NOM (News of Osaka Micropaleontologist)*, **9**, 23.
 Torii, M. and N. Ishikawa (1986) *J. Geomag. Geoelectr.*, **38**, 523.
 Tsusue, A. (1973) *Contr. Mineral. and Petrol.* **40**, 305.

**DIFFERENTIAL ROTATION OF THE EASTERN PART OF SOUTHWEST JAPAN:
PALEOMAGNETIC STUDY OF CRETACEOUS AND NEOGENE ROCKS
IN THE CHUBU AREA**

Yasuto ITOH

Department of Geology and Mineralogy, Kyoto University,
Kyoto 606, Japan

Abstract

Paleomagnetic directions have been determined on Late Cretaceous and Miocene rocks in the Chubu area, the eastern part of Southwest Japan (Fig. 1) in an effort to clarify within-block deformation of the rotated Southwest Japan. Twenty two sites are found to have reliable primary magnetic component through progressive demagnetization test using thermal and alternating field methods. Tilt-corrected paleomagnetic data in the Chubu area are divided into three stages based on the geologic age; Late Cretaceous, Early Miocene (23-15 Ma) and Middle Miocene (12-10 Ma). The formation-mean direction of 10 sites obtained from Late Cretaceous Nohi Rhyolite is $D=17.0^\circ$, $I=49.8^\circ$ and $\alpha_{95}=6.1^\circ$. The Neogene rock units which are underlain by the Nohi Rhyolite show two distinct formation-mean directions: $D=13.0^\circ$, $I=52.7^\circ$ and $\alpha_{95}=7.2^\circ$ for 8 sites of Early Miocene stage, and $D=-2.5^\circ$, $I=55.6^\circ$ and $\alpha_{95}=6.6^\circ$ for 4 sites of Middle Miocene stage.

Differential rotation is proposed between the eastern part of Southwest Japan including Chubu area and the main part of Southwest Japan which is known to have rotated

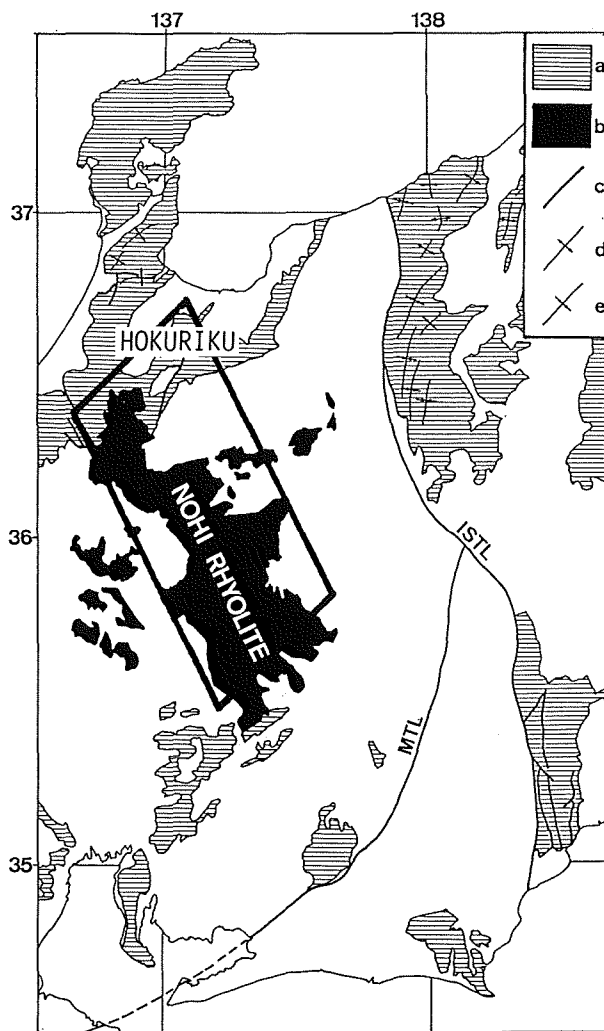


Fig. 1 Distribution of Neogene System and pre-Neogene rhyolitic rocks in the eastern part of Southwest Japan (simplified from Yamada et al., 1982). Bold enclosure shows the studied 'Chubu area'. a: Neogene System. b: Pre-Neogene rhyolitic rocks. c: fault. d: anticlinal axis. e: synclinal axis. MTL: Median Tectonic Line. ISTL: Itoigawa-Shizuoka Tectonic Line.

clockwise through about 50° around 15 Ma. The spatial distribution of contemporaneous paleomagnetic data in Southwest Japan suggests that differentially rotated two parts are connected in the western neighborhood of the Chubu area (Fig 2). It is concluded that the Chubu area had rotated counter-clockwise through 41° relative to the main part of Southwest Japan between 15 and 12 Ma.

Together with previous paleomagnetic data from Early Miocene rocks in the Kanto area which is situated to the east of the Chubu area, the present result suggests that the differential rotation of the eastern part of Southwest Japan during the period between 15 and 12 Ma is attributed to the formation of northward cusped shape of the pre-Neogene terranes which constitute the framework of Southwest Japan (Fig 3). One probable explanation of the formation of cusp is a crustal indentation caused by a collision of some landmasses on the Philippine Sea Plate against the Japan arc in Middle Miocene.

(To be submitted to Tectonics)

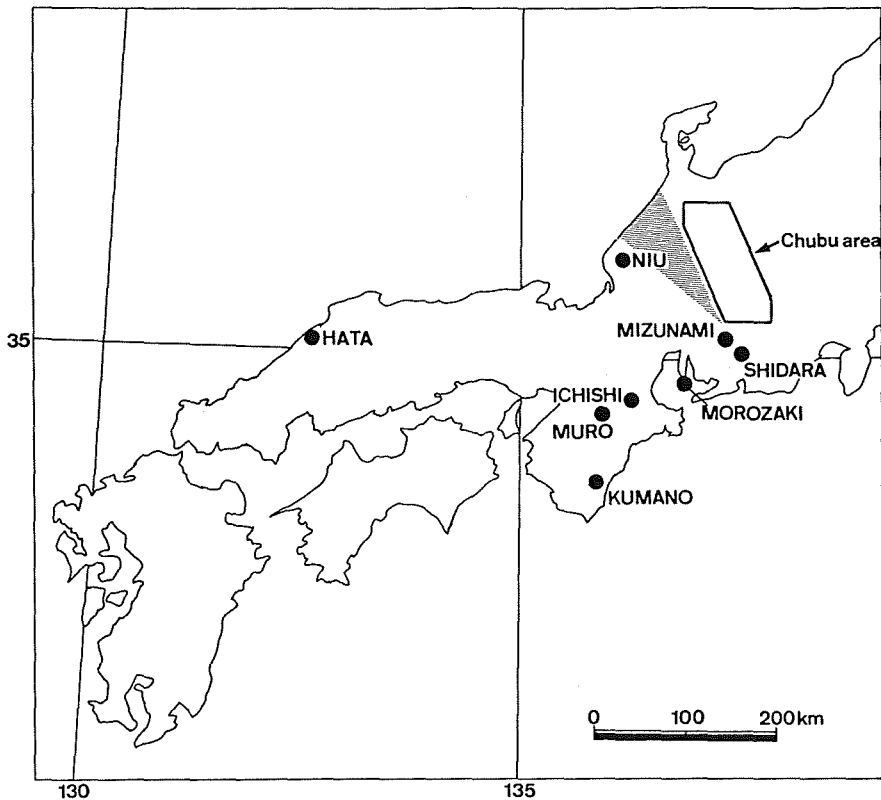


Fig. 2 Map showing the distribution of paleomagnetic data obtained from Early Miocene rock units. Solid circle indicates the data of which easterly deflection in paleomagnetic declination exceeds 40° . Shaded zone indicates possible boundary between the main part of Southwest Japan and the eastern part of Southwest Japan including Chubu area.

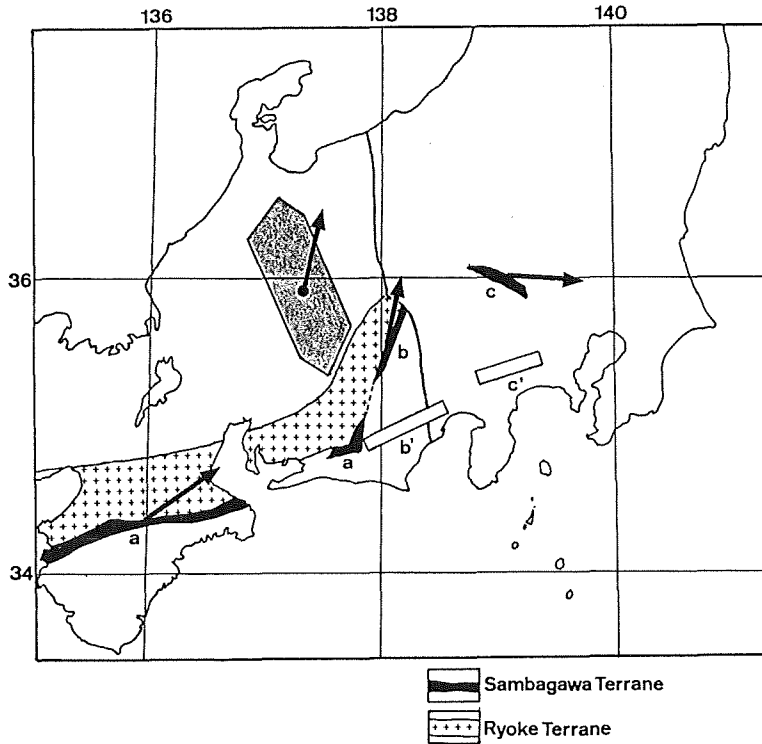


Fig. 3 Possible rearrangement of the pre-Neogene Sambagawa terrane before the differential rotation of the Chubu and the Kanto (Chichibu basin and its surrounding region) areas. Shaded enclosure and arrow in it show the studied 'Chubu area' and its paleomagnetic direction in the Early Miocene, respectively. Segment-a, b and c, which belong to paleomagnetically distinct three parts (main part of Southwest Japan, Chubu and Kanto), show the present arrangement of the Sambagawa terrane. Black arrows attached to the segments show horizontal components of mean paleomagnetic directions of each part in the Early Miocene. Segment-b and c are rotated to the rearranged position of the terrane (Segment-b' and c') so as to parallelize the paleomagnetic directions of the three parts. Rearranged segments lie almost in a straight line.

POST-OLIGOCENE TECTONIC ROTATION OF SOUTHEAST HOKKAIDO
- From Paleomagnetic Evidence -

Yoshiki FUJIWARA and Ryouichi SUGIYAMA

Department of Geology & Mineralogy Faculty of Science Hokkaido University
Sapporo, JAPAN

It is generally believed that a large scale tectonic movement had occurred during a formation of marginal sea, the Japan Sea, where locates behind the arc trench system. Since early work presented by Kawai et al (1961), many investigators have been discussed to this problem from a view point of paleomagnetism (Ito 1963, Sasajima et al. 1968, Otofujii and Matsuda 1983, Hayashida and Ito 1984, Torii et al. 1985, Hamano and Tosha 1985 etc.). These works strongly suggest that Southwest Honshu as well as Northeast Honshu were rotated independently since Early Miocene, possibly associated with the formation of the Japan Sea. Meanwhile, virtually a few paleomagnetic work has been carried out on rocks from Southeast Hokkaido which forming a northern extension of the Honshu arc.

We have determined a paleomagnetic measurements on Miocene and Pliocene rocks developed in Southeast Hokkaido in order to get correct informations concerning to tectonic rotation of the Northern Japan arc during Tertiary period.

Geologic setting of Southeast Hokkaido

Southeast Hokkaido is northern extension of the inner belt of the Honshu arc and its eastern boundary is the so-called Sapporo-Tomakomai line. This region is characterized by the predominance of various types of volcanic products ranging from late Oligocene up to Holocene in age and have generally been called the Green-tuff region. The standard sequence of the Tertiary established in this region is the followings ; the Fukuyama, Yoshioka, Kunnui, Kikonai, Assabu and the Setana stage in ascending order.

Paleomagnetic measurements

More than 200 samples were collected at 70 sites from almost entire sequence. The site mean directions and mean site directions obtained from the results of measurements of NRMs and after demagnetization using 400 Hz. alternating field are summarized in Table 1 and Fig. 1. These results clearly show that site mean declinations obtained from the Fukuyama Formation represent 46° - 69° deflected to the west and site mean declinations from the Kunnui Formation deflect 19° - 28° to the west respectively. Meanwhile, site mean declinations obtained from the Kikonai Formation represent 4° - 12° deflection to the east. Site mean directions from the Assabu Formation, the uppermost sequence in the present work, are comparable to the same direction of the present geomagnetic field.

Fission track dating was carried out on 9 stratigraphic horizons at the same time (Koshimizu et al. in press). The results of these dating are also summarized on Table 1. If we make direct comparison these fission track data with present paleomagnetic results, a large scale tectonic rotation of Southeast Hokkaido had been occurred since Late Oligocene. The rotation was anti-clockwise and possibly more than 50°

Torii(1983) proposed a rapid clockwise rotation of Southwest Japan at Middle Miocene time (15 to 13 Ma), however, the present results suggest that Southeast Hokkaido had undergone anti-clockwise rotation since Late Oligocene (24 Ma) up to Late Miocene (11 Ma).

Table 1-a Assabu Formation

Site	n	AF	D	I	k	α_{95}	rocks	FT age
A-1	3	100	332	46	19	18	tuff	
A-2	3	150	192	-56	21	17	mudstone	
A-3	3	150	187	-59	41	12	mudstone	
A-4	3	100	202	-58	21	21	mudstone	
A-5	3	200	356	44	32	14	tuff	11.2±0.7
A-6	4	150	352	40	25	13	mudstone	
A-7	3	150	162	-43	18	19	sandstone	
A-8	4	300	160	-25	14	18	tuff	8.1±0.7
A-9	3	200	195	-51	138	6	mudstone	
A-10	4	350	198	-40	11	20	tuff	7.3±0.9
A-11	3	350	195	-78	33	14	tuff	

Table 1-b Kikonai Formation

Site	n	AF	D	I	k	α_{95}	rocks	FT age
I-1	4	150	356	50	19	15	shale	
I-2	3	100	18	67	44	8	shale	
I-3	3	150	12	20	5	35	shale	
I-4	3	200	188	-50	4	45	shale	
I-5	3	200	195	-57	25	16	shale	

Table 1: Summary of site mean directions of the Tertiary rocks in Southeast Hokkaido. Detailed stratigraphic position and location of sites will be appeared in Fujiwara et al. (in preparation). n: number of samples AF: cleaning field (oe) D, I: mean direction k: Fisher's dispersion parameter α_{95} : radius of the cone of 95% FT age: fission track age (Ma)

Table 1-c Kunnui Formation

Site	n	AF	D	I	k	α_{95}	rocks	FT age
K-1	3	150	5	78	86	8	sandstone	
K-2	5	100	8	54	19	14	sandstone	
K-3	3	200	126	-63	209	5	andesite	17.1±1.6
K-4	4	200	12	58	38	10	sandstone	
K-5	3	100	165	-35	183	5	andesite	16.8±1.3
K-6	3	200	132	-50	148	6	andesite	
K-7	3	300	137	-44	21	17	sandstone	
K-8	3	250	1	18	37	16	andesite	
K-9	3	300	18	74	21	17	sandstone	
K-10	5	200	342	48	32	10	tuff	
K-11	3	300	338	40	7	30	mudstone	
K-12	3	100	297	28	7	29	sandstone	
K-13	4	150	323	50	6	27	andesite	14.5±1.4
K-14	3	250	335	67	257	5	sandstone	
K-15	3	200	46	77	5	42	sandstone	
K-16	3	200	6	63	7	30	andesite	

Table 1-d Fukuyama Formation

Site	n	AF	D	I	k	α_{95}	rocks	FT age
F-1	3	300	106	-39	89	8	andesite	
F-2	3	100	143	-50	103	7	welded tuff	21.7±1.7
F-3	6	150	108	-41	23	11	welded tuff	24.3±2.0
F-4	3	300	131	-49	15	20	volc.br.	22.3±1.8
F-5	3	400	317	43	5	33	volc.br.	
F-6	4	300	118	-55	44	10	volc.br.	
F-7	3	200	348	55	3	44	volc.br.	

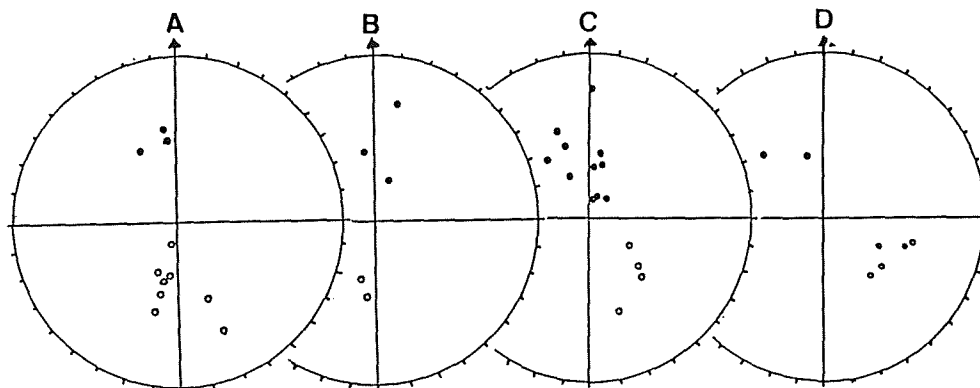


Fig. 1 Equal area projections of site mean magnetization directions after alternating field demagnetization. Bedding corrections are also made. The solid symbols refer to the lower hemisphere and the open symbols refer to the upper hemisphere. A: Assabu Formation (11.2 Ma >) B: Kikonai Formation (11.2-14.5 Ma) C: Kunnui Formation (14.5-17.1 Ma) D: Fukuyama Formation (21.7-24.3 Ma)

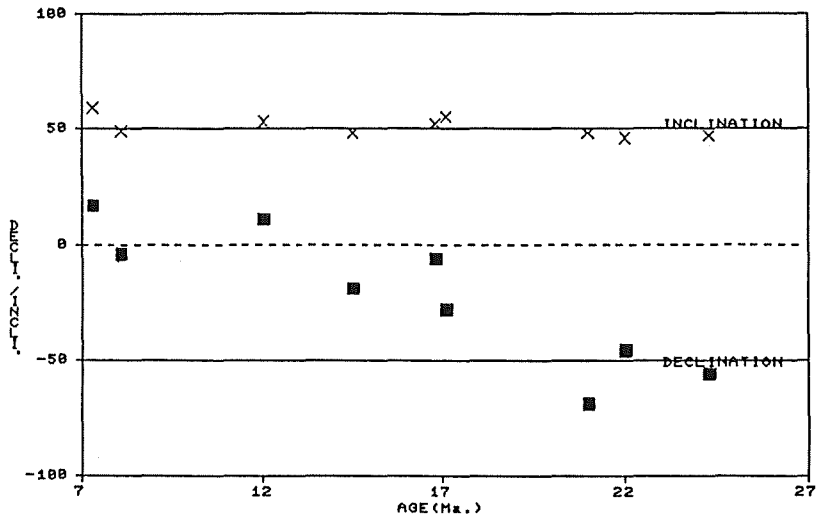


Fig. 2 Variation of declination and inclination through Tertiary period based on the paleomagnetic measurements of rocks in Southeast Hokkaido.

References

- Hamano, Y. and T. Tosha (1985) *Kagaku* 55, 8, 476-483
 Hayashida, A. and Y. Ito (1984) *Earth Planet. Sci. Lett.* 68 335-342
 Ito, H. (1963) *J. Geomag. Geoelectr.*, 15, 37
 Kawai, N., H. Ito and S. Kume (1961) *Geophys. J. Roy. Astr. Soc.* 6, 124-129
 Koshimizu, S., J. Yamazaki and M. Kato (1986) *J. Geol. Soc. Japan* 92, 11, 771-780
 Otofujii, Y. and T. Matsuda (1983) *Earth Planet. Sci. Lett.* 62, 349-359
 Sasajima, S., J. Nishida and M. Shimada (1968) *Earth Planet. Sci. Lett.* 5, 135
 Torii, M., A. Hayashida and Y. Otofujii (1985) *Kagaku* 55, 1, 47-52
 Torii, M. (1983) *Rock Mag. Paleogeophys.* 10, 77-79

(To be submitted to J. Fac. Sci. Hokkaido Univ. Ser. IV)

PALEOMAGNETIC STRATIGRAPHY OF DEEP-SEA SEDIMENTS
IN THE CENTRAL EQUATORIAL PACIFIC

Toshitsugu YAMAZAKI

Geological Survey of Japan, Yatabe, Tsukuba, Ibaraki, 305 Japan

Introduction

Paleomagnetic stratigraphy is one of the strong tools to study paleo-oceanography in the deep-sea. This report presents results of remanent magnetization measurements of deep-sea sediments in the Central Equatorial Pacific and discusses the sedimentation history.

Sediment cores were collected by a piston-corer of 8m long at closely spaced thirteen sites (Table 1) during R/V Hakurei-maru GH81-4 cruise. Topography of the study area consists of deep-sea hills of relative height of about 300m and the surrounding flat basin of about 5600m in depth. Samples are composed of mainly siliceous clay or siliceous ooze, partly pelagic clay, but no calcareous sediment was found because the water depth of this area is below the CCD (Carbonate Compensation Depth) presented at 5000m in depth (Berger and Winterer, 1974). It is known that siliceous sediments have stable remanent magnetization (Opdyke et al., 1966; Opdyke and Foster, 1970) and are suitable for study of paleomagnetic stratigraphy.

Measurements

A series of specimens for paleomagnetic measurements₃ were taken on board from split cores with small cubic cases of about 7 cm³ each. Specimens were carefully sealed for the prevention of the decay of DRM (Depositional Remanent Magnetization) due to the effect of drying (Otofuji et al., 1982). Soon after the cruise (one or two months after the sampling) measurements were carried out using an SCT's Cryogenic Rock Magnetometer. As a general rule every third specimen (about 7 cm interval) was measured, but the specimens which lay near the polarity boundary or in the weakly and/or unstably magnetized portion were continuously measured. Alternating Field (AF) demagnetization by a three-axis tumbler system was carried out

Table 1. Location of the sediment cores studied area.

Core No.	Latitude (N)	Longitude (W)	Depth (m)
P218	3°19.86'	169°35.06'	5473
P219	3°10.57'	169°44.69'	5578
P220	3°15.30'	169°40.79'	5371
P221	3°07.54'	169°27.57'	5538
P222	2°57.39'	169°38.05'	5584
P223	3°02.32'	169°31.94'	5309
P224	3°16.64'	169°41.07'	5500
P225	3°13.32'	169°41.65'	5427
P226	2°53.08'	169°34.86'	5547
P227	2°49.81'	169°38.42'	5355
P228	2°49.29'	169°41.20'	5568
P229	2°46.16'	169°40.25'	5646
P230	3°13.38'	169°35.66'	5600

P227

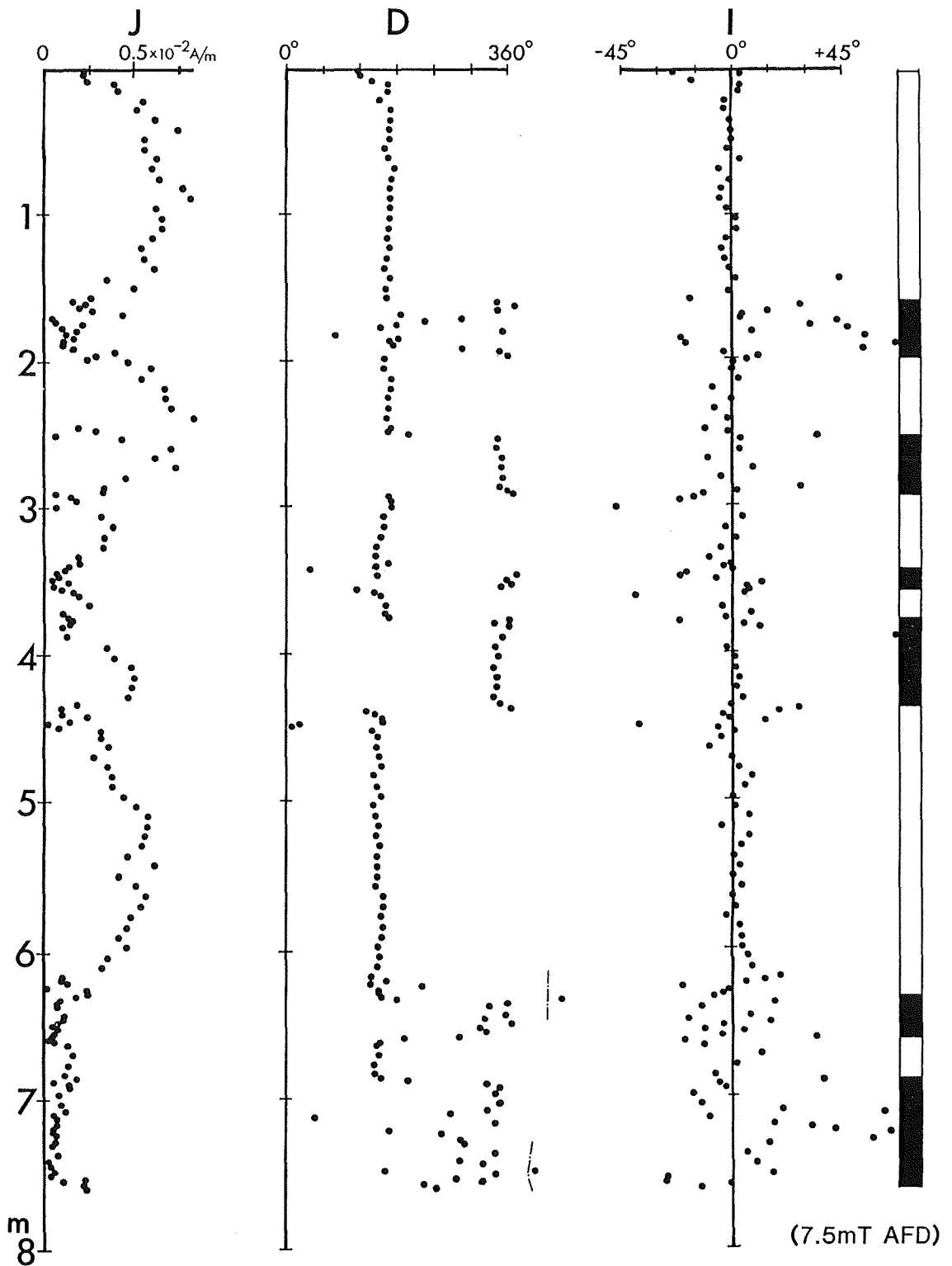


Fig. 1. Intensity (J), relative declination (D) and inclination (I) of remanent magnetization of Core P227. Right column shows the polarity of the magnetization (Solid bar represents normally magnetized part, open does reversed). Values after the magnetic cleaning by alternating field demagnetization are presented but the core had little unstable remanence. The age of the top of the core is about 3.5 Ma (See text).

to erase unstable secondary magnetization. To determine the peak field of routine AF demagnetization which should remove the secondary magnetization most effectively, the coercivity of the remanence of several pilot specimens per each core was examined by stepwise AF demagnetization. As a result, a field of 7.5 or 10 mT was adopted. Except for a few cores, the sediments were slightly overprinted by the secondary magnetization.

Direction, intensity and the polarity of remanent magnetization of a typical core, P227, are presented in Fig. 1. Paleomagnetic polarity sequences, lithology and some horizons of microfossils are summarized in Fig. 2. Descriptions of core lithology and microfossils are given in Nishimura (1986). The geomagnetic polarity time scale of Berggren et al. (1985) is adopted in the following discussion.

Age assignments

Cores P221, P222, P226, P228, P229 and P230, all from the flat basin show the polarity sequences which are in good correlation with the standard one of the Brunhes and the Matuyama Epoch. It is, therefore, inferred that these cores have had continuous sedimentation. The second normally magnetized part from the top, which is included in the Mesocena quadrangula Zone (ca. 1.3 to 0.79 Ma, Berggren et al., 1980), can be certainly correlated to the Jaramillo Event (0.91 to 0.98 Ma).

The cores from the deep-sea hills, on the other hand, have hiatuses of various durations.

Cores P218, P219, P220, P223 and P227 have no, or very thin if any, Quaternary sediments. A hiatus since the Pliocene or the late Miocene can be recognized around the top of these cores. Except for P220 the top horizon of the Spongaster pentas (latest Gilbert Epoch, Theyer et al., 1978) exists in these cores. This horizon gave a good control point to identify the Gauss and/or the Gilbert Epoch.

Cores P218 and P219 indicate the late Gilbert Epoch (4.0 Ma and 4.3 Ma respectively) at their bottoms, and about the boundary between the Gauss Epoch and the Matuyama Epoch (about 2.4 Ma and 2.7 Ma respectively) at their tops. For Core P227 existence of a hiatus between 7.30m and 7.66m is estimated from radiolarian biostratigraphy. Above the hiatus its reversal sequence corresponds well to the standard from 5.8 Ma to 3.5 Ma (Fig. 1), while below it the correspondence to the standard is unclear.

The age of Core P220 would range from 14.6 Ma to 8.7 Ma inferred from an estimated radiolarian age (10.5 to 11.2 Ma at 2.98m and 11.1 to 15.5 Ma at 7.66m) and the resemblance of its magnetic reversal pattern to the standard. At the depth of about 3.5m presence of an insignificant hiatus is supposed from that the fitness to the standard polarity time scale is not good there (Fig. 3).

For Core P223 the correspondence of its polarity sequence to the standard is quite vague. A hiatus is estimated at 4.2m (polarity boundary) from radiolarian ages and a drop in the intensity of the remanence. The reversal pattern above the hiatus would be that of the Gilbert Epoch. Below it the standard polarity sequence from 10 to 12 Ma may be fitted, which is inferred from the same radiolarian age (10.5 to 11.2 Ma, from 4.40m to 7.25m) as that of Core P220.

Cores P224 and P225 have the Quaternary sediments of a few meters thick which are underlain by the early Miocene sediments. From radiolarians, the uppermost normally magnetized part can be identified to the Brunhes Epoch, and the ages of the bottom of the cores, 7.49m (P224) and 7.20m (P225), are estimated to be the early Miocene (20.7 to 23.2 Ma). Existence of hiatuses is expected at 1.85m (P224) and 2.70m (P225) from a visually remarkable change in lithology and a drop (about an order of

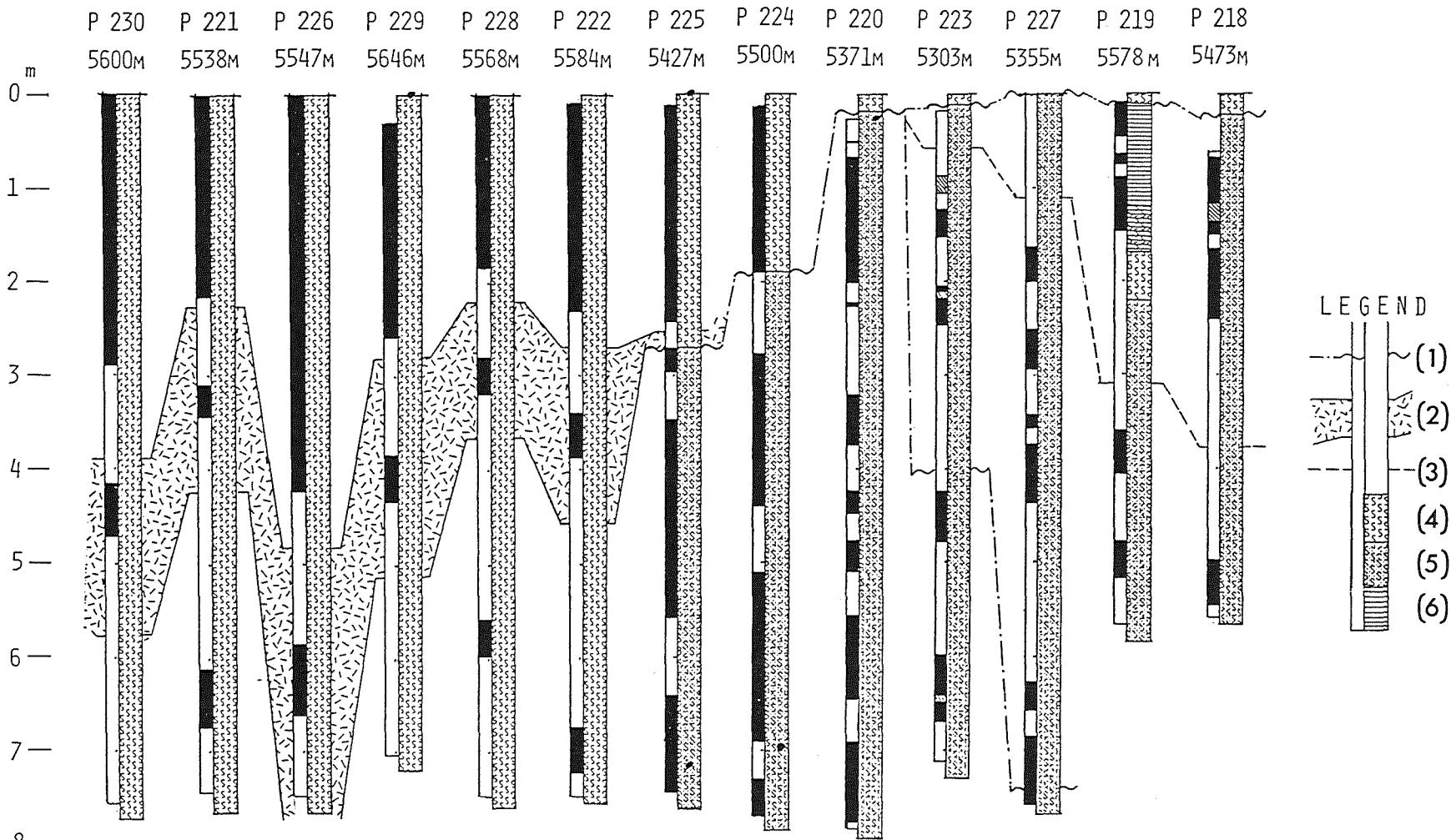


Fig. 2. Paleomagnetic stratigraphy, lithology and some horizons of microfossils (Nishimura, 1986) of all cores are summarized. (1) Hiatus, (2) *Mesocena quadrangula* Zone (ca. 1.3 to 0.79 Ma, Berggren et al., 1980), (3) Top horizon of *Spongaster pentas* (latest Gilbert Epoch, Theyer et al., 1978), (4) Siliceous clay, (5) Siliceous ooze, (6) Pelagic clay.

magnitude) of the intensity of the remanence at these horizons. The polarity sequence below the hiatus may indicate the age from 18 Ma (P224) or 19 Ma (P225) to 21 Ma, but other possibilities (from 21 Ma to 22 Ma, for example) can not be excluded.

The age of the youngest sediments below hiatuses (considering all hiatuses but the older ones in P223 and P227) is about 2.5 Ma (P218), and that of the oldest sediments above them is about 0.8 Ma (P225). It can be estimated, therefore, that the formation of a hiatus was intensified in the period from the latest Pliocene to the early Pleistocene. Presence of the hiatus at this period has been reported for some other cores from the Central Equatorial Pacific (Kobayashi et al., 1971; Opdyke et al., 1974; Theyer and Hammond, 1974; Joshima, 1982). The intensified currents of the AABW (Antarctic Bottom Water) is thought to be most responsible for the formation of the hiatus (van Andel et al., 1975).

Sedimentation rates

Fig. 3 shows the time versus depth for the thirteen cores. Variation of the sedimentation rate from the early Miocene to the Quaternary can be read from the figure.

The sedimentation rate in the Quaternary was 3 to 6 m/m.y. (the average of each core). The rate is relatively high for pelagic sediments below the CCD because the sampling sites have been beneath the zone of high productivity near the equator. Around the Jaramillo Event the sedimentation rate was at the peak, 5 to 10 m/m.y.. Subsequently the rate somewhat reduced. There is, however, a possibility that the sedimentation rates in the Brunhes Epoch is underestimated because the very surface sediments were sometimes missed during the sampling. But the thickness of the missed surface sediments would not exceed several tens of centimeters as usual, so it can be safely said that in the Brunhes Epoch the sedimentation slowed down.

The early Miocene and the early Pliocene are marked by relatively high sedimentation rate, 3 m/m.y. or more. The middle to late Miocene and the late Pliocene are, on the other hand, the periods of low rate (less than 2 m/m.y.). The paleolatitude of the study area at 20 Ma deduced from the absolute motion models of the Pacific Plate (e.g. van Andel et al., 1975) was about 3°S. The area, therefore, has been in the biologically productive equatorial belt since the early Miocene. The variation of the sedimentation rate would reflect both the rise and fall of the intensity of the bottom current (AABW) and the change of the biological productivity with time.

Conclusion

Paleomagnetic study of closely spaced thirteen cores from the Central Equatorial Pacific revealed the sedimentation history from the early Miocene.

(1) Hiatuses are expected in the cores from the deep-sea hills. Their durations are (a) from the early Miocene (about 20 Ma) to the Pleistocene (about 0.8 Ma) : P224, P225, (b) from the Pliocene or the late Miocene to almost the Recent : P218, P219 (from about 2.5 Ma); P223, P227 (3.5 Ma); P220 (8.5 Ma). The formation of a hiatus would be intensified in the period from the latest Pliocene to the early Pleistocene.

(2) The cores taken from the deep-sea basin (Cores P221, P222, P226, P228, P229 and P230) show continuous sedimentation during the Quaternary.

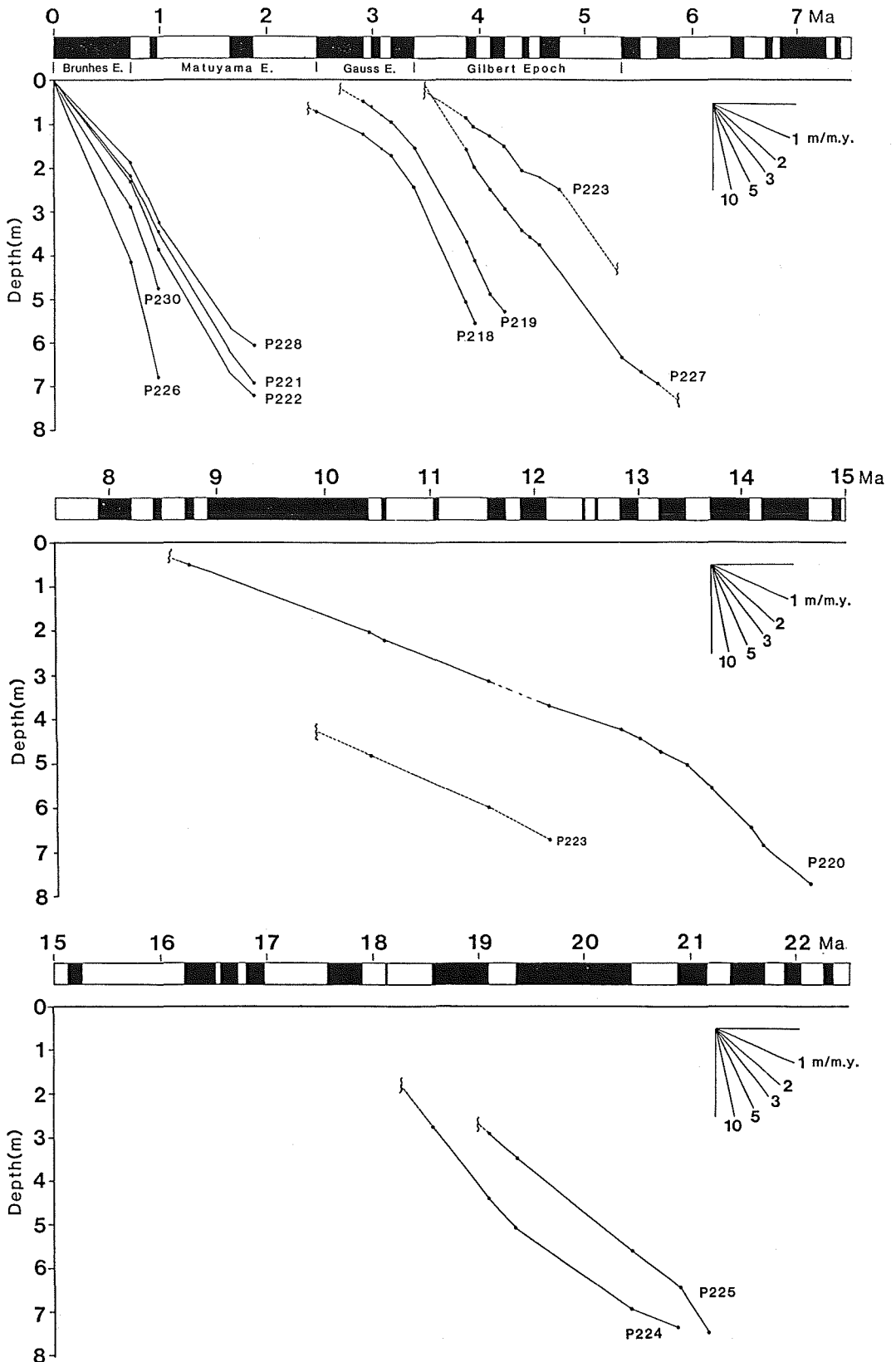


Fig. 3. Plots of the time versus depth for thirteen cores. The time scale of Berggren et al. (1985) is adopted.

(3) The sedimentation rate was 3 m/m.y. or more in the early Miocene, the early Pliocene and the Quaternary. It was less than 2 m/m.y. in the middle to late Miocene and the late Pliocene.

(4) The sedimentation rate in the Quaternary maximized around the Jaramillo Event (5 to 10 m/m.y.) and decreased in the Brunhes Epoch (3 to 6 m/m.y.).

References

- Berger, W. H. and E. L. Winterer (1974) Intern. Assoc. Sedimentologists Spec. Pub., 1, 11.
- Berggren, W. A., L. H. Burckle, M. B. Cita, H. B. S Cooke, B.M. Funnell, S. Gartner, J. D. Hays, J. P. Kennett, N. D. Opdyke, L. Pastouret, N. J. Shackleton, and Y. Takayanagi (1980) Quaternary Res., 13, 277.
- Berggren, W. A., D. V. Kent, J. J. Flynn, and J. A. Van Couvering (1985) Geol. Soc. Am. Bull., 96, 1407.
- Joshima, M. (1982) Geol. Surv. Japan Cruise Rept., 18, 276.
- Kobayashi, K., K. Kitazawa, T. Kanaya, and T. Sakai (1971) Deep-Sea Res., 18, 1045.
- Nishimura, A. (1986) Geol. Surv. Japan Cruise Rept., 21 (in press).
- Opdyke, N. D. and J. H. Foster (1970) Mem. Geol. Soc. Am., 126, 83.
- Opdyke, N. D., L. H. Burckle, and A. Todd (1974) Earth Planet. Sci. Lett., 22, 300.
- Opdyke, N. D., B. Glass, J.D. Hays, and J. Foster (1966) Science, 154, 349.
- Otofujii, Y., I. Katsura, and S. Sasajima (1982) Geophys. J. R. astr. Soc., 70, 191.
- Theyer, F. and S.R. Hammond (1974) Earth Planet. Sci. Lett., 22, 307.
- Theyer, F., C.Y. Mato, and S.R. Hammond (1978) Marine Micropaleontol., 3, 377.
- Van Andel, T. H., G. R. Heath, and T. C. Moore, Jr. (1975) Mem. Geol. Soc. Am., 143, 1.

(In press in Geol. Surv. Japan Cruise Rept. in detailed form)

LATE CRETACEOUS PALEOMAGNETIC POLE FROM THE KOTO RHYOLITE, SOUTHWEST JAPAN

Kouji FUKUMA and Masayuki TORII

Department of Geology and Mineralogy, Kyoto University,
Kyoto 606, Japan

The late Mesozoic felsic igneous rocks are widely distributed in Southwest Japan. These igneous rocks overlap onto or intrude into the accretionary terranes that make up much of the geologic backbone of Southwest Japan. Paleomagnetism of these rocks would give an important constraint for the original position of Southwest Japan. The Koto Rhyolite is located in the eastern part of Southwest Japan (Fig. 1). The distribution of these felsic rocks can be divided into the two areal subdivisions; the main body is distributed on the western foot of the Suzuka Mountains, and the other small bodies are distributed as isolated hills on the eastern coastal area of Lake Biwa. In the main body, the stratigraphic succession of the volcanic and intrusive rocks is divided into two units (Nishikawa et al., 1983). The lower unit consists of rhyolitic welded tuff and quartz porphyry, and the upper unit consists of pyroclastics and granite porphyry. The age of these rocks was recently determined by the fission track dating method and estimated to be about 70 Ma (Ito, 1986). Rb-Sr method provides the whole rock isochron age of the samples from the upper pyroclastics as 75.8 ± 2.4 Ma (Seki, 1978). Paleomagnetic study was done on the welded tuffs and related intrusive rocks from the main body of the Koto Rhyolite.

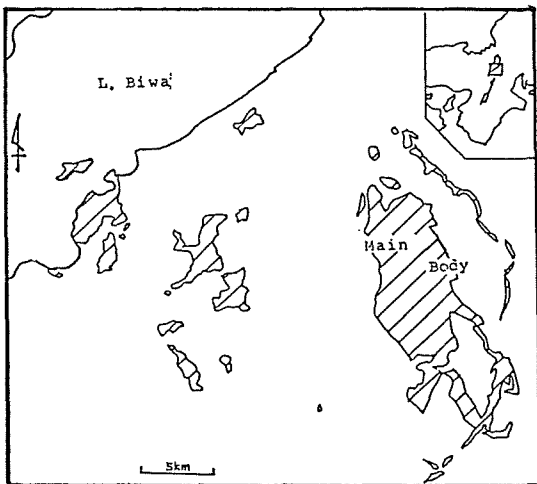


Fig. 1 Distribution of the Koto Rhyolite

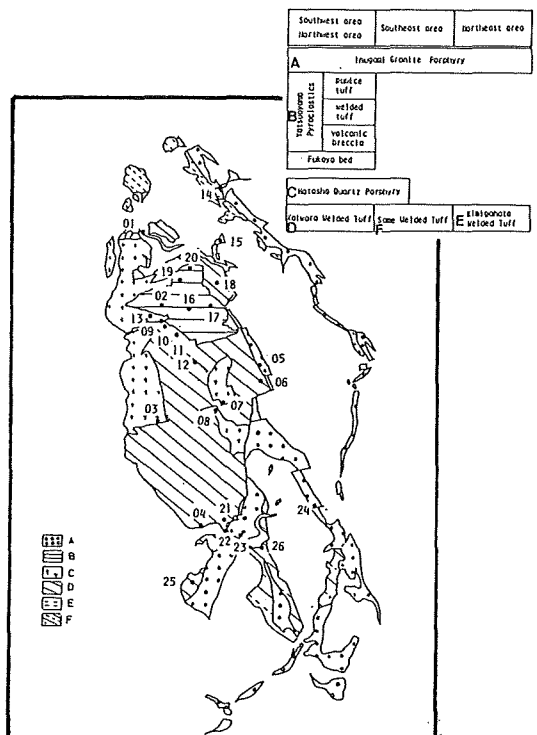


Fig. 2 Sampling sites for paleomagnetic study: base map is simplified from the geological map after Nishikawa et al. (1983).

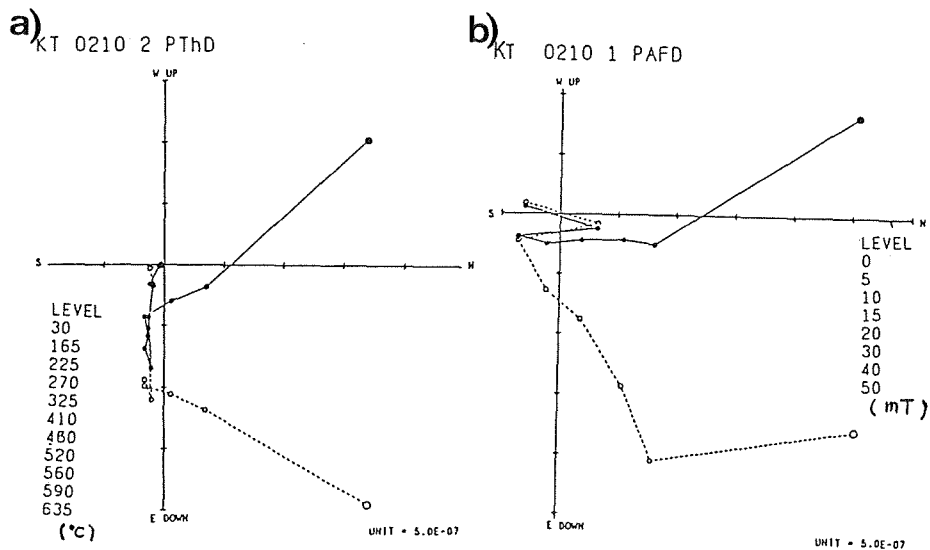


Fig. 3 Orthogonal projections of vector end points for the two specimens cut from one hand sample: a) progressive thermal demagnetization, b) progressive alternating field demagnetization. The open and solid symbols represent projections onto the vertical and horizontal plane, respectively.

We collected oriented samples at 26 sites in the whole area of the main body (Fig. 2). Natural remanent magnetizations were measured using the ScT cryogenic magnetometer. Intensity of remanence ranged from 10^{-2} A/m to 10^{-5} A/m. Progressive alternating field (AF) demagnetization was performed for one specimen per site. Progressive thermal demagnetization was carried out for three specimens cut from three independently oriented samples from each site. Behaviors of the remanence during stepwise demagnetization were examined on the orthogonal projections in order to recognize the discrete magnetic components. The characteristic remanent magnetization (ChRM), which is constantly reduced to the origin on the projection, could be visually detected from the thermal demagnetization data at 18 sites. The thermal treatment was found to be more effective than the AF demagnetization to isolate the ChRMs (Fig. 3).

At two sites (site 21, site 25), the granite porphyry intruded into the host rock of welded tuff to make baked contact zone. We could find the three components of remanent magnetization which are only revealed by the thermal demagnetization (Fig. 4a, 4b). Low blocking temperature component (below 300°C) is assumed to be a viscous remanence acquired in the present geomagnetic field. To determine the directions of other two components, the principal component analysis (Kirschvink, 1980) was adopted for the progressive thermal demagnetization data. The magnetic component, which disappear between 300°C and 550°C , are approximately antiparallel to the component of the highest blocking temperature (550°C to 580°C ; ChRM) for both sites. Further, the component of 300°C to 550°C has the same direction as those of the intrusive rock (site 23) and the severely baked host rock (site 22) near the boundary (Fig. 4c). It is evident that intrusion of the granite porphyry made thermal effect to the original magnetization of host rock; the secondary magnetizations of viscous-partial-TRM or TRM acquired in opposite sense, and the original magnetization was covered by the secondary magnetization as a function of the distance from the contact.

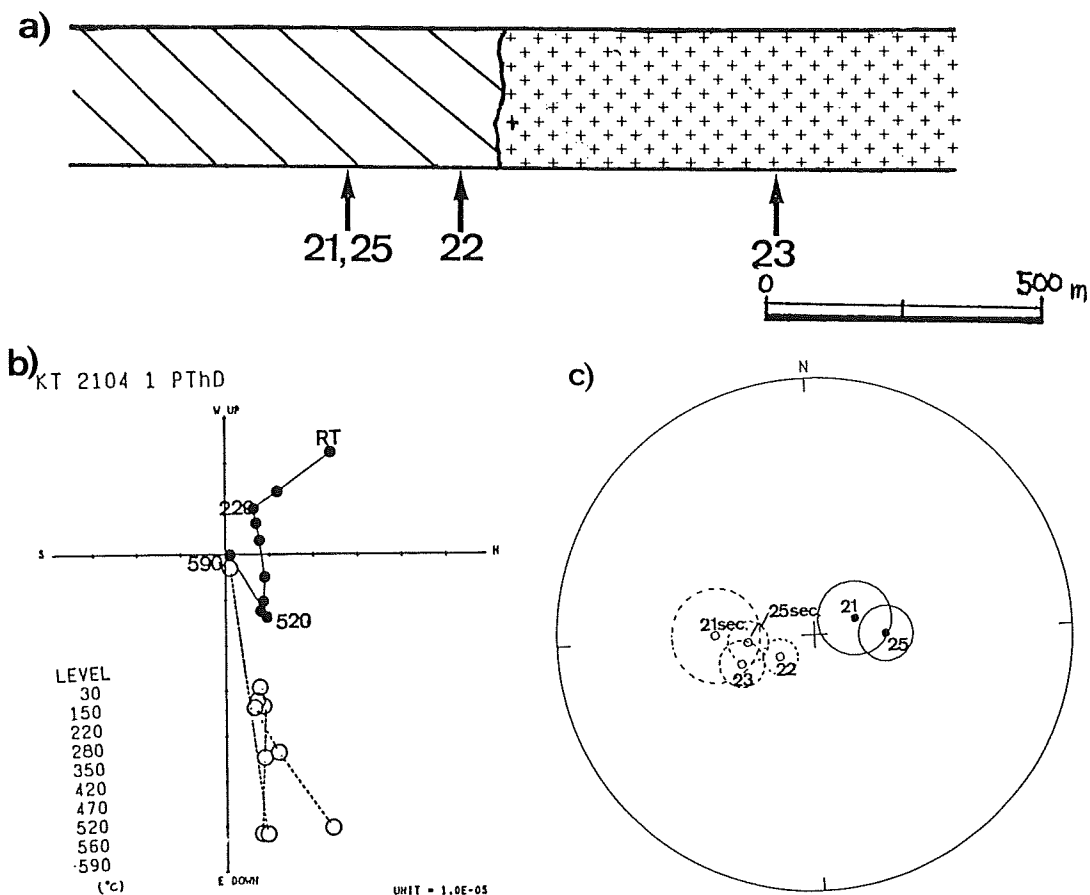


Fig. 4 Schematic view of the baked contact zone and the magnetizations around this zone. a) Schematic view of the contact zone. left: the lower welded tuff. right: the upper intrusive rock. Numerals represent the site numbers. b) Typical example of three-component magnetization. c) Directions of the magnetizations. 21, 22, 23 and 25 denote the characteristic magnetizations of site 21, site 22, site 23 and site 23, respectively. 21sec and 25sec mean the secondary magnetization of site 21 and site 25.

Characteristic remanences were ascertained through the thermal demagnetization from 18 sites. These site-mean directions are fairly well clustered (Fig. 5). Except for the one above mentioned site (site 22) of the baked contact zone, the samples from the lower units are consistently normally magnetized. Whereas antipodal reversely polarized ChRMs were found in the upper intrusive rock. These facts suggest that the ChRMs are of primary origin. The unweighted mean direction (Dec=77.9°, Inc=61.1°, α_{95} =6.5°) could be the late Cretaceous geomagnetic field direction observed at the studied area.

The paleomagnetic pole position (168.4°N, 31.4°W, α_{95} =8.5°) is obtained by averaging virtual pole positions of each site, and compared with those of the contemporaneous poles from the other regions of Southwest Japan. From Yamaguchi and Go river areas in the central part of Southwest Japan, an apparent polar wander path has been proposed for the period between 112 Ma and 14 Ma from the felsic igneous rocks (Otofujii and

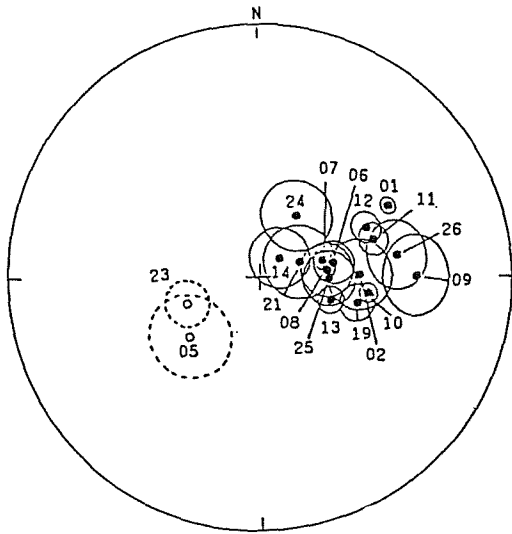


Fig. 5 Equal-area projection of site-mean directions and 95% confidence ovals of characteristic magnetizations. Numerals denote the site numbers.

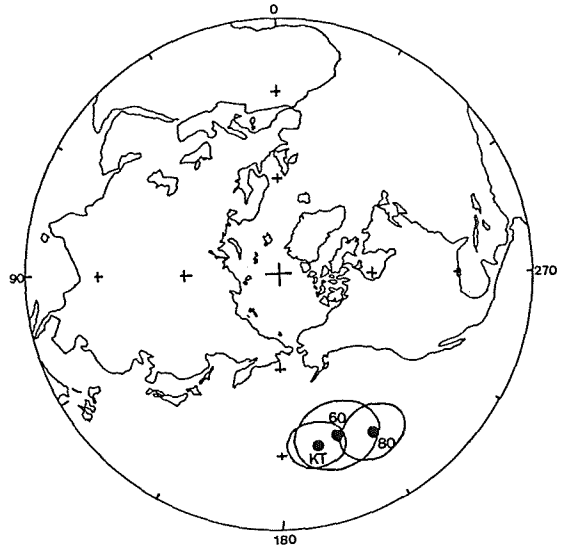


Fig. 6 Comparison of pole positions from the Koto Rhyolite (KT) and the Yamaguchi and Go river area. 80 and 60 denote 80Ma and 60Ma pole positions (Otofujii and Matsuda, 1986), respectively.

Matsuda, 1986). Our 70 Ma pole position lies between 80 Ma and 60 Ma pole positions and overlapping onto them with the confidence limit circles of 95% (Fig. 6). This fact implies that since late Cretaceous Koto area has not suffered any significant relative motion with respect to the central part of Southwest Japan. The zonal arrangement of pre-Neogene rocks of Southwest Japan gives a strong support to this implication. Otofujii and Matsuda (1986) indicate that the declination values of their studied area had kept approximately constant with respect to the expected paleomeridian of the Eurasia between 100 Ma to 20 Ma. They suggest the single phase rotation of Southwest Japan at sometime between 20 Ma and 10 Ma. While as well evidenced by the recent paleomagnetic investigations of the Neogene rocks, Southwest Japan rapidly rotated clockwise as a coherent block at 15 Ma, as the result of the opening of the Japan Sea (Otofujii et al., 1985). It is, therefore, concluded that the anomalous paleomagnetic pole of late Cretaceous from the main body of the Koto Rhyolite is largely attributed to the rotation of Southwest Japan in middle Miocene time. Further, it is confirmed that the regional extension of Southwest Japan is, at least, bounded by the Yamaguchi and Go river area on the west and by the Koto Rhyolite on the east. This land block has been composed of a rigid microplate and originated from the eastern margin of the Eurasia Continent since late Cretaceous time.

References:

- Ito, H. (1986) in this issue.
 Kirschvink, J.L. (1980) *Geophys. J. R. astr. Soc.* **62**, 699.
 Nishikawa, K., T. Nishibori, T. Kohayakawa, T. Tajima, M. Joshima, K. Mimura and M. Katada (1983) *J. Jap. Assoc. Min. Petr. Eoc. Geol.*, **77**, 51.
 Otofujii, Y., A. Hayashida and M. Torii (1985) in 'Formation of Active Ocean Margins', edited by N. Nasu et al., TERRAPUB., 551.
 Otofujii, Y. and T. Matsuda (1986) submitted to *Earth Planet. Sci. Lett.*
 Seki, T. (1978) *Mem. Fac. Sci., Kyoto Univ., Ser. Geol. Mineral.*, vol. XLV, 71.

SHORT DURATION OF MAGMATIC ACTIVITY OF THE LATE CRETACEOUS KOTO
RHYOLITE: NEW EVIDENCE FROM FISSION TRACK AGE DATING

Hisatoshi ITO and Susumu NISHIMURA

Department of Geology and Mineralogy, Kyoto University,
Kyoto 606, Japan

The Koto Rhyolite is widely distributed on the eastern area of Shiga Prefecture in Southwest Japan. The Koto Rhyolite has been recognized as one of thick piles of igneous rocks among the regional felsic magmatism in the Cretaceous period which forms backbone of Southwest Japan. Radiometric age determination has been carried out by Seki (1978) using Rb-Sr method as a part of his study on the geochronology and petrogenesis of felsic Cretaceous igneous rocks in Southwest Japan. In Seki (1978), 78.5 ± 2.4 Ma was reported as the isochron age of the Koto Rhyolite. He also mentioned about relatively older age of 121 ± 35 Ma with a large error.

It is important to determine timing and duration of this widespread felsic igneous activity occurred in Southwest Japan so as to clarify the tectonic event in Japanese arc in Cretaceous period. The Koto Rhyolite is situated in the middle of the locality of this igneous rock in Southwest Japan.

The distribution of the Koto Rhyolite is recognized in two different geographic feature. The main distribution of the Koto Rhyolite is observed on the western foot of the Suzuka Mountains. The relatively small volume of the isolated rock bodies is sporadically distributed in the eastern coastal plain of Lake Biwa. The former will be called 'the main body' and the latter 'the small bodies', hereafter. The stratigraphic relationship between these two rock units has not been well-defined. In the main body, discontinuity of the igneous activity has been recognized as the presence of thin lacustrine sediment inbetween the volcanic sequence (Mimura, 1976). No quantitative estimation of time duration of the discontinuity has been reported so far.

In order to clarify the time and duration of the igneous activity in this region, the FTD studies were made on eight samples (KT01~KT08) collected from the main body and two samples (KT09,KT10) from the small bodies. The sample locality map is shown in Fig.1.

Method

Zircon crystals were separated from 5 to 10 kg rock samples by using the procedure described by Tagami et al. (1987). External detector method (EDM) was applied to both the polished internal surface (ED1) and the natural surface (ED2) of

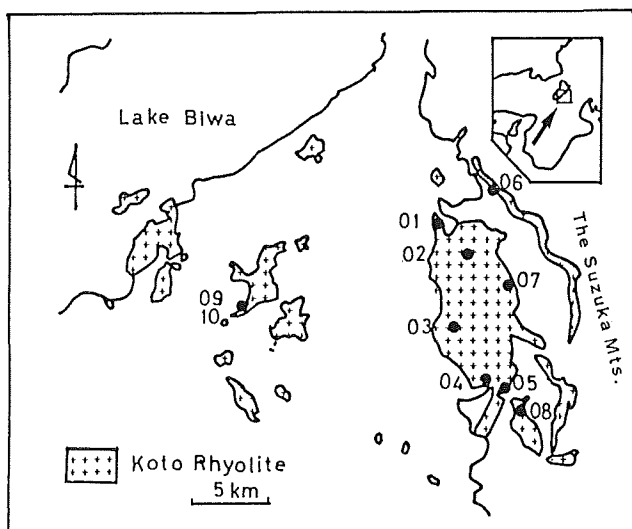


Fig. 1 Sampling sites (•) in the Koto district.

zircon crystals. Zircon crystals were etched in NaOH:KOH (1:1) for 25 to 30 hours at 252°C. Muscovite detectors were etched in 48% HF for 5 minutes at 33°C.

Ages were calculated by Zeta calibration method which was proposed by Hurford and Green (1982). For the age standard, zircon crystals separated from the Fish Canyon Tuff ($T_{STD}=27.9$ Ma; I.U.G.S. standard) in the San Juan Mountains of southern Colorado (U.S.A.) were used.

Equations are as follows:

$$T = Z \left(\frac{\rho_s}{\rho_i} \right)_{UNK} g \quad (1)$$

$$Z = \frac{T_{STD}}{\left(\frac{\rho_s}{\rho_i} \right)_{STD} g} \quad (2)$$

where, Z: Z value presented by Hurford and Green (1983),
 ρ_s : spontaneous track density (cm^{-2}),
 ρ_i : induced track density (cm^{-2}),
g: geometry factor (0.5: ED1, 1.0: ED2),
and Subscript UNK indicates the unknown age sample
and subscript STD the age standard sample.

In order to ascertain the validity of this study, ζ values were also calculated as follows.

$$\zeta = \frac{T_{STD}}{\left(\frac{\rho_s}{\rho_i} \right)_{STD} g \rho_d} \quad (3)$$

where, ζ : ζ value presented by Hurford and Green (1982),
and ρ_d : induced track density on standard glass (cm^{-2}),

ζ values obtained in this study are listed in Table 1 with those values obtained by Hurford and Green (1983) for the comparison. Table 1 shows that the values in this study are in fairly good agreement with those by Hurford and Green (1983).

Standard glass	ED1	ED2	Hurford and Green (1983)
962a	377.7±7.4	339.4±6.7	
612	368.3±6.7	350.9±6.4	339±5
CN-1	123.3±2.1	116.2±1.9	113.0±2.6
CN-2	128.5±2.3	125.2±2.2	121.0±3.6

Table 1 ζ values determined using the standard glasses. These ζ values (ED1,ED2) are calculated according to equation (3). Errors show 1σ . ζ values in the last column have been determined by Hurford and Green (1983) using ED1 method.

Results and discussion

The results are listed in Table 2. The age data obtained by ED1 and ED2 method are also shown in Fig. 2. In this figure, the agreement of the age data by ED1 and ED2 method can be examined; KT04, KT07, KT08, and KT09 give a concordant age by ED1 and ED2 method within 1σ error. Weighted mean ages of both ED1 and ED2 are shown in Fig. 3 according to stratigraphic order by Nishikawa et al (1983). Weighted mean ages of KT04, KT07, KT08, and KT09 are 70.7 ± 6.6 , 70.2 ± 6.4 , 63.3 ± 6.2 , and 70.9 ± 6.0 Ma, respectively. The other data do not show a good concordance between the results of ED1 and ED2, but almost the same age was obtained. These facts show that the igneous activity of the Koto Rhyolite took place around 70 Ma within relatively short age duration, which agrees well with the Rb-Sr isochron age of 75.8 ± 4.8 Ma reported by Seki (1978). However, we could not find any evidence for older age data reported by Seki (1978). Conclusively, the igneous activity of the Koto Rhyolite occurred around 70 Ma in both the main body area and the small bodies area. Further the present data indicate that the age discontinuity in igneous activity between the lower and upper units of the main body was probably very short.

Table 2 Fission track analytical data for the Koto Rhyolite and Fish Canyon tuff : $Z=32.8$ for ED1 and $Z=34.0$ for ED2 are calculated using Fish Canyon tuff data.

sample	method	N_s	ρ_s ($\times 10^6 \text{ cm}^{-2}$)	N_i	ρ_i ($\times 10^6 \text{ cm}^{-2}$)	T (Ma)	N	r
KT01	ED1	1555	5.26	361	1.17	86.5 ± 5.9	6	0.91
	ED2	(No data)						
KT02	ED1	824	5.62	229	1.49	71.6 ± 5.9	5	0.99
	ED2	(No data)						
KT03	ED1	1425	6.91	414	1.92	67.3 ± 4.5	7	0.22
	ED2	(No data)						
KT04	ED1	1288	6.12	337	1.53	73.8 ± 5.2	6	0.98
	ED2	1152	3.78	617	1.94	68.2 ± 4.3	5	0.99
KT05	ED1	1875	7.41	467	1.77	76.1 ± 4.8	7	0.86
	ED2	806	4.80	322	1.83	90.5 ± 6.9	4	1.00
KT06	ED1	2035	4.51	575	1.22	65.8 ± 3.9	9	0.93
	ED2	932	3.89	402	1.61	81.4 ± 5.8	5	0.99
KT07	ED1	1860	7.62	504	1.98	67.4 ± 4.2	7	0.90
	ED2	1125	3.20	534	1.45	73.3 ± 4.8	9	0.94
KT08	ED1	947	6.82	264	1.82	61.8 ± 5.5	3	0.97
	ED2	1457	4.22	777	2.16	63.9 ± 3.7	8	0.88
KT09	ED1	2312	7.19	588	1.75	69.8 ± 4.1	7	0.96
	ED2	1417	4.23	660	1.89	72.1 ± 4.3	7	0.95
KT10	ED1	901	7.06	298	2.23	52.8 ± 4.0	5	0.81
	ED2	1562	3.67	781	1.76	66.1 ± 3.8	10	0.98
Fish Canyon tuff								
	ED1	5491	6.13	3381	3.61		18	0.90
	ED2	2939	3.23	3749	3.94		18	0.89

Note: N_s , spontaneous track number N_i , induced track number
 N, number of grains r , correlation coefficient
 All minerals are zircon. Errors of age data are 1σ .

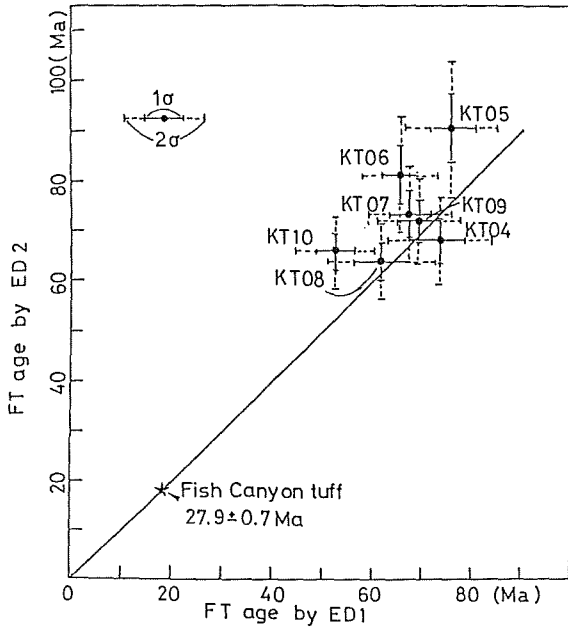


Fig. 2 The relation between ED1 and ED2 age of the Koto Rhyolite. 1σ and 2σ errors are shown using solid and dotted lines, respectively.

THE MAIN BODY		THE SMALL BODIES	
Southwest area		Southeast area	Northeast area
Northwest area			
Inugami Granite Porphyry			
(KT07) 70.2 ± 6.4 Ma		(KT05) 82.0 ± 8.0 Ma	
Yatsuoyama Pyroclastics	pumice tuff welded tuff (KT02) 71.6 ± 11.8 Ma volcanic breccia		
Fukaya bed			
Hatasho Quartz Porphyry (KT03) 67.3 ± 9.0 Ma			
Kaiwara Welded Tuff (KT01) 86.5 ± 11.8 Ma (KT04) 70.7 ± 6.6 Ma	Same Welded Tuff (KT08) 63.3 ± 6.2 Ma	Kimigahata Welded Tuff (KT06) 72.2 ± 6.6 Ma	
		Tuff layer (KT09) 70.9 ± 6.0 Ma	
		Kamewari Welded Tuff	
		Koshigoe Welded Tuff	
		Mt. Ryuseki Formation	
		Azuti Welded Tuff (KT10) 61.2 ± 5.6 Ma	

Fig. 3 The fission track dating results of the Koto Rhyolite in the stratigraphic order. Errors show 2σ .

References

- Hurford, A. J. and P. F. Green (1982) *Earth Planet. Sci. Lett.*, 59, 343-354.
- Hurford, A. J. and P. F. Green (1983) *Isotope Geoscience*, 1, 285-317
- Mimura, K., M. Katada and H. Kanaya (1976) *J. Japan Assoc. Min. Petr. Econ. Geol.*, 71, 327-338 (in Japanese)
- Nishikawa, K., T. Nishibori, T. Kobayakawa, T. Tajima, M. Joshima, K. Mimura and M. Katada (1983) *J. Japan Assoc. Min. Petr. Geol.*, 77, 51-64 (in Japanese)
- Seki T. (1978) *Mem. Fac. Sci., Kyoto Univ.*, 16, 71-110
- Tagami, T., N. Lal, R. B. Sorkhabi, H. Ito and S. Nishimura (1987) *Mem. Fac. Sci., Kyoto Univ.*, (in preparation)

**PALEOMAGNETIC STUDIES OF PALEOZOIC ROCKS FROM THE
ELLSWORTH MOUNTAINS, WEST ANTARCTICA**

Minoru FUNAKI¹ and Masaru YOSHIDA²

- 1) National Institute of Polar Research,
9-10 Kaga 1-chome, Itabashi-ku, Tokyo 174, Japan.
- 2) Department of Geosciences, Faculty of Science, Osaka City University,
3-138 Sugimoto 3-chome, Sumiyoshi-ku, Osaka 558, Japan.

1. Introduction

The Ellsworth Mountains consist of Sentinel Range in the northern part and Heritage Range in the southern part. The mountains are interested geologically in the alignments of the structural trends versus to the Pensacola Mountains of the Transantarctic Mountains; their mutual directions of the trend differ to be perpendicular, although the geological similarities are estimated (i.e. Schopf, 1969).

Paleomagnetic studies were performed for argillites collected from the upper Heritage Group (upper Cambrian Period) of Pipe Peak by Watts and Bramall (1980, 1981). They obtained significant NRM from the highest blocking temperature component (650-670°C) resulting the hematite by thermal demagnetization. The mean NRM direction as 13° inclination and 22° declination were revealed after tilt corrections and thermal demagnetization. This NRM direction and the VGP position (4°N, 269°E) differ approximately 90° counterclockwisely to those of the early Paleozoic of East Antarctic craton. They concluded therefore that the Ellsworth Mts. rotated 90° counterclockwisely versus East Antarctica.

Total of 43 hand samples with orientations from the Heritage Range, which were selected from numbers of rock samples collected for geological investigation, were used for the present study. Although the number of samples is not enough for precise paleomagnetic study, sampling sites covered wide area of the Heritage Range and the obtained paleomagnetic data appear to give some meaningful results. Rock types of these samples are estimated to be Cambrian and Permian sedimentary rocks and Cambrian to Devonian dyke rocks.

2. Experiments

Every sample was AF demagnetized to 50 mT for taking away of soft magnetic components. Based on this demagnetization results, total of 37 samples with stable NRM components are selected for thermal demagnetization and thermomagnetic analyses. The results of thermal demagnetization from 30 to 580°C in steps of 50° suggest that the original steep inclinations of several dyke rocks shift to lower inclination by thermal demagnetization over 400°C, although the declinations after that demagnetization

Table 1. Paleomagnetic results of the Ellsworth Mountains.

No.	Rock type	Tilt correction	N	Inc	Dec	K	α_{95}	pLat	pLon
1	Sedimentary rocks	after	7	-19.2	62.9	10	20.1°	14.3°N	22.2°W
2	Dyke rocks	before	7	-65.9	60.5	23	12.8	52.3°S	116.5°E

show random distribution. The most reliable NRM components against thermal demagnetization are adopted for this study. However, as the samples having clear cracks can not be heated because of break up the samples during thermal demagnetization, NRM after AF demagnetization to 15 mT were adopted for these samples.

Total of 7 sedimentary rock samples have similar NRM direction in low inclination side after tilt collections. Stable NRM from 8 dyke rocks make a cluster in the high inclination side without tilt corrections. The mean NRM directions and the VGP positions obtained from these samples are listed in Table 1. However many other samples show random NRM distributions even if any kind of treatments were attempt.

Thermomagnetic curves were obtained from room temperature to 750°C under 0.6T external magnetic field and 10^{-4} torr atmospheric pressure. The obtained curves were classified to 4 types based on reversibility of 1st run cycle; type 1 is a reversible thermomagnetic curve with clearly defined Curie point 580°C; type 2 is an almost reversible one with Curie point 580°C for main magnetic mineral associated with small amount of thermomagnetic humps at 180 to 350°C; type 3 is an irreversible one with small hump around 400°C characterized by increasing spontaneous magnetization after heat treatment and clearly defined Curie point 580°C; type 4 is a reversible one with weak spontaneous magnetization and with not well defined Curie points between 300 and 580°C; type 5 is extremely irreversible one characterized by Curie points 580 and 675°C and thermomagnetic hump at 400°C in heating curves.

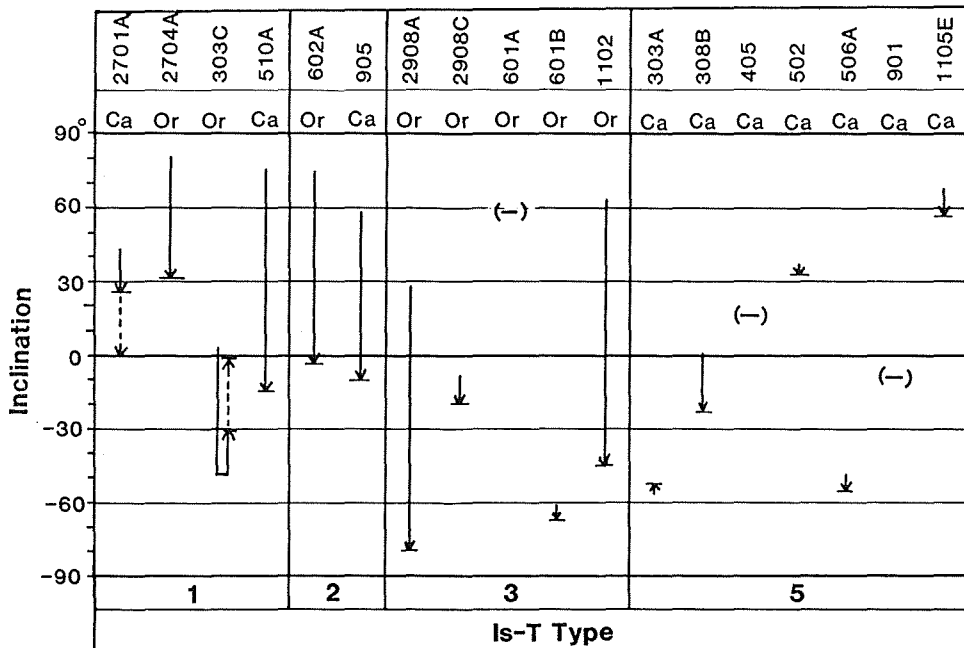


Fig. 1 NRM inclination variations against thermal demagnetization to 580°C and AF demagnetization for dyke rocks from the Ellsworth Mts. (-): inclination level by AF demagnetization. Ca: Cambrian dyke rocks. Or: Ordovician dyke rocks. Nos. 1-5: types of thermomagnetic curve (Is-T).

3. discussion

Magnetic minerals estimated from thermomagnetic analyses are magnetite for the type 1, magnetite and pyrrhotite for the type 2, titanomagnetite and magnetite for the type 4 and hematite for the type 5. The samples including magnetite or titanomagnetite grains associated with small amount of hematite grains show the typical thermomagnetic curves type 3 due to reduction of fine hematite grains by heating more than 400°C under 10^{-4} torr atmospheric pressure. The same explanation is applied to the thermomagnetic hump resulting hematite in the type 5. Thus the type 3 thermomagnetic curves probably show existence of magnetite or titanomagnetite with small amount of hematite. Therefore origin of NRM is supposed to be TRM for types 1, 2 and 4, CRM for the types 5 and TRM with partial CRM for the type 3.

The NRM inclinations from Cambrian to Ordovician dyke rocks having types 1 and 2 change from steep to flat by thermal demagnetization. However the samples of the type 5 show random distribution of inclinations which have small inclination change by that demagnetization as shown in Fig.1. Namely the magnetite grains have recorded at least two kinds of TRM decomposed into steep inclination at low temperature and flat one at high temperature, but hematite grains have recorded variable direction. If the Ellsworth Mts. was fragments of Gondwanaland, acquired NRM tends toward to be flat at the early Paleozoic, medium angle at the middle Paleozoic and steep at the late Paleozoic to the middle Mesozoic Eras (ie. McElhinny, 1973). From the geological evidences, 4 times low grade metamorphisms were estimated; twice at the pre-Devonian or Devonian Periods, once between the Devonian and Permo-Carboniferous Periods and once at the Mesozoic Era (Yoshida, 1982). The metamorphosed temperature of the Ellsworth Mts. did not exceed more than

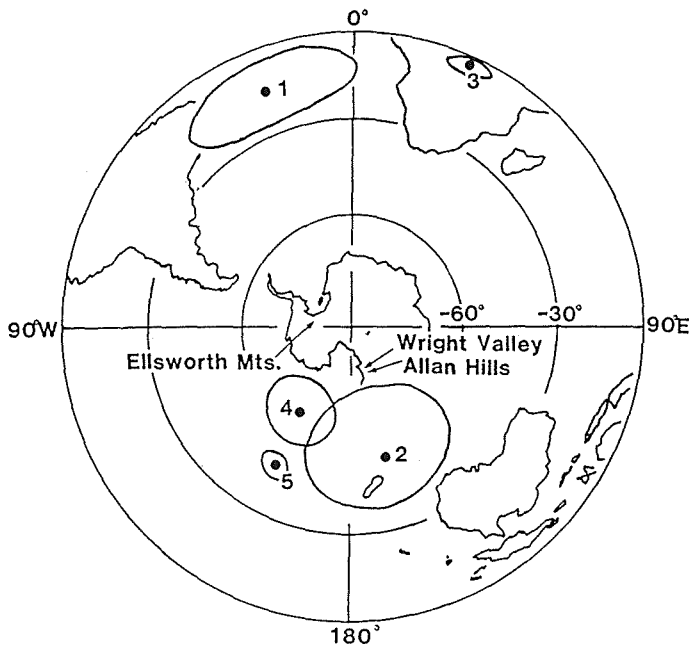


Fig. 2. VGP positions with g_5 values from Ellsworth Mts., Wright Valley and Allan Hills.
1: sedimentary rocks from the Ellsworth Mts. 2: dyke rocks from the Ellsworth Mts. 3: dyke rocks from Wright Valley. 4: Beacon Supergroup from Allan Hills. 5: Ferrar dorelite from Wright Valley

500°C through the 4 times metamorphisms. These inclination variations are understood based on the above results as follows. The flat NRM component was acquired in the Cambrian or Ordovician metamorphisms and the steep one was acquired by final metamorphism occurred from the Permian to Jurassic Periods. On the other hand, distribution of the NRM inclinations having hematite grain show that the Ellsworth Mts. experienced several times metamorphisms characterized by hematite formation in some Periods of the 4 times metamorphisms.

The NRM directions after tilt corrections of 7 sedimentary rock samples cluster with $\alpha_{95} = 20.1^\circ$ around inclination -19.2° and declination 62.9° , although that of other 15 samples scatter widely. The cluster is one of the representative NRM direction resulting DRM when the Heritage group was formed in the Cambrian Era. The calculated VGP position, as shown in Fig. 2, is given 14.3°N , 20.2°W which locates about 45° westward compared with the VGP position 3°S , 24°E (Funaki, 1984) obtained from Cambro-Ordovician dyke rocks of Wright Valley, Southern Victoria Land in the Transantarctic Mountains. The directions of NRM for 7 dyke rock samples cluster and those of other 8 samples scatter after thermal demagnetization without tilt corrections. The VGP position 52.3°S , 166.5°E with $\alpha_{95} 12.8^\circ$ (Fig. 2) is obtained from the mean NRM direction (inclination -65.9° , declination 60.5°) of the former 7 dyke rock samples. The VGP positions of Permian Beacon Supergroup (62.3°S , 151.4°S) from Allan Hills in Southern Victoria Land (Funaki, 1983b) and Jurassic Ferrar Dolerite (45.3°S , 152°W) from McMurdo Sound region (Funaki, 1983a) are known. The VGP position of the dyke rocks also locates 43° westward from the Permian and Jurassic VGPs.

These results suggest that the Ellsworth Mts. rotated about 45° counterclockwisely with respect to East Antarctica after remagnetization of Ordovician dike rocks during some periods from the late Paleozoic to Mesozoic Eras. The sense of the rotation is in harmony with the perpendicular counterclockwise rotation model of the Ellsworth Mts. proposed by Watts and Bramall(1981).

References:

- Funaki, M. (1983a), Nankyoku shiryō (Antarct. Rec.), 77, 20-32.
- Funaki, M. (1983b), Nankyoku Shiryo (Antarctic. Rec.), 78, 1-14.
- Funaki, M. (1984), J. Geomag. Geoelectr., 36, 529-563.
- McElhinny, M.W. (1973), Paleomagnetism and plate tectonics. Cambridge, The University Press, p260.
- Schopf, J.M. (1969), Science, 164, 63-66.
- Watts, D.R. and Bramall, A.M. (1980), Antarctic Journal, 15, 34-36.
- Watts, D.R. and Bramall, A.M. (1981), Nature, 293, 638-641.
- Yoshida, M. (1982), Mem. Natl. Inst. Polar Res. Spec. Issue, 21, 120-171.

A PALEOMAGNETIC RECONNAISSANCE OF SOME LATE PRECAMBRIAN TO EARLY
PALEOZOIC ROCKS OF TANSEN AREA, LESSER HIMALAYA, NEPAL

Pitambar GAUTAM

Department of Geology & Mineralogy, Faculty of Science,
Hokkaido University, Sapporo 060, Japan.

Permanent address: Department of Geology, Tribhuvan University,
Kirtipur, Kathmandu, Nepal.

Introduction

Considerable advances have been made in geological understanding of the Nepalese Lesser Himalaya, in recent years. However, the rocks have been remained virtually unstudied paleomagnetically. The paper by Yoshida & Sakai (1984) is probably the only reported case of paleomagnetic studies from the area dealing with the preliminary measurements of magnetic properties of Late Paleozoic to Cenozoic rocks of the Tansen Group in Central Nepal. The present work is a further attempt to to fullfil the gap in paleomagnetic research from the Lesser Himalaya and deals with the magnetic properties of some sedimentary and metasedimentary rocks from the Tansen area. It seems timely to make every effort to make use of the potential possibilities of paleomagnetic techniques in the Nepal Lesser Himalaya to solve the yet unresolved structural and stratigraphic problems.

Geological setting and sampling

The territory of present study is located around the town of Tansen in Central West Nepal. The area belongs to the southern part of the Lesser Himalayan zone lying mainly between the Main Boundary Thrust (MBT) in the south and middle reaches of the Kali Gandaki river in the north. Most of the previous geological works (Frank & Fuchs, 1970; Fuchs & Frank, 1970; Hashimoto et al., 1973; Fuchs, 1980; Mascle, 1980; Sharma, 1980; Arita et al., 1982; Sharma et al., 1984 and others) dealing with the area have been carried out on regional scale with emphasis on lithostratigraphic division and structural zoning. More detailed works (Arita & Yoshida, 1982; Sakai, 1983, 1984, 1985) carried out recently make possible to discuss geology of the area in more detail. The following is a brief geological description of the study area based on these recent works.

Tansen area is divided into two major stratigraphic units: the Tansen Group and the Kali Gandaki Supergroup. The Tansen Group consists mainly of clastic sediments of Late Carboniferous to Early Miocene age. The Kali Gandaki Supergroup underlies the Tansen Group disconformably. This supergroup attains a thick sequence (>10 km in thickness) of non-to weakly-metamorphosed terrigenous and carbonaceous rocks, deposited mainly under arid climates and shore-line environment. Among the reported organic

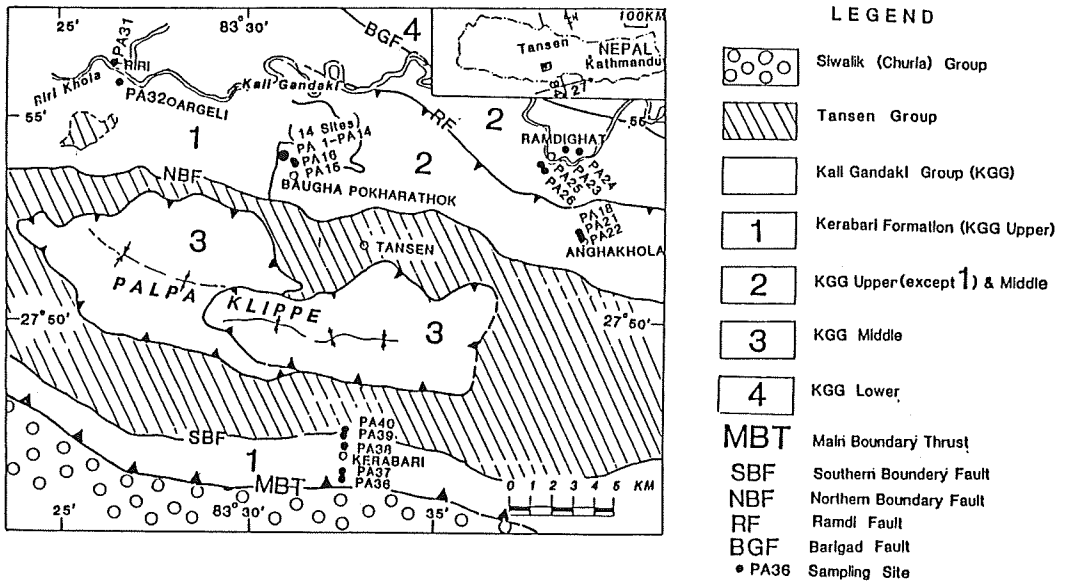


Fig. 1 Geological sketch map (after Sakai, 1983, 1985) of the area studied showing sampling sites.

		FORMATION	DESCRIPTION	THICKNESS m	AGE	SAMPLING SITES
KALIGANDAKI SUPERGROUP	TANSEN GROUP	SISHE	diamictite with sandstone and rhythmite of sandstone & shale	20-1000	Late Carb.- Permian	
	UPPER GROUP	KERABARI	upper: bedded grey dolomitic with shale, sandstone, oolite and chert beds	2150	Early Palaeozoic	PA40 PA39
			middle: bedded grey dolomitic with chert bed & lenses			PA38
			lower: algal limestone with dolomitic pebble conglomerate & bedded dolomitic			PA37 PA32 PA36 PA31
		Riri member: black laminated limestone, limy slate	PA 1, PA25 PA 2, PA26 PA 3, PA 5 PA 4, PA 6 PA 7-PA 9			
		RAHDIGHAT	upper: light brown laminated slate middle: variegated calcareous slate with limestone bands lower: black & green slate	750		PA10-PA13 PA24 PA14, PA23 PA18
	MIDDLE GROUP	SAIDI KHOLA	bioturbated rhythmite of ss & sl	180	PA10-PA13	
		KHORAIDI	dolomitic stromatolite with oolite, quartzite & rhythmite	350	PA18	
		CHAPPANI	quartzite grey clayslate with stromatolite	400	PA15 PA16 PA21 PA22	
		VIRKOT	white pink quartzite and shale with stromatolite	510		
HEKLANO		green light brown phyllitic slate with fine laminae and marl bed	800+	Late Precambrian		
LOWER GR.	NAUDAHA	white quartzite with metabasites	400+			

Fig. 2 Chart showing lithological description of strata (modified after Sakai, 1985) and stratigraphic distribution of sampling sites.

Table 1 Natural remanent magnetization (NRM) directions* of sites

Site	n(N)	D (°)	I (°)	k	a_{95} (°)	Intensity ($\times 10^{-9}$ emu/cc)	Rock type**	Bedding*** (Strike/ Dip)
PA 1	3	356	50	11	24	78	gray calc. sl.	N 8W 31NE(O)
PA 2	3	357	46	63	10	320	gray calc. sl.	N 8W 35NE(O)
PA 3	3(6)	348	20	58	7	3400	purple sl.	N15W 38NE(O)
PA 4(A)	2(3)	313	10	45	14	1100	purple sl.	N15W 18NE(O)
PA 4(B)	1(2)	347	40	-	-	3200	green sl.	N15W 18NE(O)
PA 5(A)	2	316	7	103	9	5600	purple sl.	N14W 20NE(O)
PA 5(B)	1	326	34	-	-	2600	green sl.	N14W 20NE(O)
PA 6	2(3)	334	44	120	7	250	green calc. sl.	N 7W 30NE(O)
PA 7	2	8	46	-	-	160	green sl.	N16E 35SE(O)
PA 8	1	332	37	-	-	37	black sl.	N48E 20SE(O)
PA10	2(3)	0	47	169	6	15000	ss., sl.	ON 20 E(O)
PA11	2(3)	16	53	17	19	870	ss.	N30E 13SE(O)
PA12	2(3)	339	38	40	15	780	silty sl.	N10E 34SE(O)
PA13	1	16	34	-	-	530	ss.	N40E 15SE(O)
PA14	2(4)	357	40	664	2	3600	ss.	N38E 18SE(O)
PA15	2	346	44	-	-	320	phyllitic sl.	N10E 54SE(A)
PA16	3	345	41	47	11	820	phyllitic sl.	N21E 55SE(A)
PA18	2(3)	333	45	107	7	240	ss., qtz.	N85W 18SW(O)
PA22	2	48	36	-	-	220	qtz.	N68E 30SE(O)
PA23	3(4)	11	38	53	9	130	dol., ss.	N20E 20SE(O)
PA24	3	157	84	4	37	440	sl.	N10W 30NE(A)
PA31	2	357	47	-	-	86	black calc. sl.	N60W 35NE(A)
PA32	2	354	52	-	-	98	ls.	N62W 30SW(A)
PA36	2	329	50	-	-	64	gray ls.	N85E 45NW(N)
PA37	2	346	52	-	-	140	ls.	N85E 83SE(O)
PA38	2(3)	349	26	75	9	160	dol., ls.	N83E 50NW(N)
PA39	3(7)	342	48	18	12	200	dol., ls.	N84W 85NE(N)
PA40	2(3)	13	67	5	35	280	calc. ss.	N65W 85NE(N)

* n and N are the number of samples and specimens, respectively; D is the declination of the magnetization direction, measured eastwards from north; I is the inclination of the magnetization direction, downwards positive, upwards negative; a_{95} is the semi-angle of cone of 95% confidence; k is the estimate of the Fisher's precision parameter.
(Directions not corrected for bedding)

** Abbreviations: calc. = calcareous, sl. = slate, ss. = sandstone, qtz. = quartzite, dol. = dolomite, ls. = limestone

***Bedding: (N) = Normal, (O) = Overturned, (A) = Uncertain

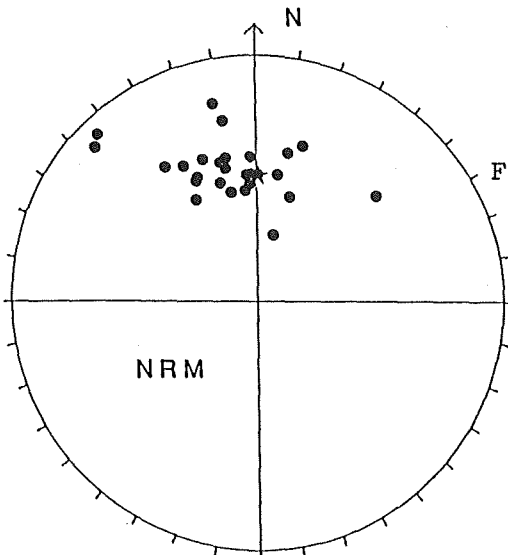


Fig. 3 Schmidt's net projection of mean NRM directions of sites (circles). All directions have positive inclinations. Star - dipole field direction for Tansen. (bedding uncorrected)

remains are stromatolites and some tiny plant remains in carbonaceous or coaliferous beds from some horizons. So, based mainly on lithostratigraphic comparison of these rocks with rock formations in other regions (Nawakot complex in Central Nepal, the Vindhya in the Indian Shield, Kumaon Himalayan rocks etc.) and the fact that these rocks underlie the glacial diamictites of the Sisne Formation, the lowest member of the Tansen Group, assigned Permo-Carboniferous age, the group is given Late Precambrian to Early Paleozoic age. It will be worth noticing that there are uncertainties concerning the upper age limit of the group and are discussed in detail in the papers mentioned above.

Three structural belts are recognized in the area: the Tansen Synclinorium, Angha Khola Recumbent fold belt and Khoraidi fold belt from south to north respectively. The first and second of them are separated by the so-called Northern Boundary Fault (NBF) while the Ramdi Fault separates the second and the third. The Tansen Group embraces the doubly plunging Tansen Synclinorium and is covered in the central part by Palpa klippe. This klippe is believed to be formed due to the overthrusting of the Angha Khola Recumbent Fold Belt upon the synclinorium. In the southern part of Palpa klippe, the Tansen Group forms an imbricate structure.

Oriented block samples were collected from 4 localities (30 sites) using a magnetic compass. The samples belong to the Middle and Upper Groups of the Kali Gandaki Supergroup. Two or three blocks were collected from each site.

A geological sketch map with sampling site locations and lithostratigraphic column with sampling levels is shown in Fig. 1 and Fig. 2. The bedding data from the sampling sites and lithology of the samples is presented in Table 1.

Laboratory measurements

Normally two cylindrical specimens (2.54 cm in diameter, 2.5 cm in length) were drilled from each sample in the laboratory. The remanent magnetization was measured using a Schoenstedt SSM1A spinner magnetometer.

The initial NRM data are presented in Table 1. The mean NRM intensity for sites shows a variation between 1.5×10^{-5} to 3.7×10^{-8} (emu/cc), most of samples having intensity of 10^{-7} order. Except the sandstone from site PA10 the reddish purple slate specimens from the Ramdighat Formation possess highest intensities (10^{-6} emu/cc). An equal-area projection of NRM directions is presented in Fig. 3.

Alternating field (AF) demagnetization studies were carried out on an apparatus, which utilizes a 400 Hz alternating field, without specimen rotation. At least one specimen from each site was demagnetized in increasing peak fields of 100, 200, 300, 400, 500 and 530 Oersteds. In some cases, however specimens could not be subjected to all these steps owing to the rapid decay of intensities reaching to the noise level of the instrument.

A visual analysis to assess the directional stability and coercivity spectrum of each specimen was done using orthogonal

Table 2 Magnetization directions of sites after demagnetization*

Site	AFD (Oe)	THD (°C)	(Bedding not corrected)			//	(Bedding corrected)			
			D (°)	I (°)	k	a_{85} (°)	D (°)	I (°)	k	a_{85} (°)
PA 1	300		354	51	17	19				
PA 2	300		14	51	13	21				
PA4(B)	300		343	44	-	-				
PA 6	200		337	33	90	8				
PA10	200		4	47	216	5				
PA11	200		19	51	-	-				
PA13	100		22	43	-	-				
PA18	200		333	45	107	7				
PA23	200		3	32	72	8				
PA31	200		347	46	-	-				
PA32	200		353	36	-	-				

PA 3	300		346	14	77	9	335	-11		
PA4(A)	300		304	9	10	24	22	-21		
PA5(A)	300		312	7	-	-	16	-18		
Mean(3 sites)			320	10	13	21	4	-18	10	24

PA36	300		313	3	-	-	305	-24		
PA37	300		259	65	-	-	330	-4		
PA38	300		0	6	4	40	2	-44		
PA39	300		336	28	19	12	326	-47		
PA40	300		2	41	66	9	2	-40		
Mean(5 sites)			334	32	4	29	335	-34	9	20
/ PA36-PA40 /										
Mean(3 sites)			352	25	13	21	350	-45	28	15
/ PA38-PA40 /										

* The number of samples and specimens for site is same as in Table 1.
 AFD = Alternating Field demagnetization, Peak field value (Oersted)
 THD = Thermal demagnetization, Temperature (degree Celcius)
 Other conventions, same as in Table 1.

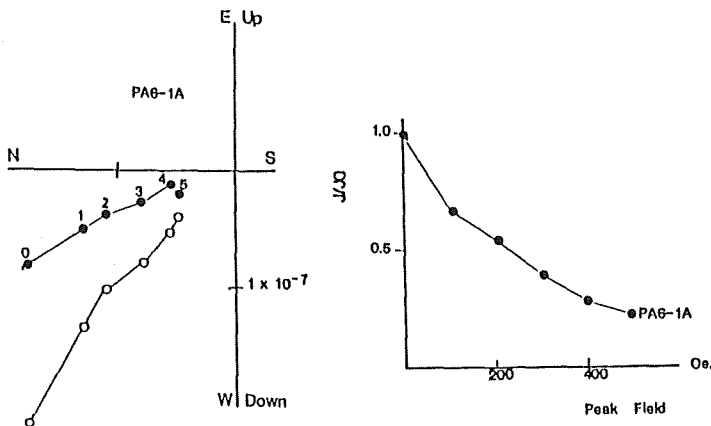


Fig.4 AFD results for a specimen PA6-1A.
 a. Zijderveld plot, showing projections of the end-point of the resultant vector during successive demagnetization in peak fields indicated by numbers 1,2,3,4,5 corresponding to 100, 200, 300, 400 and 500 Oersteds. 0 indicates NRM. Solid (open) circles represent projections on the horizontal (N-S vertical) plane.
 b. Normalized intensity response curve.

component plots (Zijderveld, 1967), normalized intensity decay curves, and Schmidt's equal-area net plots of directional changes for successive demagnetization steps. On the basis of such analysis the following three groups of specimens were distinguished:

First group of specimens which show that relatively soft components become reduced after 200-300 Oersted treatment reaching a relatively stable direction. The normalized intensity curves for these specimens show that about 50% of intensity reduces during AF treatment up to 500 Oersted (e.g., specimens PA 6-1A, Fig. 4).

Second group of specimens shows elimination of unstable soft components around 300 Oersted. At the same time, 60-90% of initial intensity becomes reduced. Further treatment in higher fields leads to the decrease in intensity to the noise level of the instrument (e.g., specimen PA39-2A, Fig. 5)

And, the third group of specimens exhibiting a "hard" component, where less than 10% of the initial intensity becomes reduced during AF treatment up to 550 Oersted without any notable changes in directions (e.g., Purple slate from Ramdighat Formation).

Thermal demagnetization (THD) was carried out on pilot specimens from each formation. Progressive heating of the pilot specimens was done in 6-10 steps up to a maximum temperature of 550(°C) in air. The remanent magnetization was measured after cooling to the room temperature after each successive heating step. The heating-cooling process was carried out in a magnetically field-free space. The same type of analysis applied for AF demagnetization data was made for THD data. It was established that thermal treatment is not applicable to first and second groups of specimens (mentioned above) due to rapid decay of the magnetization intensity to the noise-level of the instrument soon after one or two heating steps. Only third group specimens were found suitable for THD studies because of their relatively higher initial intensities. The orthogonal component plots for the purple slate specimens showed that a relatively stable direction is reached after 300°C (Fig. 6). Some of the specimens exhibited "hard" direction during THD (e.g., specimen from site PA10.)

Based on the results of demagnetization studies on pilot specimens, the rest of the specimens were subjected to either AFD (optimum peak fields of 200 and 300 Oersted) or THD (optimum temperature of 300°C), depending on their magnetic behavior during cleaning. Table 2 is the listing of results of the magnetic cleaning studies.

Discussions and conclusions

It is evident from Fig. 3 that the NRM directions form a cluster around the axial dipole field direction at present for Tansen ($I = 47^\circ$). After cleaning, for most of the sites, neither the grouping of mean directions for specimens within a site is improved nor the site-mean directions do show any significant departure from the NRM site-mean directions. Such a behavior can be interpreted in terms of largely overprinting or complete

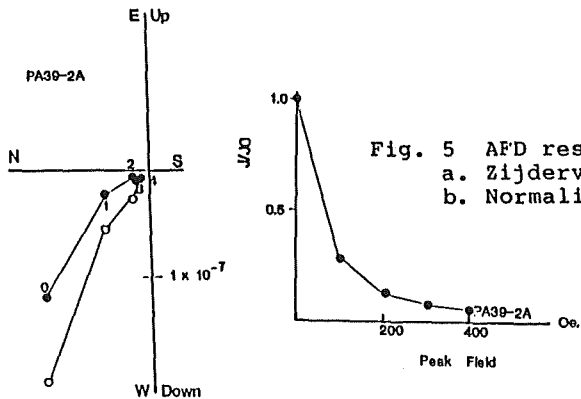


Fig. 5 AFD results for a specimen PA39-2A.
 a. Zijdeveld plot.
 b. Normalized intensity decay curves.

Fig. 6 Thermal demagnetization results for a specimen PA3-3.
 a. Zijdeveld plot. The numbers 0,1,2,3,4 and 5 indicate NRM, 100,200,300,400 and 500 degree centigrades heating temperatures.
 b. Normalized intensity response curve.

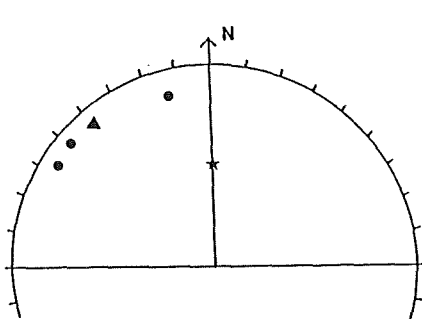
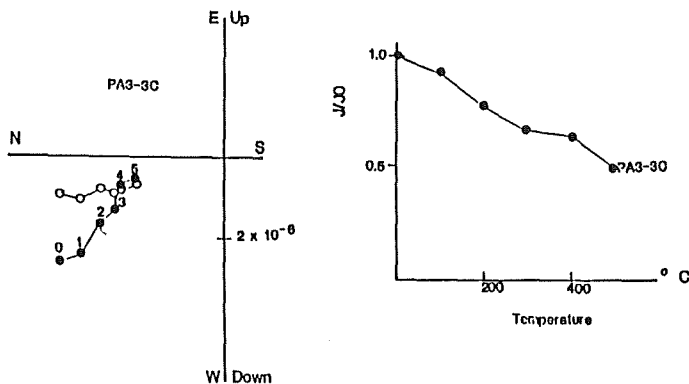


Fig.7 Projections of mean directions of sites PA 3, PA4(A) and PA 5(A) after thermal cleaning at 300 °C. Triangle - mean of 3 sites (not corrected for bedding).

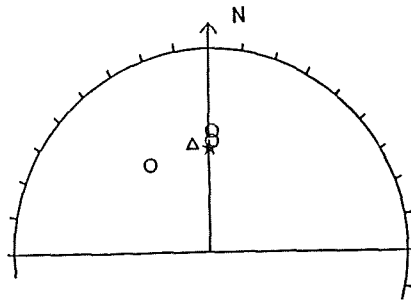


Fig. 8 Projections of mean magnetization directions from sites PA38, PA39 and PA40 after cleaning at 300 Os. peak fields (open circles). Triangle is the mean of three sites (bedding correction applied).

remagnetization of the rocks in the recent magnetic field.

The mean directions for 3 sites belonging to the Ramdighat Formation yield a mean-site with NNW declination and shallow downward inclination (Fig.7). There is no improvement in the grouping of the directions after bedding correction (Table 2). Thermomagnetic analysis of the purple slate specimen suggests hematite as the carrier of remanence. Microscopic examination of the specimens showed the distribution of larger part of opaque minerals (mainly hematite) along the cleavage rather than along the primary laminations. These facts favour the secondary nature of the revealed magnetization. The inclination (before bedding correction) suggests a shallow northern paleolatitude (5°N) of acquisition. This direction may be correlatable with the well reported "Collision component" observed in other parts of the Himalaya (e.g., in Tibetan Sedimentary Series, Nepal Himalaya, Klootwijk & Bingham, 1980).

The site-mean directions from Kerabari area show an improvement in grouping after bedding correction suggesting positive fold test. If the directions from two sites PA36 and PA37 are discarded (the directions are based on only 2 specimens in each site and the rocks in these sites are structurally highly disturbed because of their closeness to the MBT), the remaining 3 sites yield better grouping (Table 2, Fig. 8). This direction is believed to be characteristic for the Kerabari formation. However, absence of precise stratigraphic control and lack of previous paleomagnetic data from the Lesser Himalaya does not enable at present to make further interpretation.

The conclusions drawn from this study are as follows:

(1) Most of the rocks are magnetically weak with their intensity of 10^{-7} order, in emu/cc. The NRMs of these rocks represent either complete or partial overprinting in the recent geomagnetic field. Application of AF (upto 530 Oe) or TH demagnetization can not unveil the primary magnetic component either because of the rapid decay of the intensity to the instrument noise level after a few cleaning steps or owing to the presence of very hard secondary recent field component.

(2) The purple slate rocks from Ramdighat Formation and carbonates from Kerabari formation are likely suitable for further paleomagnetic research. The former can be easily measured because of their higher intensities although the magnetization is believed to be of secondary origin, while the latter seem to possess primary magnetization which can be determined after AF cleaning treatment though they are relatively weakly magnetized. However, an extensive sampling coverage with collection of several samples from each site is needed to get meaningful data.

References

- Arita, K., D. Hayashi and M. Yoshida (1982) Jour. Nepal Geol. Soc., 2, Special issue, 5.
Arita, K. and M. Yoshida (1982) Jour. Nepal Geol. Soc., 2, Special issue, 51.
Bingham, D. K. and C.T. Klootwijk (1980) Nature, vol.284, 336.
Collinson, D. W. (1983) Paleomagnetism. Techniques and

- instrumentation (Chapman & Hall, London), 502.
- Frank, W. and G. R. Fuchs (1970) Geol. Rdsch., 59, 552.
- Fuchs, G. R. (1980) In: K. S. Valdiya and S. K. Bhatia (Editors), Stratigraphy and correlations of Lesser Himalayan formations (Hindustan Publishing Corp., Delhi), 163.
- Fuchs, G. R. and W. Frank (1970) Jahrb. Geol. Bundesanst., 18, 103.
- Hashimoto, S., Y. Ohta and Ch. Akiba (Editors) (1973) Geology of the Nepal Himalayas (Saikon Publ., Tokyo), 292.
- Irving, E. (1964) Paleomagnetism and its application to geological and geophysical problems (John Wiley and Sons, New York), 399.
- Khramov, A. N. and L.E. Sholpo (1967) Paleomagnetism. Principles, methods and geological applications of paleomagnetology, in Russian (Nedra publ., Leningrad) 252.
- Klootwijk, C. T. and D.K. Bingham (1980) Earth and Planet. Sci. Letters, 51, 381.
- Masclé, G. H. (1980) In: K. S. Valdiya and S. K. Bhatia (Editors), Stratigraphy and correlations of Lesser Himalayan formations (Hindustan Publishing Corp., Delhi) 191.
- Sakai, H. (1983) Mem. Fac. Sci., Kyushu Univ. ser. D, Geol., vol. xxv, 1, 27.
- Sakai, H. (1984) Jour. Nepal Geol. Soc., 4, Special issue, 53.
- Sakai, H. (1985) Mem. Fac. Sci., Kyushu Univ. ser. D, Geol., vol. xxv, 3, 337.
- Sharma, C. K. (1980) In: K. S. Valdiya and S. K. Bhatia (Editors), Stratigraphy and correlations of Lesser Himalayan formations (Hindustan Publishing Corp., Delhi), 174.
- Sharma, T., D. R. Kansakar and K. Kizaki (1984) Bull. College of Science, Univ. of the Ryukyus, 38, 57.
- Yoshida, M. and H. Sakai (1984) Jour. Nepal Geol. Soc. 4, Special issue, 53.
- Zijderveld, J.D.A. (1967) In: D. W. Collinson, K. M. Creer and S. K. Runcorn (Editors), Methods in Paleomagnetism (Elsevier, Amsterdam), 254.

(Submitted to Jour. Fac. Sci., Hokkaido Univ., IV)

K-Ar, ^{40}Ar - ^{39}Ar AGE AND Sr ISOTOPE STUDIES
ON VOLCANIC ROCKS OF SEAMOUNTS FROM THE JAPAN SEA

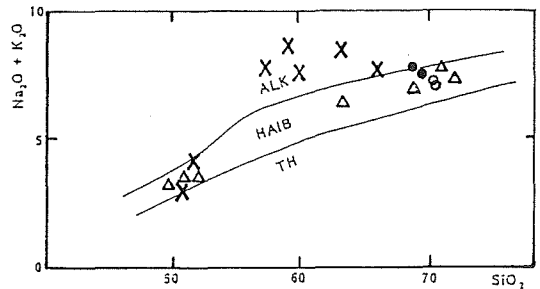
Ichiro KANEOKA*, Kenji NOTSU**, Yutaka TAKIGAMI***,
Kantaro FUJIOKA**** and Hitoshi SAKAI****

- * Earthquake Research Institute, University of Tokyo, Bunkyo-ku, Tokyo 113
- ** Institute of Chemistry, University of Tsukuba, Sakura-mura, Ibaraki 305
- *** Geophysical Institute, Faculty of Science, University of Tokyo, Bunkyo-ku, Tokyo 113
- **** Ocean Research Institute, University of Tokyo, Nakano-ku, Tokyo 164

The Japan Sea is regarded to be a typical example of a back-arc basin, which has been developed between the Asian continent and the Japanese Islands. In order to understand the mechanism of the evolution of a back-arc basin, it is important to reveal the chronological sequences and the characteristics of the erupted rocks in this area. Although there are many studies concerning the evolution of the Japan Sea (e.g., Hilde and Wageman, 1973), the formation age of the Japan Sea has not yet been settled definitely. Furthermore, the characteristics of the rocks of the ocean floor in this area are not yet clear. In order to get information concerning these problems, K-Ar, ^{40}Ar - ^{39}Ar age studies together with Sr isotope studies were performed on some volcanic rocks dredged from seamounts in the Yamato Basin of the Japan Sea.

Samples were dredged from Yamato Seamounts, located as a chain from the southwest to the northward in the Yamato Basin, during the KH84-3 cruise of the Hakuho-maru. They include both andesites and basalts. Their chemical compositions suggest that they are rather island-type volcanic rocks. Some examples are shown in Fig. 1, where some volcanic rocks dredged from the Okinawa Trough are included for comparison.

K-Ar ages were determined for whole rocks by the conventional method. K contents were analysed by a flame photometer. ^{40}Ar - ^{39}Ar ages were determined for neutron-irradiated samples by the JMTR of the Tohoku University. The experimental procedures were the same as reported before (Kaneoka, 1980). For these analyses, the most fresh samples were selected among the dredged samples from each site. However, we have no definite guarantee that they have never experienced the secondary effect which might have caused some radiogenic ^{40}Ar loss. Further, their glass content is not so large, implying that they do not contain significant amounts of excess ^{40}Ar . Hence, the obtained K-Ar age would probably indicate the younger limit for the



OKINAWA TROUGH

△ LAVA

○ } PUMICE

JAPAN SEA

X LAVA

Fig.1. The $\text{Na}_2\text{O} + \text{K}_2\text{O}$ vs. SiO_2 diagram for dredged volcanic rocks. Analyst: H.Haramura. Data for samples from the Okinawa Trough are taken from Kimura et al. (1986).

formation age of these samples.

In Fig. 2, one example is shown for a volcanic rock dredged from the Yamato Seamount which shows a plateau ^{40}Ar - ^{39}Ar age of 10.8Ma. However, only several samples show plateau ^{40}Ar - ^{39}Ar ages and the others show rather irregular patterns. In latter cases, total ^{40}Ar - ^{39}Ar ages are adopted, which are equivalent to conventional K-Ar age.

Present results are summarized in Fig. 3, where some reported data are also included. Except for samples from the Yamato Ridge area and the Oshiam Plateau area, most samples show the ages of 10-20Ma. Younger K-Ar ages are mostly dredged from the fringing areas of the Japanese Islands and probably related to the volcanism during the evolution of the Japanese Islands and would not directly relate to the formation of the back-arc basin. One sample from the midst of the Yamato Basin shows a K-Ar age of about 7Ma. Since this sample is a little altered, however, this value might indicate the younger limit for the formation age of the floor.

In Fig. 4, the results for $^{87}\text{Sr}/^{86}\text{Sr}$ ratio analyses are summarized for present samples together with reported data. The $^{87}\text{Sr}/^{86}\text{Sr}$ ratios were analysed on a VG-Micromass MM-30 mass spectrometer after the same procedures reported before (Notsu, 1983). It is noteworthy that volcanic rocks dredged from Yamato Seamounts show rather uniform $^{87}\text{Sr}/^{86}\text{Sr}$ ratios of about 0.7036. Such values are similar to those reported for some Quaternary volcanic rocks from the northeast Japan, located as zones between the volcanic front and the Japan Sea side. For volcanic rocks from the Yamato Ridge area, the dredged volcanic rocks show the higher $^{87}\text{Sr}/^{86}\text{Sr}$

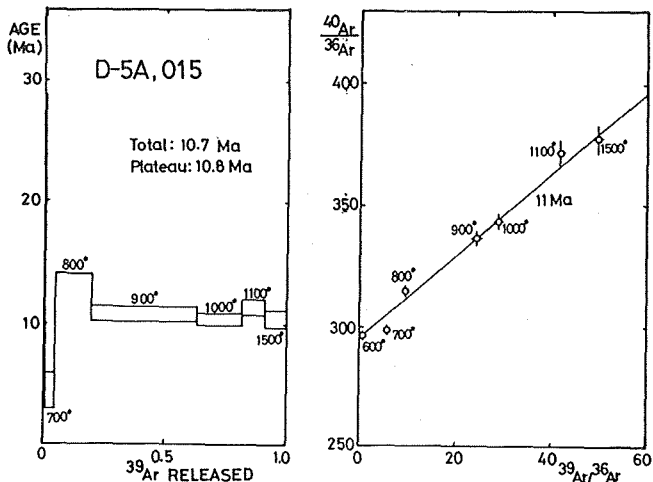


Fig. 2. ^{40}Ar - ^{39}Ar age diagram for a volcanic rock dredged from the Yamato Seamount (D-5A, 015).

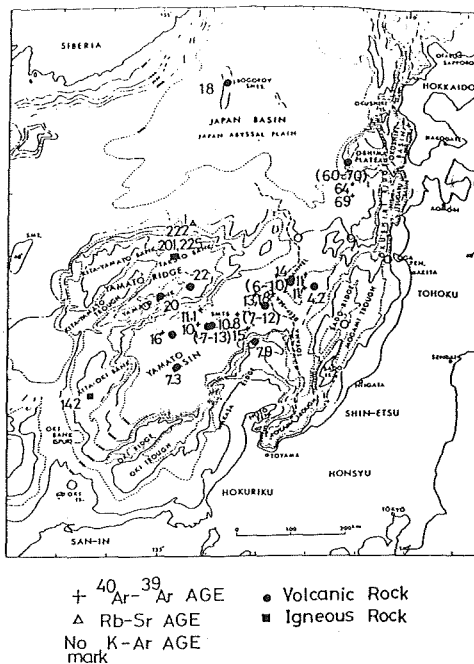


Fig. 3. Summary of radiogenic ages for igneous rocks dredged from the Japan Sea. Results for present samples together with other data summarized in Kaneoka (1986) are plotted.

ratios than the samples of the Yamato Seamounts. The latter samples would probably reflect the larger contamination by the relatively old continental crustal materials.

Since the Yamato Seamounts are located almost in the midst of the Yamato Basin as a chain, it is expected to have been formed rather in the later stage of the evolution of the Japan Sea floor. Hence the formation age of these seamounts would reflect the ages of the latest volcanic activity during the formation history of the Yamato Basin area. Further the $^{87}\text{Sr}/^{86}\text{Sr}$ ratios suggest that they still keep the characteristics of the island-arc type volcanism. This may imply that the opening of the Japan Sea might have stopped before completely pure MORB-type materials could appear on the floor of the Japan Sea without being affected by crustal materials.

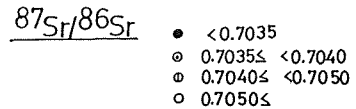
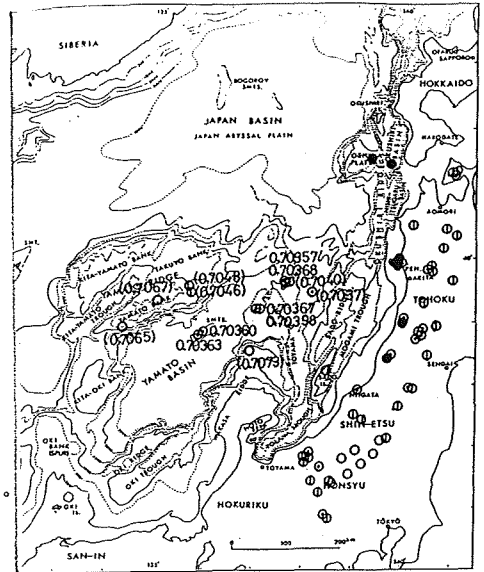


Fig.4. Summary of $^{87}\text{Sr}/^{86}\text{Sr}$ ratios for volcanic rocks dredged from the Japan Sea. Data by Ueno et al. (1974) are included. Data for Quaternary volcanic rocks of the northeast Japan are taken from Notsu(1983).

References

- Hilde, T.W.C. and J.W.Wageman (1973) In "The Western Pacific: Island Arc, Marginal Seas, Geochemistry" ed. by P.J.Colemann, (W. Australian Univ. Press), 415.
- Kaneoka, I. (1980) Earth Planet. Sci. Lett., 46, 233.
- Kaneoka, I. (1986) J. Geomag. Geoelectr., 38, 475.
- Kimura, M., I. Kaneoka, Y. Kato, S. Yamamoto, I. Kushiro, H. Tokuyama, H. Kinoshita, N. Isezaki, H. Masaki, A. Oshida, S. Uyeda and T.W.C. Hilde (1986) Bull. Earthq. Res. Inst., 61, 269.
- Notsu, K. (1983) J. Volcanol. Geotherm. Res., 18, 531.
- Ueno, N., I. Kaneoka and M. Ozima (1974) Geochem. J., 8, 157.

PALEOMAGNETISM OF A PHOSPHORITE NODULE COLLECTED FROM
OFF NEW ZEALAND

Hayao MORINAGA, Hiroo INOKUCHI, Katsumi YASKAWA,
Toshikatsu MIKI^o and Motoji IKEYA^o

Faculty of Science, Kobe University, Rokkodai-cho, Kobe 657, Japan
^oTechnical College, Yamaguchi University, Tokiwadai, Ube 755, Japan

Phosphorite nodules are seemed to grow up through much the same process as manganese nodules. Growth layers of both nodules are thought to show syngenetic horizons of the growth. If remanent magnetizations of each growth layer can be measured, ages and thus resultant growth rates of the nodules must be roughly estimated from magnetic polarity changes in the magnetizations kept in the nodules. In the case of manganese nodules, they contain a reasonably stable natural remanent magnetization (NRM) of about the same magnitude as deep-sea sediments, and the ages and resultant growth rates have been already estimated from the recording of magnetic reversals (Crececius et al., 1973).

Phosphorite nodules have been investigated for major and minor elements included in them (Burnett, 1977; Suess, 1981; Thompson et al., 1984), and for U and Th isotopes to establish their ages and hence to obtain clues for their mode of formation (Veeh et al., 1973; Burnett and Veeh, 1977; Thompson et al., 1984). The studies indicate that the phosphorite nodules are currently forming in the areas of intense oceanic upwelling; the continental margin of Peru-Chile, South-West Africa (Namibia) and East Australia (O'Brien and Veeh, 1980). Ages of the nodules dated by U-series methods almost range from late Pleistocene to Recent.

A phosphorite nodule sample was collected from the sea floor off New Zealand. This sample was in the shape of a mound with a relatively flat plane. As a black spot was present near the center, this sample must have grown radially around this spot. The growth layers, however, were comparatively parallel on the side containing the flat plane from the spot and those on the other side were curved owing to its radial growth. This sample was cut by four planes perpendicular to the flat plane, and was re-formed into a block of 15×20×24 mm³. This block was divided into sixteen slabs of about 1mm thick parallel to the flat plane. These slab specimens were named 1, 2,, 16 in a descending order from the flat plane side (Fig.1). The black spot was included in a specimen (8).

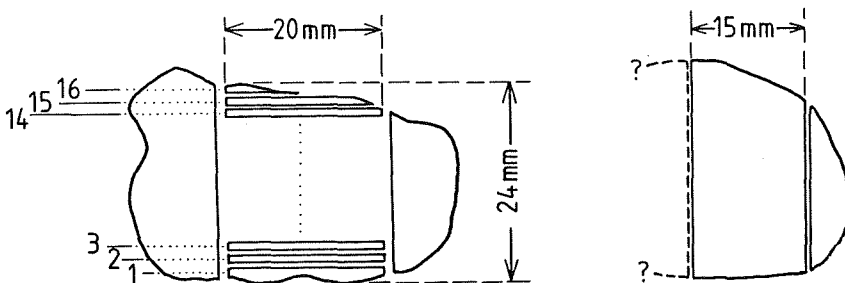


Figure 1. Schematic views of the phosphatic nodule sample.

SPECIMEN	INTENSITY (10^{-11}) [Am ²]	DECLINATION [°]	INCLINATION [°]	POLARITY
1	11.70	20.5	-43.1	Normal
2	6.80	0.0	-53.9	Normal
3	4.12	14.0	0.0	Normal
4	5.85	30.9	-4.9	Normal
5	1.11	0.0	-26.5	Normal
6	2.69	-116.5	33.8	Reverse
7	5.09	161.5	51.6	Reverse
8	2.06	180.0	14.0	Reverse
9	3.60	180.0	33.6	Reverse
10	2.23	90.0	63.4	??
11	23.95	-112.2	-7.1	??
12	3.20	-161.5	-8.9	??
13	7.28	0.0	74.0	??
14	5.22	0.0	-16.6	Normal
15	7.34	8.1	-15.7	Normal
16	5.31	168.6	16.3	Reverse

Table 1. The results of NRM measurements.

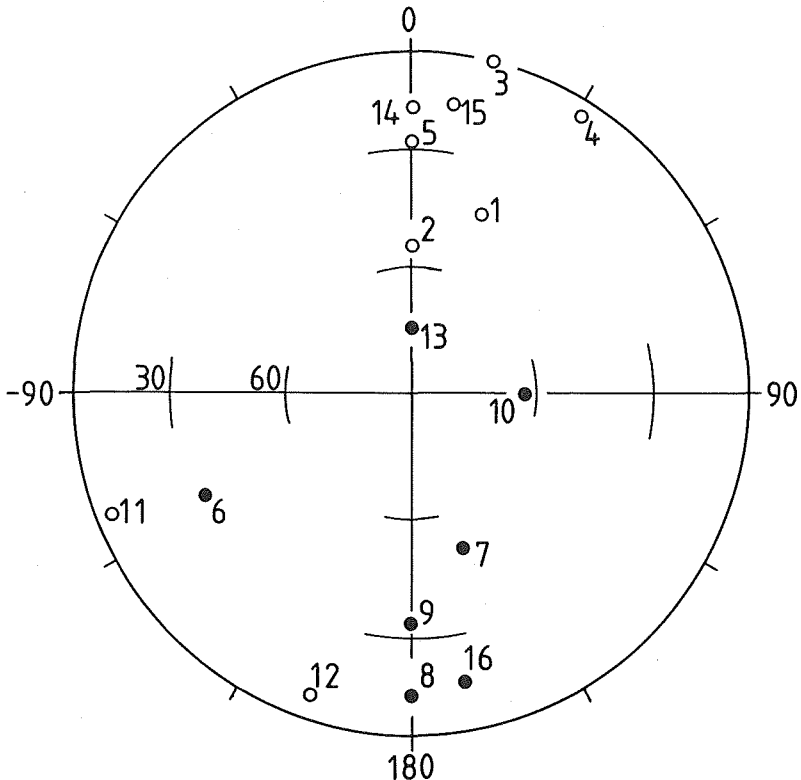


Figure 2. The direction of NRM plotted on Schmidt equal area projection [○; upper hemisphere, ●; lower hemisphere].

The NRM measurements of these slabs were carried out using SCT superconducting rock magnetometer, whose sensitivity is 10^{-11} Am². The results of the NRM measurements are shown in Table 1 and Fig.2. In the Table 1, a column 1 corresponds to specimen number, a column 2 indicates a intensity of magnetic moment of each specimen and columns 3 and 4 indicate a declination which was measured clockwise from a certain direction and a inclination which was measured downwards from the flat plane respectively. The NRM intensities are very weak of the order of 10^{-10} to 10^{-11} Am².

Fig.3 shows change in magnetizations of specimen (1) during a progressive alternating-field (AF) demagnetization. Although each direction is fairly fluctuating during the demagnetization as shown in Fig.3, each magnetic polarity never changes. On the supposition that this nodule has continued to grow till its sampling, the polarities of all specimens can be decided only using the NRM directions and are shown in a column 5 of Table 1. In this column, 'Normal' corresponds to a direction satisfying a declination of the first and the second quadrants and a minus inclination, and 'Reverse' corresponds to the opposite direction in the case of 'Normal'.

The NRM directions of all specimens except for those of 10-16 containing curved growth layers are separated into two mutually opposite groups as shown in Fig.2. Mean 'Normal' direction for specimens of 1-5 is calculated to be Dec=14.2° and Inc=-26.2° ($\kappa=9.7$ and $\alpha_{95}=25.8^\circ$), and mean 'Reverse' direction for specimens of 6-9 is calculated to be Dec=-168.8° and Inc=37.2° ($\kappa=6.4$ and $\alpha_{95}=39.3^\circ$). If this nodule has constantly grown with its rotation, these direction data must be distributed at random on this net. In addition, a presence of the flat plane and growth layers parallel to the plane must obstruct its rotation and must usually face this flat plane side downwards. Supposing its growth without rotation, this separation of the direction data occurs in two following cases;

- (i) this nodule oppositely rotated once before,
- (ii) a polarity reversal occurred once before.

As the case (i) is hard to occur commonly, the case (ii) is reasonable as a origin of this separation. Each NRM direction of specimens 10-16 is unreliable because they contain curved layers.

As the result of magnetic measurements, it was found that a polarity reversal occurred during the growth of this nodule and this nodule started to grow at reversed epoch because a polarity of specimen 8 is 'Reverse'. If this nodule has continued to grow till its sampling, it is no doubt that this nodule started to grow in Matuyama reversed epoch and a Matuyama-Brunhes boundary corresponds to a position between specimens of 6 and 5. Thus, mean

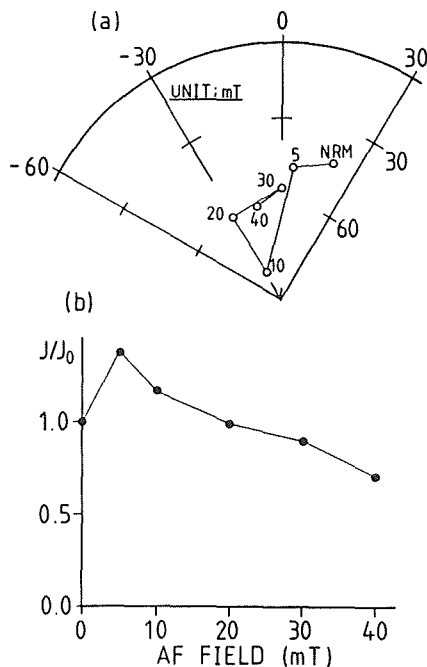


Figure 3. Change in direction (a) and intensity (b) of a remanence of a specimen (1) during a progressive AF demagnetization.

growth rate of this nodule can be estimated to be about 0.012 mm per 1000 years.

References

- Burnett W. C. (1977) *Geol. Soc. Am. Bull.*, 88, 813.
Burnett W. C. and H. H. Veeh (1977) *Geochim. Cosmochim. Acta*, 41, 755.
Crececius E. A., R. Carpenter and R. T. Merrill (1973) *Earth Planet. Sci. Lett.*, 17, 391.
O'Brien G. W. and H. H. Veeh (1980) *Nature*, 288, 690.
Suess E. (1981) *Geochim. Cosmochim. Acta*, 45, 577.
Thompson J., S. E. Calvert, S. Mukherjee, W. C. Burnett and J. M. Bremner (1984) *Earth Planet. Sci. Lett.*, 69, 341.
Veeh H. H., W. C. Burnett and A. Soutar (1973) *Science*, 181, 844.

(To be submitted to *Earth Planet. Sci. Lett.*)

NRM ACQUISITION MECHANISMS FOR SNOW INVOLVING ROCK DUSTS

Minoru FUNAKI¹ and Hideo SAKAI²

1: National Institute of Polar Research. 9-10, Kaga 1-chome
Itabashi-ku, Tokyo 173

2: Department of Earth Sciences Faculty of Science,
Toyama University. Gofuku 3190, Toyama 930, Japan

1. Introduction

Yellow colored dirt-ice layers involving volcanic ashes were reported by Nishio et al.(1984) and Katsushima et al.(1984) from blue ice fields of Yamato Mountains at Enderby Land and Allan Hills in Southern Victoria Land of East Antarctica. Funaki and Nagata (1985) studied NRM of the layers collected from Allan Hills. They reported fairly stable NRMs against AF demagnetization up to 50 mT. The NRM intensities were order of magnitude 10^{-6} Am²/kg which was 10^{-3} Am²/kg converted into amount of the involving volcanic ashes. The NRM directions measured from 10 samples with orientation from a dirt-ice block sample were almost parallel as shown $\alpha_{95} = 2.1^\circ$ and $K=347$. The NRM intensity converted into volcanic ashes was similar to TRM rather than DRM. It is difficult to estimate the NRM acquisition mechanisms in the Antarctic ice sheet, because the meteorological environment on Antarctica is highly different from sedimentation of volcanic ashes due to strong katabatic wind compared with deep sea or lake sedimentation. As the first step for search the NRM acquisition in dirt-ice layers, NRM acquisition process in dirt-snow involving rock dust was investigated.

Two kinds of low temperature laboratory were used in this study. Their temperatures were kept -20 and -10°C in day time, although the respective temperatures rose several degrees from constant temperature in night time. The geomagnetic field (GMF) of these rooms were 45μT in intensity and 58° in inclination.

2. Magnetic properties of block sample and rock dust

An andesite block sample collected from Izu peninsula was used for preparation of rock dusts less than 105μm in diameter instead of volcanic ash.

Magnetic hysteresis curves of the block sample and the rock dusts were measured at room temperature from -1.4 to 1.4 T in external steady magnetic field. Saturation magnetization I_S , saturation remanent magnetization I_R , coercive force H_C and remanent coercive force H_{RC} were determined as shown in Table 1. The I_S values of block and rock dusts have small difference, suggesting small heterogeneous distribution of magnetic grains in the rock. The rock dusts have larger values of $H_C=1.4$ and $H_{RC}=3.9$ mT than those of $H_C=1.1$ and $H_{RC}=2.6$ mT in the block sample.

Table 1. Basic magnetic properties of Izu andesite.

Sample	NRM	VRM (231 ^m)	I_S	I_R	H_C	H_{RC}	I_R/I_S	H_{RC}/H_C
			Am^2/kg	Am^2/kg	mT	mT		
Block sample	$3.30 \pm 0.36 \times 10^{-4}$	1.35×10^{-5}	1.43	0.21	11	26	0.14	2.36
Rock dusts 105μm		1.65×10^{-5}	1.78	0.29	14	39	0.16	2.79
Unit	Am^2/kg	Am^2/kg	Am^2/kg	Am^2/kg	mT	mT		

Thermomagnetic curves were obtained in the range of room temperature to 630°C under the condition of 10^{-4} torr in atmospheric pressure with 0.6 T of external magnetic field. The 1st run curve showed irreversible reactions with main Curie point 450°C in a heating curve and 300°C in a cooling curve. Original spontaneous magnetization decreased from 1.8 to 1.6 Am^2/kg after heat treatment up to 600°C. The 2nd run curve was reversible to the 1st run cooling one. These thermomagnetic analyses suggest major role of titanomaghemite for a magnetic mineral.

AF demagnetization curves of NRM for block samples were obtained up to 50 mT. Original NRM intensity $3.7 \times 10^{-4} \text{Am}^2/\text{kg}$ was demagnetized smoothly up to 20 mT and then zigzagged to 50 mT. Its directional changes were also small to 20 mT but then became large.

Acquisition test of viscous remanent magnetization (VRM) was carried out for a demagnetized block and rock dusts samples under the GMF. In case of this test, the rock dusts were fixed into a non-magnetic sample holder by bond. Both VRM acquisitions were almost saturated after 20 minutes and the values after 231 hours were 1.35 and 1.65 $\times 10^{-5} \text{Am}^2/\text{kg}$ for block sample and rock dusts, respectively.

3. NRM acquisitions for dirt-snow samples

In order to search for NRM acquisition process, total of 5 and 7 dirt-snow samples, involving 5.4 wt% of rock dusts, were set in -20 and -10°C laboratories respectively. The NRM changes were measured at 0.7, 1.7, 3.7, 5.7, 23.7, 27.7, 47.7, 72.7, 103, 120 and 1201 hours from making of the samples, as shown in Fig. 1.

The NRM intensity curves at -20°C was roughly divided on logarithmic time scale from first to final as following sequences; increased smoothly up to $0.40 \times 10^{-4} \text{Am}^2/\text{kg}$ from 0.7 to 23.7 hours (1st stage), decreased down to $0.32 \times 10^{-4} \text{Am}^2/\text{kg}$ from 23.7 to 72.7 hours (2nd stage), increased up to $1.00 \times 10^{-4} \text{Am}^2/\text{kg}$ from 72.7 to 1201 hours (3rd stage). Maximum intensities of the

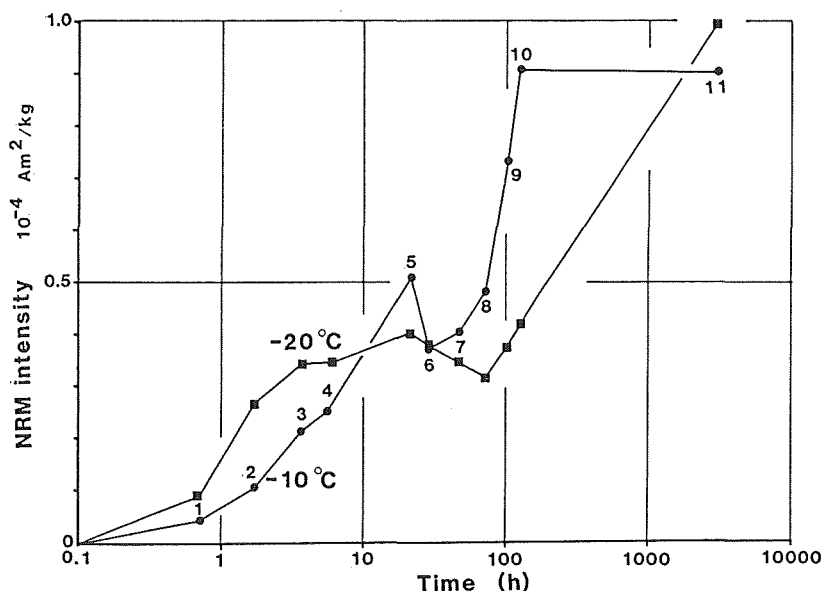


Fig. 1. Mean NRM intensity acquisition curves of dirt-snow samples at -20 and -10°C .

5 samples were observed at 1201 hours in all cases. On the other hand, the NRM intensity at -10°C was slightly different and its acquisition curve was divided into following sequences from first to final; increased smoothly up to $0.51 \times 10^{-4} \text{Am}^2/\text{kg}$ from 0.7 to 23.7 hours (1st stage), decreased down to $0.37 \times 10^{-4} \text{Am}^2/\text{kg}$ from 23.7 to 27.7 hours (2nd stage), increased up to 0.91×10^{-4} from 27.7 to 128 hours (3rd stage), kept plateau from 128 to 1201 hours (4th stage). The maximum NRM intensities at -10°C are observed between 103 and 1201 hours. In general, the intensity acquisition rates at -10°C were large between 10 and 128 hours in comparison with that of -20°C one.

Change of mean NRM directions and their α_{95} values at -20°C are shown in Fig. 2. The directions changed irregularly first from 0.7 to 27.7 hours and systematically from 47.7 to 1201 hours, although the NRM directions were in parallel with the GMF direction taking into consideration of their α_{95} values. The α_{95} value decreased systematically from 0.7 to 128 hours, but then increased at 1201 hours. The mean NRM at 128 hours was the closest to the GMF direction (inclination 55.1° , declination 1.9°) and the smallest α_{95} value (16.8°). In case of -10°C as shown in Fig. 3, the directions shifted toward to the GMF direction from 0.7 to 27.7 hours. However all NRM directions, except the direction at 1.7, 3.7 and 5.7 hours, were not consisted with that direction taking consideration of α_{95} values. The NRM directions from 44.7 to 1201 hours shifted to lower inclination side holding the northward declinations; the directions went away along the north meridian from the GMF direction. The α_{95} values decreased gradually down to 2.8° observed at 128 hours and then increased up to 5.4° after 1201 hours.

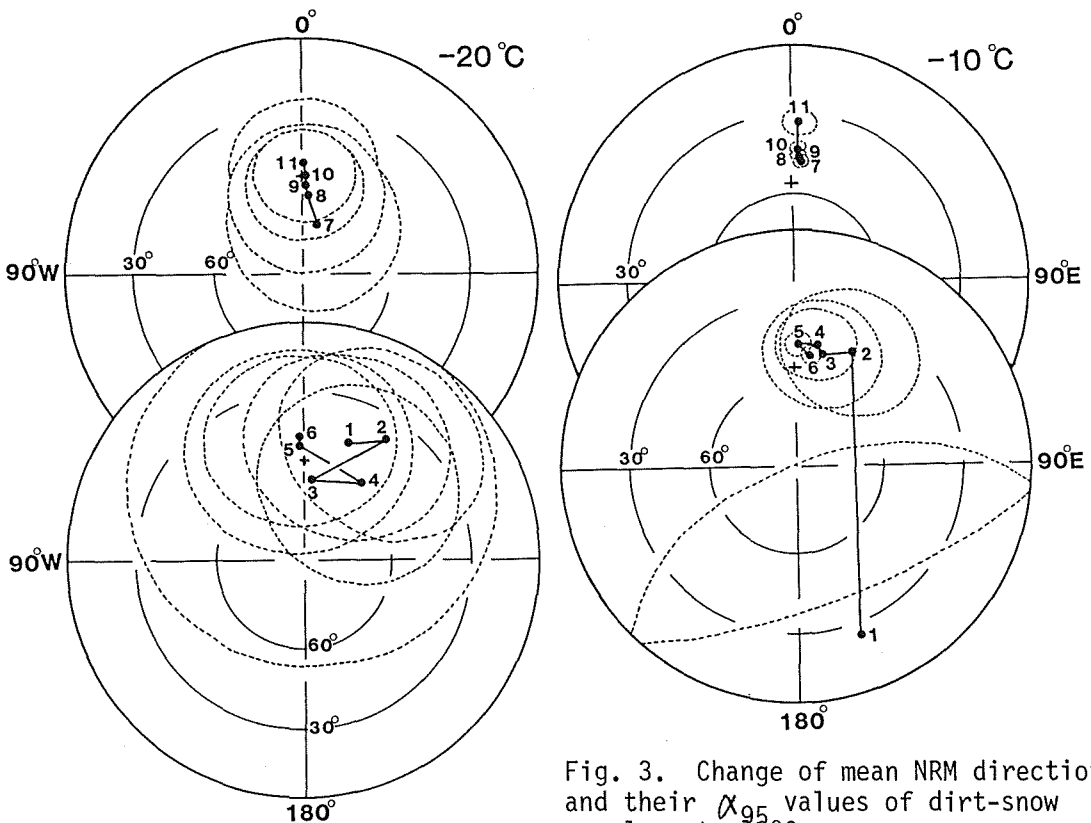


Fig. 2. Change of mean NRM directions and their α_{95} values of dirt-snow samples at -20°C . Numbers from 1 to 11 correspond to the respective measurement times in Fig. 1. +: GMF direction.

Fig. 3. Change of mean NRM directions and their α_{95} values of dirt-snow samples at -10°C .

4. Discussions

Individual magnetic grains in the rock dusts had chemical remanent magnetization (CRM) essentially resulting from the dominant occurrence of titanomaghemite, which was stable up to 20 mT against AF demagnetization. Magnetic domain structures of both samples were estimated to be pseudosingle domain (PSD) structure based on the classification of domain structures using the ratios of I_R/I_S and H_{RC}/H_C (Table 1) proposed by Day et al. (1977). The saturated VRM intensity $1.65 \times 10^{-5} \text{Am}^2/\text{kg}$ of rock dust was fairly small as compared with original NRM one $3.30 \times 10^{-4} \text{Am}^2/\text{kg}$ of block sample. Therefore, there is no possibilities of remagnetization toward the GMF direction for each magnetic grain during these experiments. Plausible NRM acquisition may be explained by the rotation of magnetic grains toward the GMF direction.

The mean NRM intensities probably saturated during the time from 103 to 128 hours at -10°C and from 128 to 1201 hours at -20°C . The saturated intensities 1.00×10^{-4} at -20°C and $0.91 \times 10^{-4} \text{Am}^2/\text{kg}$ at -10°C were converted into amount of involving rock dusts as 1.85×10^{-3} and $1.69 \times 10^{-3} \text{Am}^2/\text{kg}$ respectively. As the original NRM intensity of block sample was $3.30 \pm 0.36 \times 10^{-4} \text{Am}^2/\text{kg}$, the NRM intensities of dirt-snows were very strong, being consistent with the results of dirt-ice reported by Funaki and Nagata (1985). The directions at -20°C changed systematically to the GMF direction having a gradual decrease of α_{95} value up to 128 hours. In case of -10°C , the directions went away clearly from the GMF direction with the time to the lower inclination side holding the northward declination after 47.7 hours. This tendency was also observed in the experiment at -20°C , but only after 1201 hours. The α_{95} values decreased smoothly with time to get minimum value at 128 hours but they increased after that time.

From these results, following two kinds of NRM acquisition mechanism are estimated. The first idea is a similar mechanism to the post detrital remanent magnetization (pDRM). The temperature controls in the laboratories was not good enough; they change from -4 to -10°C for -10°C laboratory and -13 to -21°C for -20°C one. In the condition of these temperature variations, snow particles repeat vaporization and solidification due to variation of vaporized pressure according to changing temperature. Furthermore, smaller snow particles are absorbed by larger ones by surface energy differentiation. If small magnetic grains adhere to the surfaces of the small snow particles, the grains drop on the surface of under laying snow particles with rotation to adjust their NRM to the GMF directions. When this mechanism operated and repeated in the dirt-snow, the magnetic grains were rearranged exponentially to the GMF direction. This idea resembles to the NRM acquisition mechanism for sediments during their dehydration and solidification process (pDRM).

The second idea is estimated that the magnetic grains are rotated to the GMF direction adjusting in parallel with their NRM directions by the interaction of NRM and the GMF intensities, because snow surfaces have water layers of several angstrom thick at least -50°C , the water layers perform the lubrication between magnetic particles and solid snow surfaces.

During NRM acquisitions of the dirt-snow, the new snow particles change to depth hoar through packed snow stage, suggesting the growth of snow grains. A possibility is estimated for stepwise NRM intensities acquisition of 4 stages from this snow conditions based on first idea; magnetic grains are first dropped to lower level during formation of packed snow (1st stage); magnetic grains can not be dropped to lower snow layers because of formation of stable packed snow (2nd stage); magnetic grains are dropped again during formation of depth hoar (3rd stage); magnetic grains can not drop any more to lower snow layers by the formation of stable depth hoar (4th stage). Probably both of the first and second ideas are performed simultaneously adjusting in parallel with the NRM and the GMF directions. On the other hand, movement of snow grains by compactness disturbs NRM

alignment.

The magnetic grains magnetized to their principal grain axes aligned to the GMF direction. Namely the principal axes of magnetic grains represented by ellipsoid are tilted to 58° statistically. On the other hand, the dirt-snows are compacted by its deadweight simultaneously. These phenomena affects toward flattening of the inclination. This is the reason why the mean NRM directions shift to lower inclination side keeping the northward declination. The flattening process also affects snow grains. As the snow grains with shape anisotropy distribute at random, the flattening acts disturbance of the clustering NRM direction. If drop of magnetic grains stops by development of large snow grains (depth hoar), only flattening affects to the dirt-snows. That is why the increases χ_{95} and K values at 1201 hours are estimated.

References:

Day, R., Fuller, M. and Schmidt, V.A. (1977), *Phys. Earth Planet. Inter.*, 13, 260-267.

Funaki, M. and Nagata, N. (1985), *Mem. Natl. Inst. Polar Res., Spec. Issue*, 39, 209-213.

Katsushima, T., Nishio, F., Ohmae, H., Ishikawa, M. and Takahashi, S. (1984), *Mem. Natl. Inst. Polar Res., Spec. Issue*, 34, 174-187.

Nishio, F., Katsushima, T., Ohmae, H., Ishikawa, M. and Takahashi, S. (1984), *Mem. Natl. Inst. Polar Res., Spec. Issue*, 34, 160-173.

CHEMICAL COMPOSITION OF MAGNETITE
FROM THE HYDROTHERMAL ALTERATION ZONE OF
QUARTZ DIORITE BODIES, CHICHIBU MINING AREA, JAPAN.

Hiroto UENO

Institute of Mineralogy, Petrology and Economic Geology,
Faculty of Science, Tohoku University,
Sendai 980, Japan.

Introduction

The Chichibu mining area (36°01' N, 138°49' E) is situated in Nakatsugawa, Saitama Prefecture, about 90 km NNW of Tokyo. The deposits of the mine are of pyrometasomatic type. Quartz diorite bodies around the deposits are partly subjected to hydrothermal alteration. The unaltered fresh part of quartz diorite bodies has the thermoremanent magnetization (TRM), while the hydrothermally altered part may have the chemical remanent magnetization (CRM). However, carriers of magnetization of both fresh and altered sites are magnetite. In this paper, chemical compositions of magnetite from altered sites as compared those from fresh sites are described briefly.

General Geology

The sedimentary formation in the mining area consist of the Nakatsugawa group of the Chichibu Paleozoic Formation (Fujimoto, et al., 1950). The group is divided into three formations, the Ishibune, Ryogami and Okawamata Formations in ascending order (Fujimoto et al., 1957; Ishii, 1962; Okubo and Horiguchi, 1969). The Ishibune Formation is widely exposed in the mining area (Fig. 1), and consists of massive sandstone, slate, limestone and chert. The formation is the most important country rock of the ore deposits. The Ryogami Formation is distributed along the north side of the Ishibune Formation, and conformably overlies the Ishibune Formation. The siliceous facies, forming steep mountains such as Mt. Ryogami (1724 m), are the chief component of the lower part of the formation. The Okawamata Formation consists of sandstone and subordinate interbedded chert, slate and limestone. This formation is in fault contact with the Ishibune Formation about 2 kilometers to the south of the mapped area.

The Paleozoic sediments generally strike WNW, and dip steeply NNE. Those are disturbed by the intrusion of quartz diorite bodies. There are many faults of NS and EW systems. The mineralization was controlled by them (Shoji et al., 1969; Miyazawa, 1970). It is thought that the Ishibune Formation belongs to Carboniferous, and Ryogami and Okawamata Formations to Permian. However, Koike et al. (1971) have reported Triassic conodonts in the chert of the Ryogami Formation, and the stratigraphy and structure in this area remain further problems.

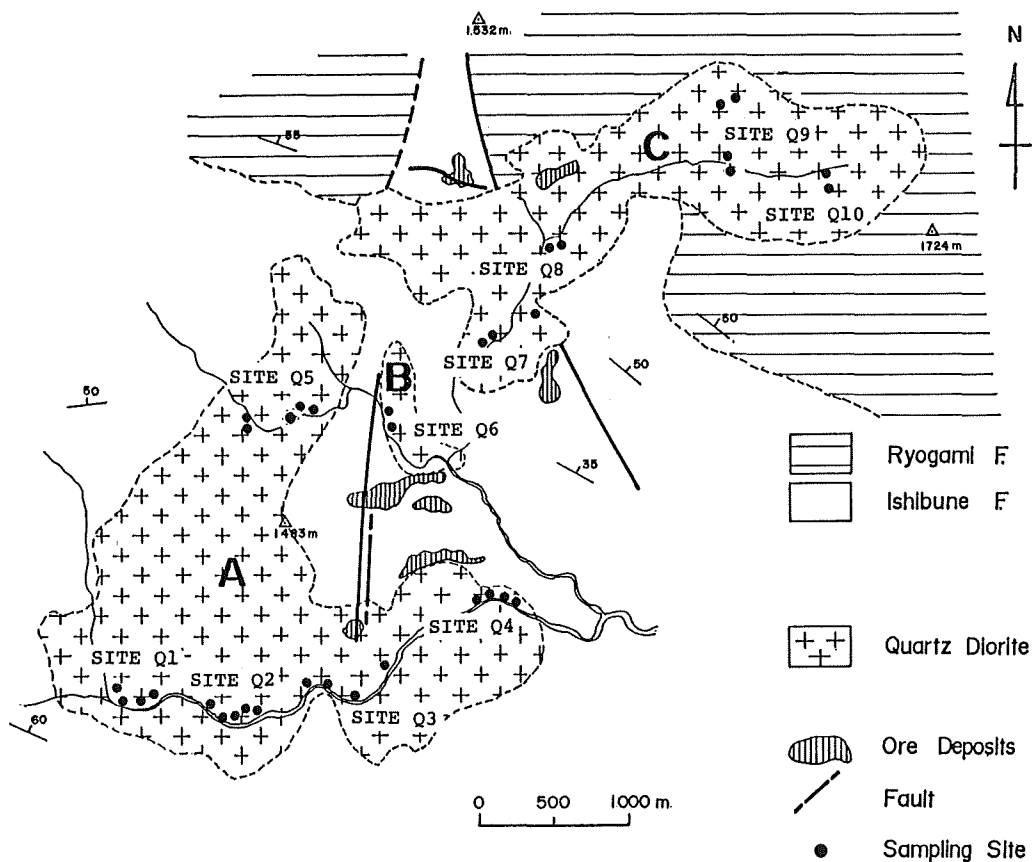


Fig. 1. Geological map of the Chichibu mining area.

The igneous rocks intrude into the Paleozoic formations. Quartz diorite shows the wide exposure and quartz porphyry and porphyrite occur as small dykes. As shown in Figure 1 there are three rock bodies of quartz diorite and they are called A, B and C bodies for convenience. The K-Ar and fission track ages from the quartz diorite A and C bodies are of Late Miocene in age (Ueno et al., 1978; Ueno and Shibata, 1985). The quartz diorite A body appears to be almost contemporary with or slightly prior to the quartz diorite C body.

Many ore deposits which are of pyrometamorphic type occur mostly in limestone of the Ishibune Formation (Fig. 1). Those are Doshinkubo, Akaiwa, Wanaba, Daikoku, Takiue, Nakatsu ore deposits. The ores are mainly composed of magnetite, pyrrhotite, pyrite, sphalerite, galena, chalcocopyrite, arsenopyrite and hematite. Skarn minerals consist of garnet, clinopyroxene, epidote, actinolite, vesuvianite, ilvite, wollastonite and others (Kaneda and Watanabe, 1961; Miyazawa et al., 1970).

Quartz Diorite Body and Opaque Mineral

Consisting rocks of quartz diorite bodies are mainly clinopyroxene-orthopyroxene-cummingtonite bearing biotite-hornblende quartz diorite. Rock facies is medium grained and massive. According to the occurrence of Fe-Ti oxide minerals and alteration degree of silicate minerals; sampling sites in quartz diorite bodies are divided into three groups. The first is fresh sites. Sites Q1, Q2 and Q5 of the quartz diorite A body, and sites Q9 and Q10 of the quartz diorite C body correspond to fresh sites. Magnetite is euhedral or subhedral, and 150 μm or less in size. Occasionally ilmenite occurs in contact with magnetite or as exsolution lamellae in magnetite.

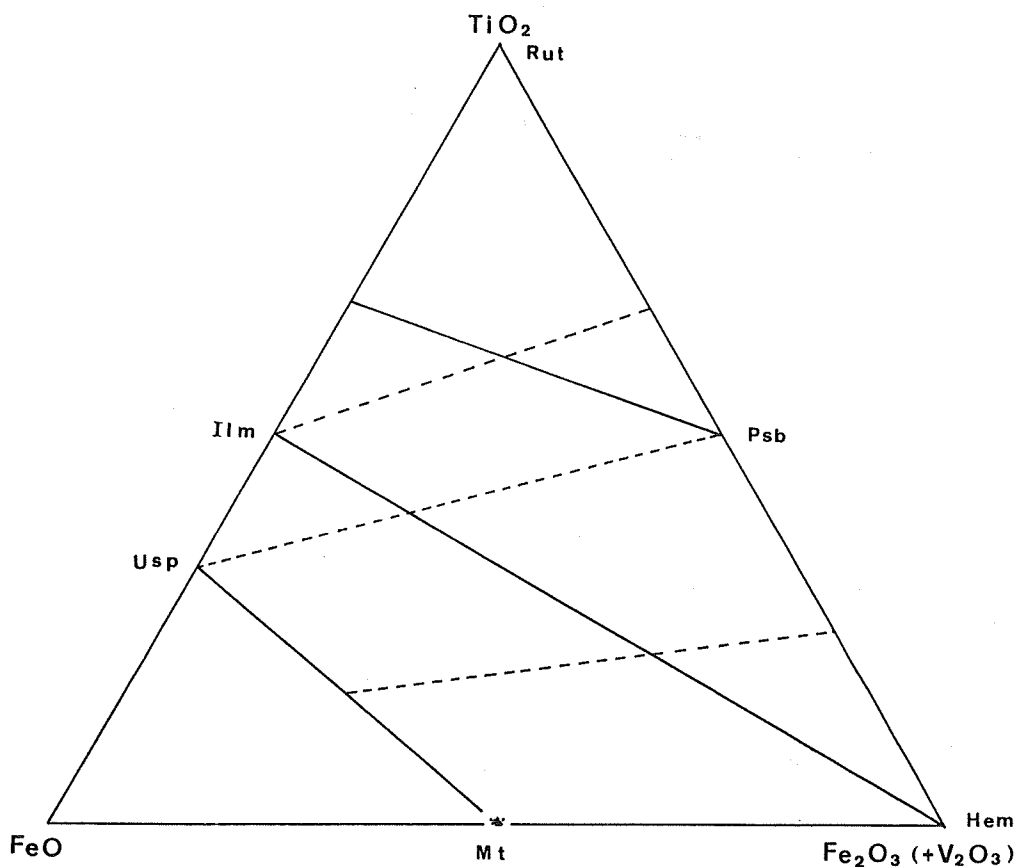


Fig. 2. Chemical composition of magnetite from fresh and hydrothermally altered sites of quartz diorite bodies.

The second is altered sites. They are site Q3 of the quartz diorite A body and sites Q7 and Q8 of the quartz diorite C body, and distribute near ore deposits. Biotite is mostly altered to chlorite. Aggregates of small recrystallized magnetite grains of about 10 μm in size appear generally. Also some grains of subhedral magnetite are present.

The third is extremely altered sites which are site Q4 of the quartz diorite A body and site Q6 of the quartz diorite B body. These rocks include large amount of pyrite, and their silicate minerals are almost altered. Biotite has changed to chlorite, and plagioclase is sericitized. Magnetite is recrystallized to fine grains or replaced by pyrite around its margin. Sphalerite, chalcopyrite or pyrrhotite occur occasionally.

Altered sites and extremely altered sites mentioned above are merely treated as hydrothermally altered sites, because altered sites and extremely altered sites are same from the standpoint of recrystallization of magnetite.

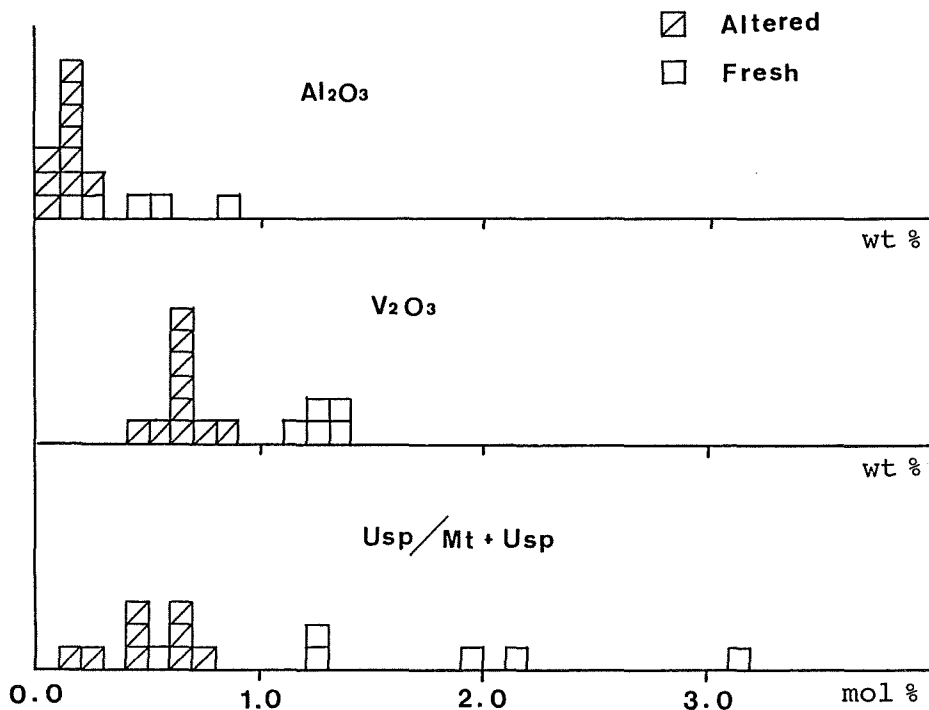


Fig. 3. Al_2O_3 , V_2O_3 and ulvospinel mole contents in magnetite.

Chemical Composition of Magnetite

Chemical compositions of magnetite were determined by an ARL electron probe microanalyzer. Macroscopically the composition of magnetite from both fresh and hydrothermally altered sites are plotted at a small area near pure magnetite as shown in Figure 2. Those are concordant with previous published results of acidic plutonic rocks. However, minor elements in magnetite from hydrothermally altered sites are different from those from fresh sites. As shown in Figure 3, Al_2O_3 , V_2O_3 and ulvospinel mole in magnetite from hydrothermally altered sites are lower than those from fresh sites. Those elements appear to be removed from original magnetite of a rock forming mineral by recrystallization during hydrothermal alteration. Cr_2O_3 , MnO and MgO are contained less than 0.2 wt%, and significant difference between fresh and hydrothermally altered sites is not recognized (Fig. 4).

It is evident that recrystallized magnetite become pure. It is possible to discriminate between the original rock forming magnetite and the recrystallized magnetite of alteration products. By this analogy the CRM due to recrystallized magnetite in the hydrothermal alteration zone may be distinguished from the TRM due to original magnetite, if the altered Fe-Ti oxide mineral is magnetite as found in the Chichibu mining area.

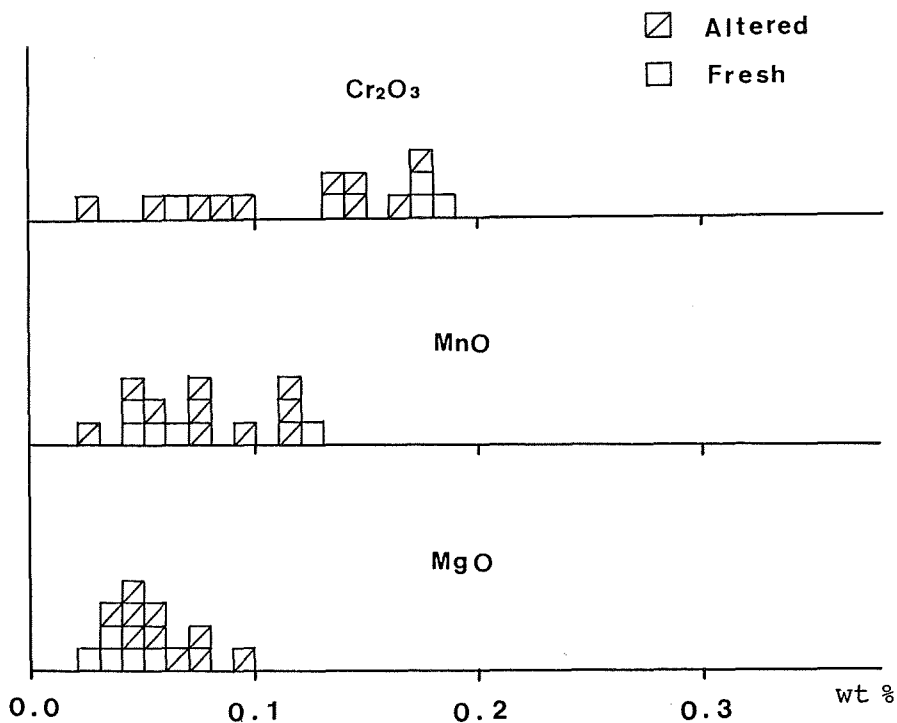


Fig. 4. Cr_2O_3 , MnO and MgO contents in magnetite.

References

- Fujimoto, H., Kawada, K., Miyazawa, T., Morikawa, R., Arai, F., Takano, T., Yoshida, S., Hara, K., Tazuke, H., and Madoo, H. (1950) Bulletin Chichibu Museum Natural History, no.1, 1-28 (in Japanese).
- Fujimoto, H., Miyazawa, T., Kawada, K., Asano, K., and Kaneda, M. (1957) Geological Society Japan 64th Annual Meeting Excursion Guide Book, 1-31 (in Japanese).
- Ishii, A. (1962) Bulletin Chichibu Museum Natural History, no. 1-22 (in Japanese).
- Kaneda, M., and Watanabe, A. (1961) Mining Geol., 11, 481-490 (in Japanese).
- Kitamura, K. (1975) Econ. Geol., 70, 725-738.
- Koike, T., Igo, H., Takizawa, S., and Kinoshita, T. (1971) Jour. Geol. Soc. Japan, 77, 165-168.
- Metal Mining Agency of Japan (1975) Report on the regional geological survey, Chichibu district: Ministry International Trade Industry, Tokyo (in Japanese).
- Miyazawa, T., Hashimoto, M., and Harada, K. (1970) IMA-IAGOD Joint Meeting 1970 Excursion Guidebook 5, 49 p.
- Okubo, M. and Horiguchi, M. (1969) Japan Geological Survey, Quadragle series, Tokyo, no.26, 66 p. (in Japanese).
- Shoji, T., Ootsuka, M., and Imai, H. (1969) Jour. Mining Metallurgical Institute Japan, 85, 765-770 (in Japanese).
- Ueno, H., and Shibata, K. (1986) Jour. Japan. Assoc. Mineral. Petr. Econ. Geol., 81, 77-82.
- Ueno, H., Tonouchi and Shibata, K. (1978) Abstracts of IAGOD Fifth Symposium held at Snowbird, USA, p. 194.

THERMOMAGNETIC STUDY ON ROCKS FROM RYOKE BELT IN YANAI-OSHIMA
DISTRICTS, SOUTH-EAST END OF YAMAGUCHI PREFECTURE, WEST JAPAN

Haruo DOMEN

Institute of Physical Sciences, Faculty of Education,
Yamaguchi University, Yamaguchi 753, Japan

Several metamorphic rock samples were taken from the Ryoke belt, which is a well-known metamorphic belt in the western Japan. And those thermomagnetic (Js-T) properties were examined by means of a balance. Both the Js-T curves thus obtained and the concentration of the ferromagnetic constituents are shown in this brief note.

Fig. 1 is a map showing a rough sketch of the geology of the sampling area, a part of the Ryoke metamorphic belt at the southeastern Yamaguchi Prefecture; Yanai and Oshima Islet districts and of sampling sites. As has been seen, the sites are on the north-south line acrossing perpendicularly to the strike of the metamorphic zone roughly speaking.

Table 1. Rock type and the concentration of the
ferromagnetics of test specimen.

	Site No.	Rock type	Ferromagnetics content in wt%	
Yanai, Main Island	NNW ↑	2 Granite	3.5×10^{-4}	
		3 Biotite banded gneiss	$5.8 \times "$	
		4 Hornbrende biotite granodiorite	$3.0 \times "$	
		5 Siliceous banded gneiss	2.8×10^{-3}	
		6 Siliceous banded gneiss	8.7×10^{-5}	
		8 Aplite	$1.1 \times "$	
		9 Siliceous banded gneiss	7.7×10^{-3}	
		↓	10 Amphibolite	$5.2 \times "$
	Oshima, Islet	↑	11 Aplite	very few
			18 Granodiorite	very few
		19 Biotite banded gneiss	5.2×10^{-4}	
↓ SSE		21 Biotite granodiorite	3.5×10^{-3}	

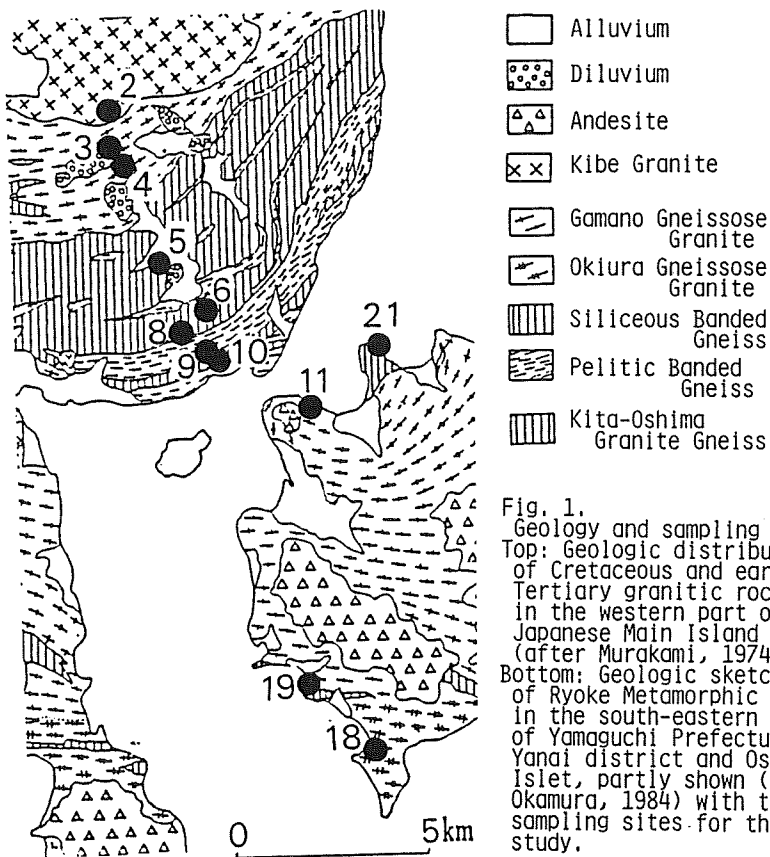
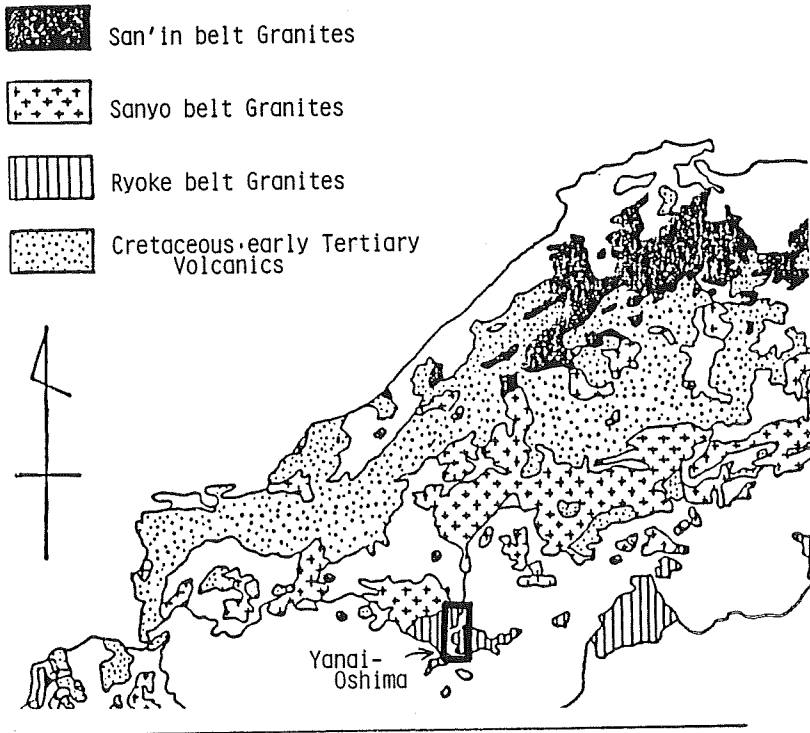


Fig. 1.
 Geology and sampling sites.
 Top: Geologic distribution of Cretaceous and early Tertiary granitic rocks in the western part of Japanese Main Island (after Murakami, 1974).
 Bottom: Geologic sketch map of Ryoke Metamorphic belt in the south-eastern end of Yamaguchi Prefecture; Yanai district and Oshima Islet, partly shown (after Okamura, 1984) with the sampling sites for this study.

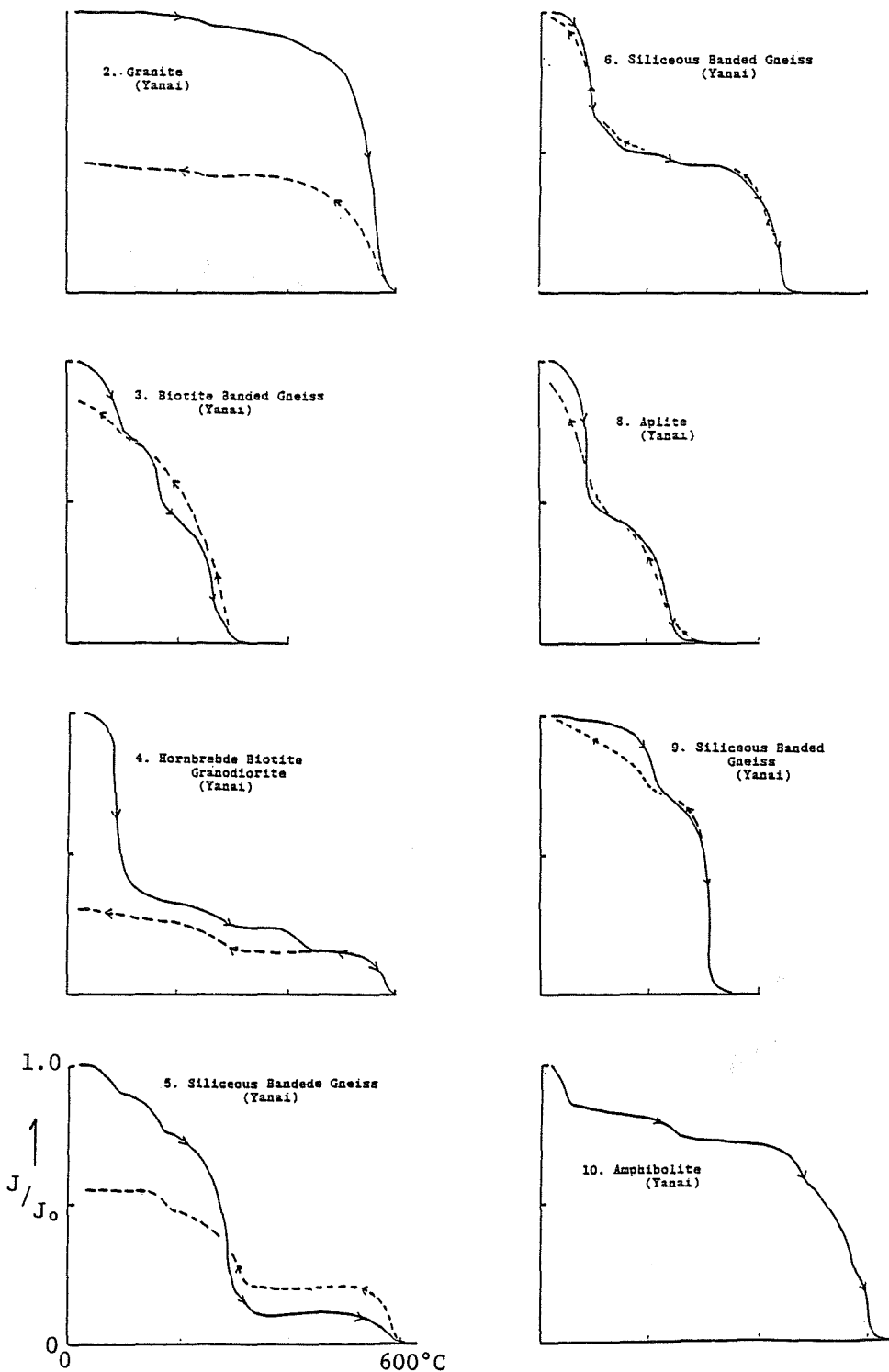


Fig. 2(a) Thermomagnetic (J_s - T) curves for the Ryoke metamorphic rocks. Yanai district, SE Yamaguchi Pref., west Japan. (in open air, $H_{ex} = 3 \text{ kG}$)

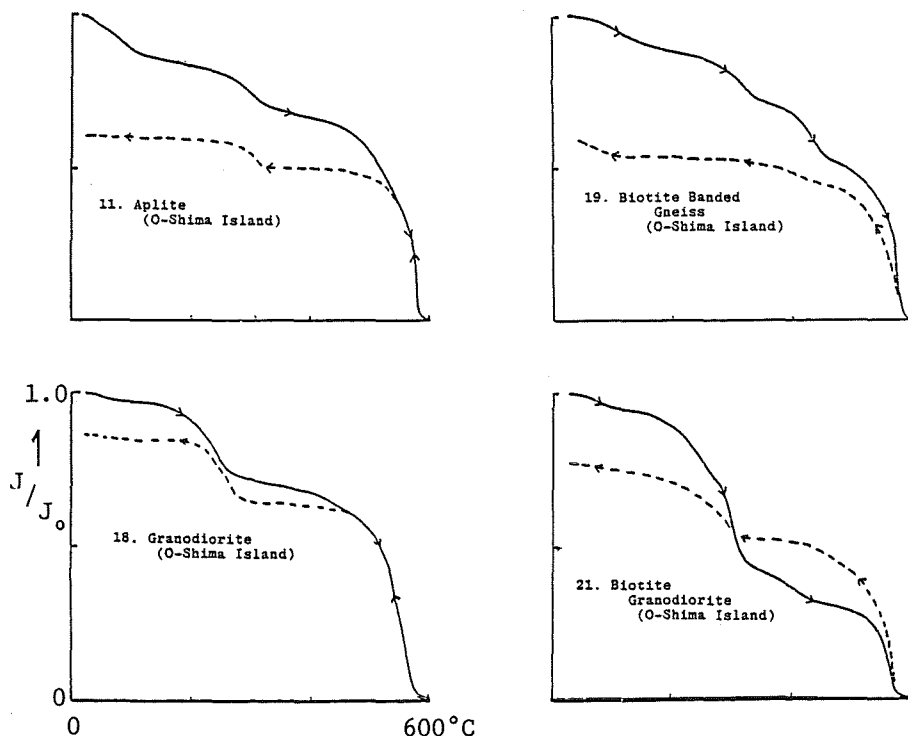


Fig. 2(b) Thermomagnetic curves for the Ryoke metamorphic rocks.
Oshima Islet, SE Yamaguchi Pref., west Japan.
(in open air, Hex = 3 kG)

The specimen submitted to the Js-T analysis was prepared such as the hand sample of each rock was crushed into fine powder of the order less than 80 meshes (0.8 mm in diameter), then the ferromagnetic rock forming minerals were picked up from the powder thus pulverized by a hand magnet at the room temperature. For the Js-T analysis, a semi-automatic home-made thermomagnetic balance (Domen, 1977) was employed. The analysis for all specimens was carried out in the open air and in the magnetic field strength of Hex = 3 kG in this time.

In Table 1, the rock type and the concentration as the weight % of the ferromagnetic constituents of the respective sample are shown. The typical examples of Js-T curves for these samples are shown in Fig. 2.

As has been seen in those figures, the mode of Js-T curves thus obtained are rather reversible in heating- and cooling-processes in spite of the analysis performing in the open air. Most of all curves show that the poly-phased ferromagnetics are contained within the specimen, roughly speaking.

On the specimens from the Site Nos. 2 and 10; both belonged to Yanai district, and also of Oshima Islet specimens, the highest Curie points are suggesting that the main ferromagnetic constituents are magnetite. But, the specimens come from the Site Nos. 3, 8 and 9 of Yanai samples show rather low temperatures for the Curie points, say 300 -- 350°C. The mode of Js-T curves for the Site Nos. 4 and 5 are rather characteristic.

Previously, the highly metamorphosed rocks from the Ko-Yama district, northeastern end of Yamaguchi Prefecture were examined (Domen, 1985), and it was clarified that the Js-T curves for the rocks highly metamorphosed of that district are fairly irreversible to the thermal treatment and the mode of Js-T curves for the Ko-Yama rocks are different in comparison with that of the specimens of the Ryoke belt examined by the present study. This difference might be due to the different type of the metamorphism, for instance, the Ko-Yama metamorphism was caused by the thermal one mainly and that of the Ryoke rocks was dynamic more than thermal.

So far as the present study is concerned, it is difficult to find any positive correlation between the mode of the Js-T curves and the degree of the metamorphism to the Ryoke rocks.

On the other hand, some preliminary test shows that the natural remanent magnetic intensity of each rock sample from the Ryoke belt are rather weak, say, of the order of 10^{-8} -- 10^{-9} emu/g. Because of this, the directions of the natural remanent magnetization are not decided yet, but the result on those may be appeared in the near future.

References

- Domen, H. (1977) Bull. Fac. Educ. Yamaguchi Univ., 27, 17.
Domen, H. (1985) Rock Mag. Paleogeophys., 12, 77.
Murakami, N. (1974) in "Chugoku Chiho" (eds. Imamura et al, 1984, Asakura Book Co.), 193.
Okamura, Y. (1984) *ibid*, 208.

RIKITAKE TWO-DISK DYNAMO AND PALEOMAGNETISM

Masaru Kono

Department of Applied Physics, Tokyo Institute of Technology
Ookayama 2-12-1, Meguro-ku, Tokyo 152, Japan

Introduction

The two-disk dynamo, or coupled-disk dynamo, was first introduced by Rikitake in 1958. The system consists of two disks and two coils which are interconnected with each other. With an appropriate selection of units for the variables, the equations describing this system can be written as

$$\begin{aligned}\frac{dx_1}{dt} + \mu x_1 &= x_2 y_1, & \frac{dx_2}{dt} + \mu x_2 &= x_1 y_2 \\ \frac{dy_1}{dt} &= \frac{dy_2}{dt} = 1 - x_1 x_2\end{aligned}$$

where x_1 , x_2 and y_1 , y_2 are the non-dimensional current and angular velocity of disks 1 and 2 and t is the non-dimensional time. The equations contain four dependent variables x_1 , x_2 , y_1 , y_2 , but as y_1 and y_2 are linearly related, the Rikitake dynamo has three degrees of freedom. This is one of the typical examples of chaos which shows complex behavior in spite of the small number of parameters and the simple differential equations governing the system (Ito, 1980).

If the time derivatives are set equal to zero, the stationary solution for this system is obtained as $x_1 = \pm k$, $x_2 = \pm k^{-1}$, and $y_1 = \mu k^2$, $y_2 = \mu k^{-2}$, where k is an arbitrarily chosen constant depending on the initial condition (Rikitake, 1958).

As the Rikitake dynamo exhibits reversals of currents which resemble the occasional reversals of the geomagnetic field, the transient behaviors of this system have been extensively studied by Allan (1962), Cook and Roberts (1970), and others. In recent years, the interest in the Rikitake dynamo was revived by the realization that it is a good example of chaos. Ito (1980) carried out a detailed analysis and obtained a phase diagram in the (k, μ) space. Shimizu and Honkura (1985) compared the behavior of the Rikitake dynamo with other coupled disk systems, while Miura and Kai (1984) studied detailed chaos structure of the coupled three-disk dynamo first introduced by Lebovitz (1959).

The Rikitake dynamo has often been employed as an analog of the geomagnetic field. For example, Cox (1968) used the Rikitake dynamo as a base in deriving his stochastic model of the geomagnetic reversals. Although his model is inconsistent with the paleomagnetically observed distribution of the magnitudes of the geomagnetic dipole moment (Kono, 1972), it is still an attractive model when considering reversal process. It is therefore very interesting to know how far the analogy holds between the model and the actual geomagnetic field.

Statistical Properties of the Geomagnetic Field

The most important statistical properties of the geomagnetic field observed by paleomagnetism, which should be related to the fundamental dynamo process in the core of the earth, are,

1. dominance of the dipole term in the surface field
2. occasional reversals of the dipoles
3. exponential distribution of the polarity interval lengths
4. bi-normal distribution of the dipole intensities

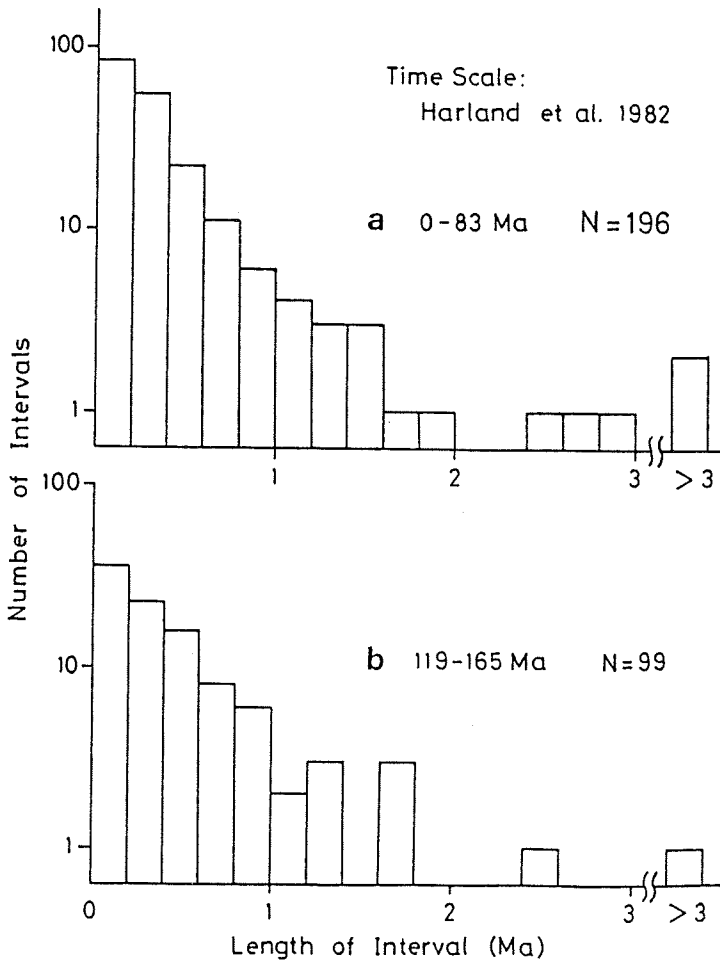


Fig. 1. Frequency distribution of the lengths of polarity intervals for (a) 0 to 83 Ma (b) 119 to 165 Ma (after the time scale of Harland et al., 1982).

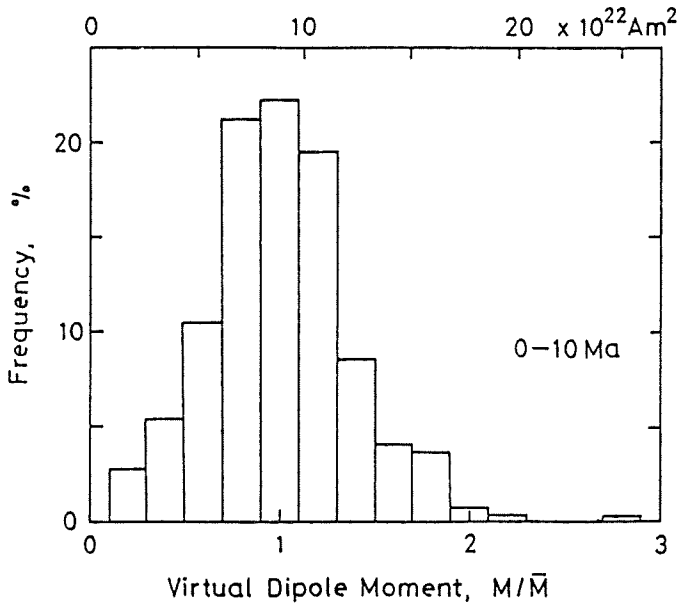


Fig. 2. Frequency distribution of the VDM for the period of 0 to 10 Ma compiled by Kono (1971) from paleointensity data obtained by the Thelliers' method.

These are the most important characteristics of the geomagnetic dipole. Other properties such as the dipole offset and the latitude dependence of paleosecular variation may be regarded as secondary in importance in comparison with these, as they are concerned with the non-dipole components of the geomagnetic field.

Figure 1 shows the frequency distributions of the lengths of polarity intervals constructed from a recent geomagnetic reversal time scale of Harland et al. (1982). Figure 1 gives separate distributions for periods before and after the Cretaceous long normal period, but it is evident from the shape of the two distributions that the combined distribution (including or excluding the long normal period) is again of the same type. The figure shows that the distribution of polarity intervals is well approximated by an exponential distribution. Of course, the fit with theoretical distribution is not perfect; there are too many long intervals. There has been some controversy whether polarity intervals follow an exponential distribution or a gamma distribution (e.g., Cox, 1968; Naidu, 1971). However, McFadden and Merrill (1984) showed that there is strong evidence that the reversal process is essentially Poisson. It is therefore reasonable to conclude that the lengths of polarity intervals follow an exponential distribution, with an addition of some longer intervals.

Figure 2 shows the distribution of the virtual dipole moment (VDM, Smith, 1967) in the last 10 Ma, as compiled by Kono (1971) from paleointensity data obtained by the Thelliers' method (Thellier and Thellier, 1959). In this compilation, polarity of the geomagnetic field was neglected, so that the abscissa is the absolute value of the VDM. It is seen from this figure that the VDM follows a normal distribution, with a mean of 8.9×10^{22} Am² and a standard deviation of 3.4×10^{22} Am². Recently, McFadden and McElhinny (1982) performed a similar analysis on a newer and larger data set and confirmed the earlier findings of Kono (1971), obtaining similar distributions for the last 5 Ma separately for normal and reversed periods. An important point to note is that the occurrence of very low dipole intensity in the paleomagnetic record is very rare. The low intensities are usually observed only for periods of polarity transition and excursion (e.g., Prevot et al., 1985), and the scarcity of low paleointensities corresponds to the short time interval covered by these abnormal periods ($2 - 4 \times 10^3$ years for a reversal) compared to the average length of polarity intervals (2×10^5 years for the last 10 Ma).

Time Dependent Behavior of Two-Disk Dynamo

The statistical properties of the Rikitake dynamo were obtained by computing the time dependent behavior of the system for various combinations of k and μ . The computation was done by the Runge-Kutta method of fourth and fifth order, with an accuracy of 10^{-10} . Since the disk dynamos do not simulate the actual physical conditions in the core, the approach taken here was to search for *any* model in the chaotic region that can successfully reproduce the observed statistical properties of the field mentioned above. Following the results of Ito (1980), several combinations of parameters (k, μ) were selected as representing a variety of cases. As the obtained system behavior can be divided into two typical types according to both polarity length and field intensity statistics, only two such combinations, (2, 1) and (4, 2.5), are used in the following to illustrate the model behavior. Models with other combinations of parameters belong to either of the two types or a combination of both, in polarity length as well as in intensity statistics.

For the case of $k = 2$ and $\mu = 1$, the system seems to be stationary; i.e., the manner of current fluctuation does not change with time. In contrast, very different behavior is observed for the combination of $k = 4$ and $\mu = 2.5$ when different portions of the time series are taken. Very long periods of constant polarity are sometimes observed but short period flippings are also seen interspersed between the long ones.

For such cases as (4, 2.5), it is necessary to follow the system behavior for quite a long

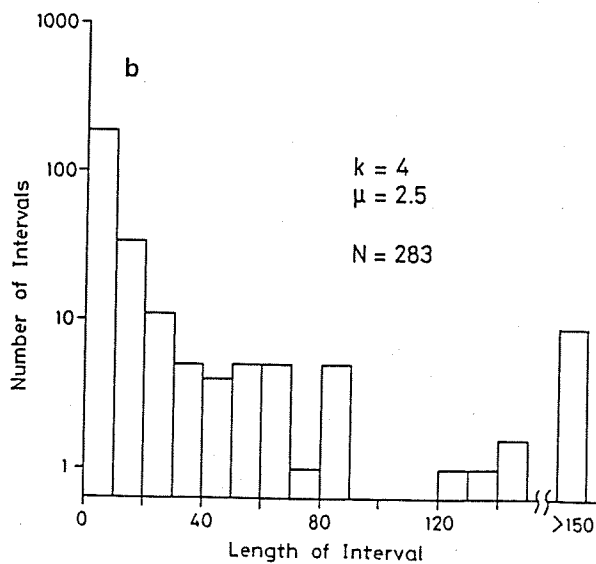
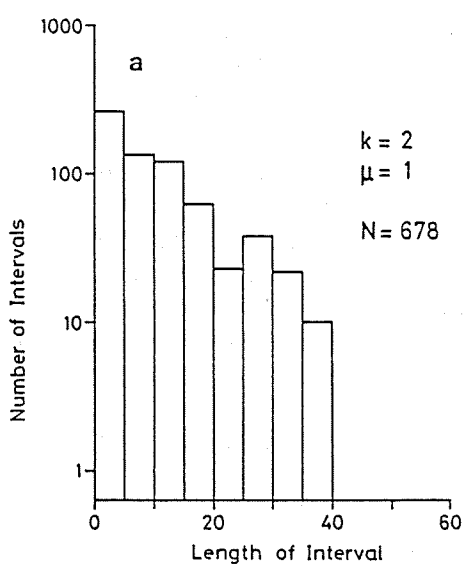


Fig. 3. Frequency distribution of the lengths of polarity intervals observed for the two-disk dynamo. (a) $k = 2$ and $\mu = 1$. (b) $k = 4$ and $\mu = 2.5$.

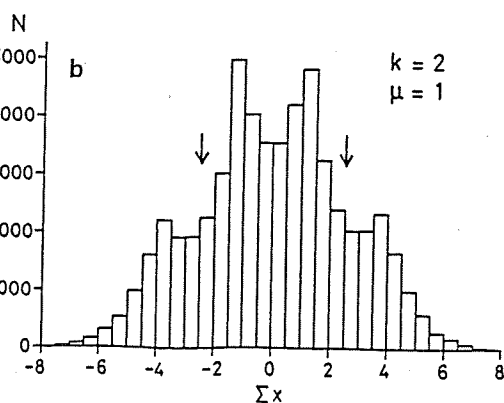
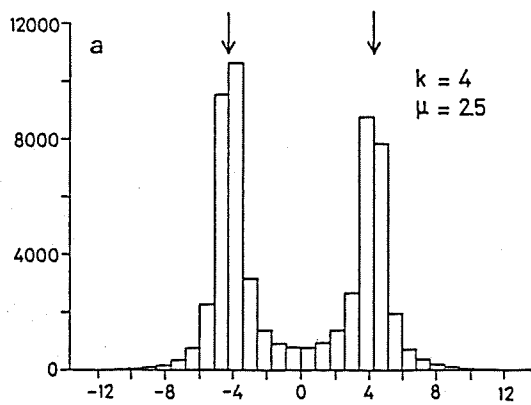


Fig. 4. Frequency distribution of the sum of currents $x_1 + x_2$ in the two-disk dynamo. Arrows indicate the equilibrium values $k + k^{-1}$. (a) $k = 2$ and $\mu = 1$. (b) $k = 4$ and $\mu = 2.5$.

time to obtain the true statistical properties of the system. For each combination of parameters used in the present study, it was found that about ten thousand non-dimensional time units is enough to average out statistical fluctuations of the system, and calculations for individual combinations of k and μ were carried out up to $t = 10,000$.

Figure 3 shows histograms of polarity intervals in the two-disk dynamo. For the case of $k = 2$ and $\mu = 1$ (Figure 3a), the shorter polarity intervals follow an exponential distribution quite well. However, there is a distinct cutoff in the observed data at about $t = 40$. In other words, longer polarity intervals are absent in the data where the exponential distribution predicts a substantial number of occurrences. In this respect, the system does not behave like a Poisson process.

On the other hand, too many long intervals are observed for the case of $k = 4$ and $\mu = 2.5$ (Figure 3b). The number of intervals decreases exponentially only up to $t = 40$; afterwards the distribution is nearly flat to $t = 90$, and many intervals exist even beyond $t = 100$. Again, the system does not appear Poisson. As noted above, a number of quite long polarity intervals exist in the geomagnetic record exceeding the expectation from the exponential distribution (Figure 1). However, the occurrence frequency in the two-disk dynamo model is much larger, and the resulting distribution is significantly different from an exponential distribution (Figure 3b).

Figure 4 shows the frequency distributions of the currents, or, equivalently, magnetic field intensities of the two-disk dynamo. For the case of $k = 2$ and $\mu = 1$ (Figure 4a), the system spends too much time near zero, and the distribution is not similar to the paleomagnetically observed one (Figure 2). The case for $k = 4$ and $\mu = 2.5$ (Figure 4b) appears more promising. But on closer examination, it can be seen that the distribution is not normal and that there are still too many probabilities for the system to attain very low intensities. The distribution of the current intensities (for one polarity) seems to be a combination of broad normal distribution and a narrow one concentrated near the equilibrium value.

Discussion and Conclusions

Although an exhaustive search has not yet been carried out in the (k, μ) space, the results summarized in the above section apply to each case treated in this study. Comparison with the results given by Ito (1980) suggests that the following conclusions are applicable to the Rikitake dynamo in a general manner.

1. The process is not usually Poisson. There are either too few or too many long polarity intervals. However, with an appropriate selection of parameters, the polarity intervals may reasonably approximate exponential distribution.
2. It is hard to obtain two normal distributions for the intensity of the currents flowing through coils. By making k larger, distributions with two distinct maxima can be obtained, but they are not normal distributions. Also, low intensities occur too frequently in every model.
3. To obtain an exponential distribution of polarity intervals and to have bi-normal distribution for field intensities seems to be mutually exclusive. The models with frequent reversals can simulate exponential distribution of polarity intervals (Figure 3a), but spend too much time near the transition so that quite low intensities are very frequent (Figure 4a). The models with two distinct intensity maxima (Figure 4b) tend to oscillate quite a long time near the equilibrium value, and the polarity intervals deviate from exponential distribution.
4. Therefore, the Rikitake dynamo has a limited applicability to be used as a direct analog of the geomagnetic field.

There are some ways to circumvent the above difficulties and to make the disk dynamo model behave more like the geomagnetic field. For instance, Shimizu and Honkura (1985) showed that the inhomogeneous N-disk dynamo is a good candidate to simulate geomagnetic

reversals. A similar conclusion was reached by Honkura and Shimizu (1985) for a model of a homopolar dynamo with perturbed coil current (simulating the effect of the non-dipole component of the field). However, these models introduce either too many degrees of freedom (e.g., N-disk dynamo), or ill-controlled parameters into the system. The Rikitake model is more attractive than these because the system is completely described by a set of simple differential equations with only two parameters. This is more so because of geometrical differences between disk dynamos and the geodynamo.

References

- Allan, D.W., *Proc. Cambridge Phil. Soc.*, 58, 671-693, 1962.
- Cook, A.E., and P.H. Roberts, *Proc. Cambridge Phil. Soc.*, 68, 547-569, 1970.
- Cox, A., *J. Geophys. Res.*, 73, 3247-3260, 1968.
- Harland, W.B., A.V. Cox, P.G. Llewellyn, C.A.G. Picton, A.G. Smith, and R. Walters, *A Geologic Time Scale*, pp. 63-84, Cambridge Univ. Press, London, 1982.
- Honkura, Y., and M. Shimizu, *J. Geomag. Geoelectr.*, 37, 1147-1155, 1985.
- Ito, K., *Earth Planet. Sci. Lett.*, 51, 451-456, 1980.
- Kono, M., *Earth Planet. Sci. Lett.*, 11, 10-17, 1971.
- Kono, M., *Phys. Earth Planet. Inter.*, 5, 140-150, 1972.
- Lebovitz, N.R., *Proc. Cambridge Phil. Soc.*, 56, 154-173, 1959.
- McFadden, P.L., and M.W. McElhinny, *J. Geomag. Geoelectr.*, 34, 63-189, 1982.
- McFadden, P.L. and R.T. Merrill, *J. Geophys. Res.*, 89, 3354-3362, 1984.
- Miura, T., and T. Kai, *Phys. Lett.*, 101A, 450-454, 1984.
- Naidu, P.S., *J. Geophys. Res.*, 76, 2649-2662, 1971.
- Prevot, M., E.A. Mankinen, R.S. Coe, and C.S. Gromme, *J. Geophys. Res.*, 90, 10417-10448, 1985.
- Rikitake, T., *Proc. Cambridge Phil. Soc.*, 54, 89-105, 1958.
- Shimizu, M., and Y. Honkura, *J. Geomag. Geoelectr.*, 37, 455-497, 1985.
- Smith, P.J., *Geophys. J. Roy. Astron. Soc.*, 12, 239-258, 1967.
- Thellier, E., and O. Thellier, *Ann Geophys.*, 15, 285-376, 1959.

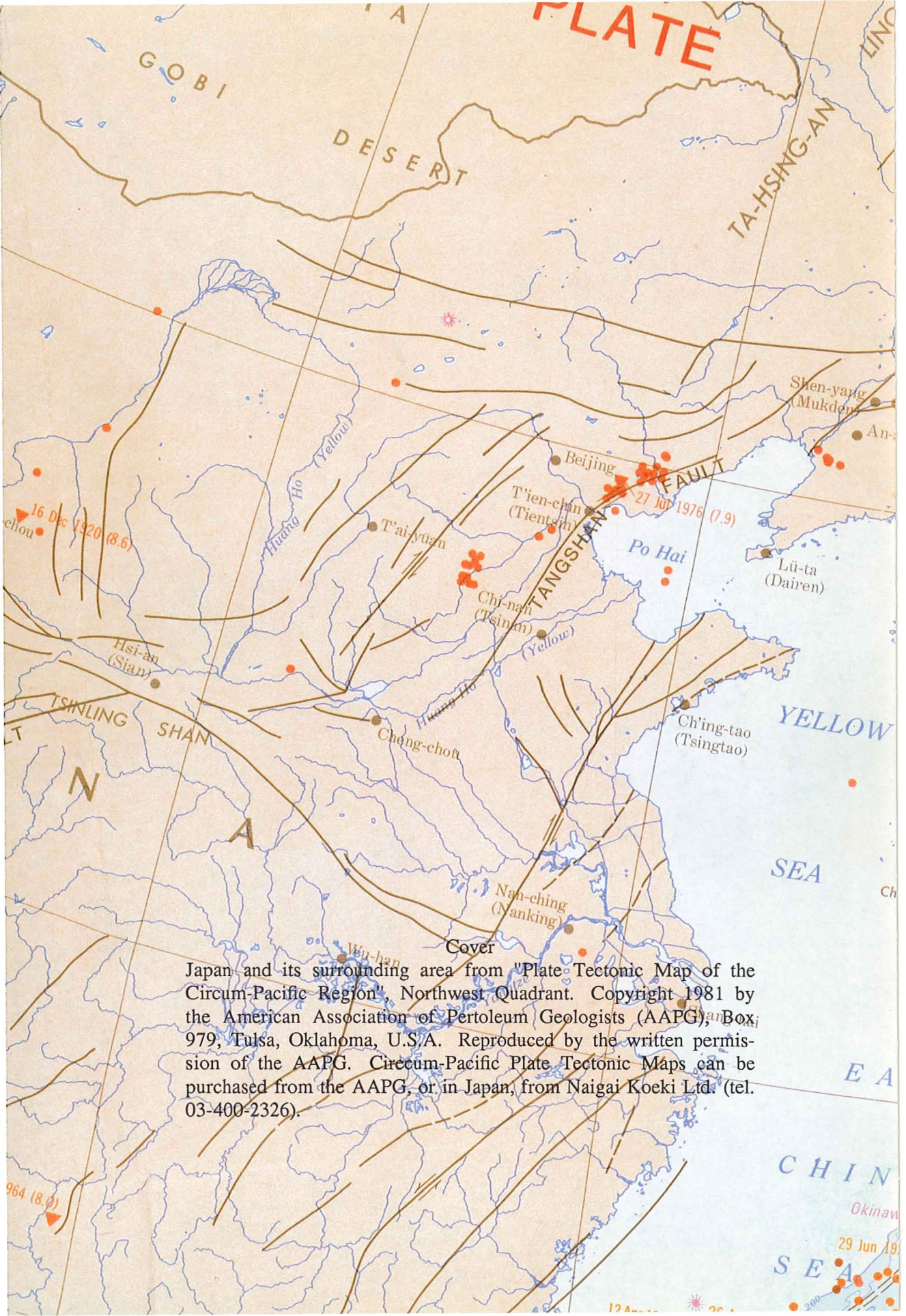
(in press in Geophysical Research Letters)

AUTHOR INDEX

DOMEN, Haruo	66
FUJIOKA, Kantaro	see Kaneoka et al.
FUJIWARA, Yoshiki and R. Sugiyama	15
FUKUMA, Kouji and M. Torii	26
FUNAKI, Minoru and H. Sakai	55
FUNAKI, Minoru and M. Yoshida	35
GAUTAM, Pitambar	39
IKEYA, Motoji	see Morinaga et al.
INOKUCHI, Hiroo	see Morinaga et al.
ISHIKAWA, Naoto	see Torii and Ishikawa
ISHIKAWA, Naoto and M. Torii	8
ITO, Hisatoshi and S. Nishimura	30
ITOH, Yasuto	12
KANEOKA, Ichiro, K. Notsu, Y. Takigami, K. Fujioka, and H. Sakai	48
KONO, Masaru	71
MATSUDA, Takaaki	see Otofujii and Matsuda
MIKI, Toshikatsu	see Morinaga et al.
MORINAGA, Hayao, H. Inokuchi, K. Yaskawa, T. Miki, and M. Ikeya	51
NISHIMURA, Susumu	see Ito and Nishimura
NOTSU, Kenji	see Kanioka et al.
OTOFUJI, Yo-ichiro and T. Matsuda	6
SAKAI, Hideo	see Funakai and Sakai
SAKAI, Hitoshi	see Kaneoka et al.
SUGIYAMA, Ryouichi	see Fujiwara and Sugiyama
TAKIGAMI, Yutaka	see Kaneoka et al.
TORII, Masayuki and N. Ishikawa	1
TORII, Masayuki	see Fukuma and Torii
TORII, Masayuki	see Ishikawa and Torii
UENO, Hiroto	60
YAMAZAKI, Toshitsugu	19
YASKAWA, Katsumi	see Morinaga et al.
YOSHIDA, Masaru	see Funaki and Yoshida







Japan and its surrounding area from "Plate Tectonic Map of the Circum-Pacific Region", Northwest Quadrant. Copyright 1981 by the American Association of Petroleum Geologists (AAPG), Box 979, Tulsa, Oklahoma, U.S.A. Reproduced by the written permission of the AAPG. Circum-Pacific Plate Tectonic Maps can be purchased from the AAPG, or in Japan, from Naigai Koeki Ltd. (tel. 03-400-2326).